



Assessment of Climate resilience capacity of a smart city of Haryana: Gurugram city

File Number : PDF/2023/002753

Submitted By : Dr. Pardeep Kumar
[SERB Qualified Unique Identification Document: SQUID-1992-PK-2895]
Submission Date : 10-Aug-2023

PROPOSAL DETAILS

(PDF/2023/002753)

Principal Investigator	Mentor & Host Institution
Dr. Pardeep Kumar pardeepranga001@gmail.com NPDF(University School of Environmental Management) Contact No : +919711833608 Date of Birth : 15-Oct-1992 Name of Father/Spouse :	Produt Bhattacharya produtbhattacharya@yahoo.com Professor(University school of environmental management) Guru Gobind Singh Indraprastha University Sector 16 c, dwarka, delhi, New delhi, Delhi-110078 Contact No. : +919560866868 Registrar Email : registrar@ipu.ac.in No. of PHD Scholars : 7 No. Post-Doctoral Fellow : 0

Details of Post Doctorate

Ph.D. (Environmental sciences) [Degree Awarded on : 27-May-2023]

Aquifer mapping of middle Andaman using geospatial, geophysical and machine learning approach

Research Supervisor/Guide & Institution :

Professor Saumitra Mukherjee

Jawaharlal Nehru University

Brief details of Thesis work :

My PhD work includes the hydrogeochemistry of middle Andaman. In one of objective i analysed the impact of limestone cave and seawater intrusion on coastal aquifer of middle Andaman and identified zones of seawater intrusion with aquifer depth. In second objective, surface manifestation of groundwater hydrology with geological structure and vegetation anomaly includes spatial temporal mapping of natural resources, geological structures like pediment plain, lineaments, weathered sandstone and patches of ophiolites in the region, groundwater potential zone mapping included use of support vector machine analysis for most prospect groundwater recharge zones in the region, geochemical and mineralogical analysis includes paleoclimates, geological mapping of rocks and minerals of middle Andaman. Last objective on hydrogeochemistry and water quality evaluation for drinking and irrigation purposes was used to identifying processes, sources of contamination, quality estimation of the groundwater.

Technical Details :

Research Area : Earth & Atmospheric Sciences (Earth & Atmospheric Sciences)

Project Summary :

A city is a complex structure of interdependent system of social, economic, and natural systems. Each system has its values and an operational infrastructure supporting the functioning of the city. **City resilience is the working capability of a city to run efficiently for people working and living in it especially the poor and vulnerable, enduring and flourishing against any shock or stress they encounter.** Resilience emphasizes improvising or enhancing the capacity of a city when it encounters multiple threats or hazards rather than mitigating or preventing the damage of resources due to a particular event (Labaka et al., 2019; Reiner and McElvaney, 2017; Index, 2014). The baseline of thriving a city is a question of debate and many agreed on voice, identity, inclusivity, opportunity, and equitable resources in the era of urban expansion and globalization (Morgan and Waskow, 2014). United Nations has drafted 17 Sustainable Development Goals to achieve till 2030 in which SDG 11 focuses on inclusive, safe, resilient, and sustainable cities and human settlement (Takase, 2018). Indian government has promised to construct 100 new smart cities with latest technologies, inclusive development, sustainability, robust infrastructure and greenfield development (Mission Smart cities). Gurugram, a smart city of Haryana, part of National Capital Region witnessing rapid expansion of population and urbanisation, increasing industrialisation, decreasing green cover, immigration of working class. The effect of climate change and man-made hazards requires a holistic assessment of resilience capacity of the city. Research questions: What is the pattern of expansion of the city and socio-demographic status of immigrants? What are the best zones for expansion of the green space in the city? What are key infrastructures and their status in smooth running of city against stress or shocks? What are the probable climate hazards, risk zone and vulnerability of inhabitant and immigrants? What is resilience capacity of the city against any climate or man-made stress or shocks? What is the nature-based-solutions to be recommended to increase the efficiency of resilience of the city? References <https://smartcities.gov.in/> Index, C. R. (2014). City resilience framework. The Rockefeller Foundation and ARUP, 928. Labaka, L., Maraña, P., Giménez, R., & Hernantes, J. (2019). Defining the roadmap towards city resilience. Technological Forecasting and Social Change, 146, 281-296. Morgan, J., & Waskow, D. (2014). A new look at climate equity in the UNFCCC. Climate Policy, 14 (1), 17-22. Reiner, M., & McElvaney, L. (2017). Foundational infrastructure framework for city resilience. Sustainable and resilient infrastructure, 2(1), 1-7.

Objectives :

- 1. Climate hazard and risk zone mapping of the city
- 2. Identification and clustering of vulnerable populations living in the city
- 3. Assessment of key infrastructure of built environment sustaining the livelihood of the city
- 4. Scope of urban green space (UGC) planning for reducing urban heat island effects and increasing biodiversity of the city
- 5. Integration of resilient variables using traditional methods and machine learning algorithms

Keywords :

Resilient Capacity, Smart cities, Rockefeller-Arup, Climate

Expected Output and Outcome of the proposal :

- Spatial map of socio-economic status of population and their education or skills in preparedness of resilient city
- Spatial map of availability and functioning of key infrastructure per 1,00,000 population
- Time series maps of Climate hazard and risk maps of the city and classification in different zone of impact.
- Spatial map of zone of least resilient, intermediate and most resilient part of the city
- Nature-based solution recommendation to policy-maker for shaping a resilient city.

Reference Details :

S.No	Reference Details
1	Professor Alokes Chatterjee, Flat 1C Russa Road East First lane, Kolkata[+9830715625] alokesh@yahoo.com
2	Professor Saumitra Mukherjee, Lab 207, School of Environmental Sciences, Jawaharlal Nehru University, New Delhi[+913908512] saumitramukherjee3@gmail.com

Study area

Gurugram (previously Gurgaon) is a smart city of India lies in the southeastern part of Haryana state (Anand et al., 2018) (Figure 1). It is also known as the cyber city of Haryana. It has an area of 1258 km² with a 15,14,085 population, 84.4% literacy Rate, 4 Sub-divisions, 4 Development-blocks, 291 Revenue-estates and 193 Villages with 6 urban local bodies (<https://gurugram.gov.in/>). Gurugram is a financial and industrial hub of Haryana and witnessing rapid population growth recently. It has become the best place for industry giants, multinational companies, software companies, and call centers. It has 9.24 % forest cover in the category of moderate and open forest given by the forest survey of India. There is no dense forest cover region in the district. The region falls into the least fire-prone region covering major tree species. Eucalyptus species, Dalbergia sissoo, Prosopis cineraria, Azadirachta indica, and Populus species (FSI, 2021)

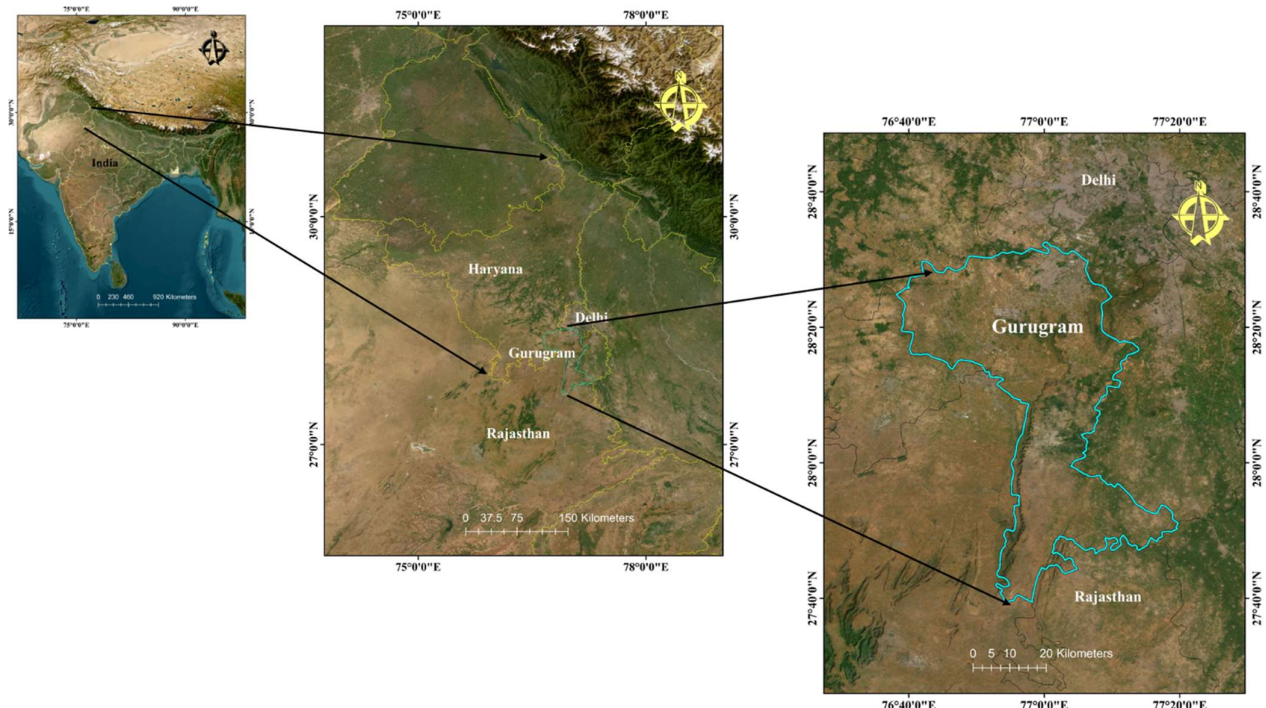


Figure 1. Study area map of Gurugram district

Methodology

Software:

Bhuvan, Google Earth, and Toposheet of Survey of India will be used for visualization and mapping of natural and urban features of the city.

ArcGIS 10.8 and QGIS 3.32 will be used for the integration of non-spatial data into geospatial data.

ENVI 5.2, ERDAS 2014, and SNAP 9.0.0 will be used for preprocessing, integration, and fusion of satellite data.

ArcGIS 10.8, Google Earth Engine, R, and Tensorflow will be used for the integration and processing of data for final results.

Satellite data

ResourceSat-1-2, Sentinel 1-2 and Landsat 1-9 will be used for the estimation of changes in land use and land cover, infrastructure, urban density, and green spaces in the city.

MODIS, ALOS PALSAR, Sentinel 1, and Landsat 5-9 for thermal profile, wetness, greenery, and water resources in the city.

Social and economic data

Research articles, magazines, government and NGO reports for past decisions of government and stakeholders.

Census 2011 will be used for the socio-economic demography of the city.

Field Survey will be used for the socio-economic demography of immigrants in the city.

Rockefeller-Arup City Resilience Index will be used to estimate the resilience of the city. The index will be calculated by using 52 indicators of a resilient city.

Flow chart of research work

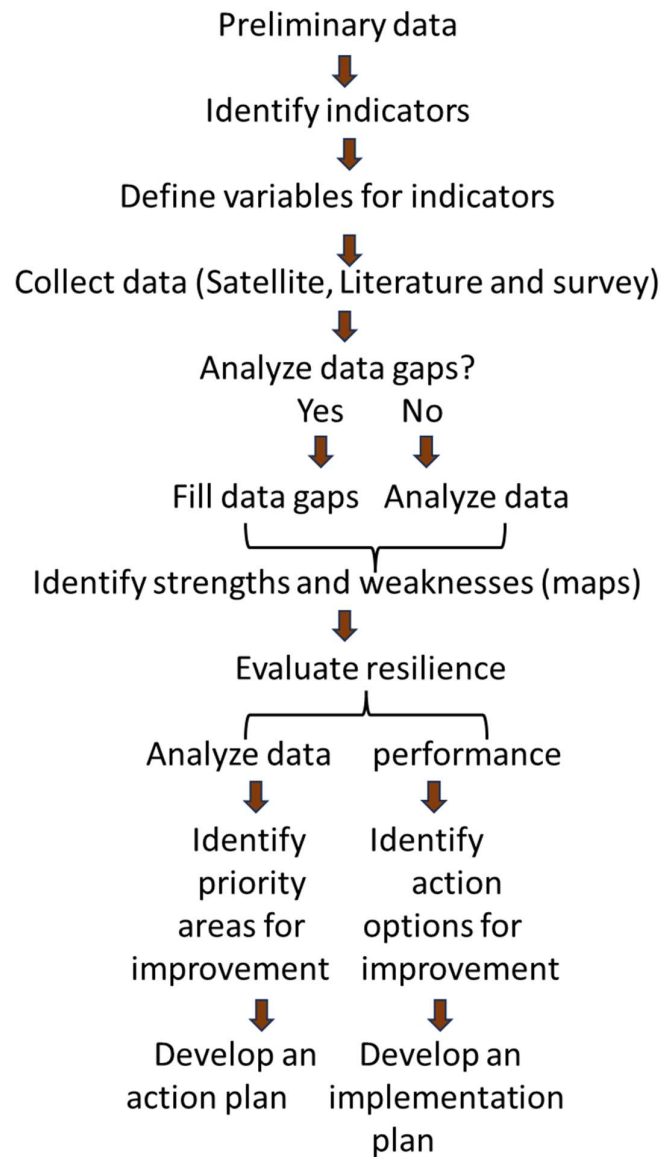


Figure 2. Flowchart of the research work

BIO-DATA

1. Name and full correspondence address: Pardeep Kumar, Lab 211, School of Environmental Sciences Jawaharlal Nehru University New Delhi, Pin 110067
2. Email(s) and contact number(s): pardeepranga001@gmail.com, +919711833608
3. Institution: Jawaharlal Nehru University, New Delhi
4. Date of Birth: 15-10-1992
5. Gender: Male
6. Category: SC
7. Whether differently abled: No
8. Academic Qualification (Undergraduate Onwards):

	Degree	Year	Subject	University/Institution	% of marks
1	B.Sc.	2014	Physics, Chemistry, Mathematics	Maharshi Dayanand University, Rohtak	59.17
2	M.Sc.	2016	Environmental Sciences	Jawaharlal Nehru University, New Delhi	66
3	M.Phil..	2019	Environmental Sciences	Jawaharlal Nehru University, New Delhi	76
4	Ph.D.	2023	Environmental Sciences	Jawaharlal Nehru University, New Delhi	76

9. Ph.D thesis title, Guide's Name, Institute/Organization/University, Year of Award: Ph.D. thesis on **Aquifer mapping of middle Andaman using geospatial, geophysical, and machine learning approach**, under the supervision of **Prof. Saumitra Mukherjee** from **School of Environmental Sciences, Jawaharlal Nehru University, 2023**.

10. Work experience (in chronological order).

S.No.	Positions held	Name of the Institute	From	To	Pay Scale
1	Research scientist	Jawaharlal Nehru University	01-03 2017	20-09-2017	250000/m

11. Professional Recognition/ Award/ Prize/ Certificate, Fellowship received by the applicant.

S.No	Name of Award	Awarding Agency	Year
1	Reviewer	Frontiers of Earth Science, Section- Environmental informatics and Remote sensing	2023
2	Reviewer	Journal of Earth System	2023

		Science, Springer Published by the Indian Academy of Sciences	
3	Summer school “Virtual School on Resilient Cities”	International Society for Photogrammetry and Remote Sensing and Beijing University of Civil Engineering and Architecture	2022
4	Faculty development program- Basic of Machine learning- Mathematics Inside	Netra Lab, Department of Computer Applications, Sikkim University	2021
5	Post graduate certificate in climate change	IGNOU	2020
6	Post graduate certificate in Geoinformatics	IGNOU	2019
7	Junior Research fellow	UGC-CSIR	2017

12. Publications (*List of papers published in SCI Journals, in year wise descending order*).

S.No.	Author(s)	Title	Name of Journal	Volume	Page	Year
1	Kumar Pardeep, Chandrashekhar Azad Vishwakarma, Priyadarshini Singh, Harshita asthana, Vikas Rena, Carolyne chinneikim mate, Saumitra Mukherjee	Hydrogeochemical characterization and water quality evaluation for drinking and irrigation purposes of coastal aquifers of Middle Andaman	Journal of Hydrology: Regional Studies	Under review		2023
2	Kumar Pardeep, Priyadarshini Singh, Harshita Asthana, Bhawna Yadav, Saumitra Mukherjee	Groundwater Potential Zone Mapping of Middle Andaman Using Multi-Criteria Decision Making and Support Vector Machine	Groundwater for sustainable development	Under review doi-10.2139/ssrn.4489541		2023
3	Kumar Pardeep, Saumitra Mukherjee	Impact of climate change and catastrophic events on Forest cover of Middle Andaman using Remote sensing, GIS and support vector machine	Forests	Under review doi: 10.20944/preprints202307.0103.v1		2023
4	Singh Garima, Pardeep Kumar, Saumitra Mukherjee	Forest Fire Risk Mapping in Pauri Garhwal district of Uttarakhand	Forests	Under review doi: 10.20944/preprints202307.0132.v1		2023
5	Kumar, Pardeep, and Saumitra Mukherjee	Impact of limestone caves and seawater intrusion on coastal aquifer of middle Andaman	Journal of Contaminant Hydrology	256	104197	2023
6	Rena, Vikas, Chandrashekhar Azad Vishwakarma, Priyadarshini Singh,	Hydrogeological investigation of fluoride ion in groundwater of Ruparail and Banganga basins,	Environmental Earth Sciences	81	17	2022

	Nidhi Roy, Harshita Asthana, Vikas Kamal, Pardeep Kumar, and Saumitra Mukherjee	Bharatpur district, Rajasthan, India				
7	Asthana, Harshita, Chandrashekhar A. Vishwakarma, Priyadarshini Singh, Pardeep Kumar, Vikas Rena, and Saumitra Mukherjee	Comparative analysis of pixel and object-based classification approach for rapid landslide delineation with the aid of open-source tools in Garhwal Himalaya	Journal of the Geological Society of India	96	65-72	2020
8	Singh, Priyadarshini, Harshita Asthana, Vikas Rena, Pardeep Kumar, Jyoti Kushawaha, and Saumitra Mukherjee	"Hydrogeochemical processes controlling fluoride enrichment within alluvial and hard rock aquifers in a part of a semi-arid region of Northern India	Environmental Earth Sciences	77	1-15	2018

13. Detail of patents. NA

S.No	Patent Title	Name of Applicant(s)	Patent No.	Award Date	Agency/Country	Status

14. Books/Reports/Chapters/General articles etc. NA

S.No	Title	Author's Name	Publisher	Year of Publication

15. Any other Information (maximum 500 words) NA



Pardeep Kumar

Undertaking by the Principal Investigator

To

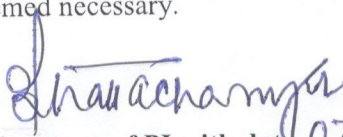
The Secretary
SERB, New Delhi

Sir

I Prof. Prodyut Bhattacharya

herby certify that the research proposal titled Assessment of Climate resilience capacity of smart-city of Haryana: Gurugram City submitted for possible

funding by SERB, New Delhi is my original idea and has not been copied/taken verbatim from anyone or from any other sources. I further certify that this proposal has been checked for plagiarism through a plagiarism detection tool i.e. 06 % approved by the Institute and the contents are original and not copied/taken from any one or many other sources. I am aware of the UGCs Regulations on prevention of Plagiarism i.e. University Grant Commission (Promotion of Academic Integrity and Prevention of Plagiarism in Higher Educational Institutions) Regulation, 2018. I also declare that there are no plagiarism charges established or pending against me in the last five years. If the funding agency notices any plagiarism or any other discrepancies in the above proposal of mine, I would abide by whatsoever action taken against me by SERB, as deemed necessary.


Signature of PI with date 07/8/2023

Name / designation Professor

Prof. Prodyut Bhattacharya

University School of Environment Management
GGS Indraprastha University
University School of Environment Management
Block-A, Sector-16C, Dwarka, New Delhi-110078

Prof. Prodyut Bhattacharya



No.

210307



प्ररूप संख्या 5

(देखिए नियम 8)

जन्म प्रसाण - पत्र

हरियाणा सरकार स्वास्थ्य विभाग

जन्म और मृत्यु रजिस्ट्रीकरण अधिनियम, 1969 की धारा 12/धारा 17 के अधीन जारी किया गया जन्म प्रमाण-पत्र।

यह प्रमाणित किया जाता है कि निम्नलिखित सूचना जन्म के मूल रिकार्ड से ली गई है, जो (स्थानीय क्षेत्र) तहसील १

प्रस्ताव को पाए गए राज्य हरियाणा के रजिस्टर में है।

नाम एस/ए एमी

लिंग _____

जन्म तिथि 15-10-1992 रजिस्ट्रेशन संख्या 189

जन्म स्थान —८८१ रजिस्ट्रेशन तिथि ०६/०५/१६

माता का नाम _____
माता का युआईडी नं० (यदि कोई है) _____

पिता का नाम _____ **रामचल**

पिता का यूआईडी नं० (यदि कोई है) _____

माता पिता का स्थाई पता _____ २८.५७.२०२३ तिथि १२३ वर्ष/पर

जन्म तिथि (शब्दों में) पन्द्रह अक्टूबर बारह से बाले

Vide cmo letter 306/214/16
प्राप्ति संख्या ०१४८५-१५८
तिथि 06/5/16 वा ०८-१८/५/१६ जारी करने वाले विधिकारी के हस्ताक्षर
प्राप्ति संख्या ०१४८५-१५८ वा ०८-१८/५/१६ जारी करने वाले विधिकारी के हस्ताक्षर

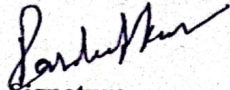
Scanned by TapScanner

Undertaking by the Fellow

I, PARDEEP KUMAR, Son/Daughter/Wife of Shri. RAMPHAL, resident of -
BHILWANI, HARYANA agree to undertake the following, If I am offered the SERB
N-PDF

1. I shall abide by the rules and regulations of SERB during the entire tenure of the fellowship.
2. I shall also abide by the rules, discipline of the institution where I will be implementing my fellowship
3. I shall devote full time to research work during the tenure of the fellowship
4. I shall prepare the progress report at the end of each year and communicate the same to SERB through the mentor
5. I shall send two copies of the consolidated progress report at the end of the fellowship period.
6. I further state that I shall have no claim whatsoever for regular/permanent absorption on expiry of the fellowship.

Date: 07-08-2023


Signature
(PARDEEP KUMAR)

Endorsement Certificate from the Mentor & Host Institute

This is to certify that:

- I. The applicant, Dr. Pradeep Kumar, will assume full responsibility for implementing the project.
- II. The fellowship will start from the date on which the fellow joins University/Institute where he/she implements the fellowship. The mentor will send the joining report to the SERB. SERB will release the funds on receipt of the joining report.
- III. The applicant, if selected as SERB-N PDF, will be governed by the rules and regulations of the University/ Institute and will be under administrative control of the University/ Institute for the duration of the Fellowship.
- IV. The grant-in-aid by the Science & Engineering Research Board (SERB) will be used to meet the expenditure on the project and for the period for which the project has been sanctioned as indicated in the sanction letter/ order.
- V. No administrative or other liability will be attached to the Science & Engineering Research Board (SERB) at the end of the Fellowship.
- VI. The University/ Institute will provide basic infrastructure and other required facilities to the fellow for undertaking the research objectives.
- VII. The University/ Institute will take into its books all assets received under this sanction and its disposal would be at the discretion of Science & Engineering Research Board (SERB).
- VIII. University/ Institute assume to undertake the financial and other management responsibilities of the project.
- IX. The University/ Institute shall settle the financial accounts to the SERB as per the prescribed guidelines within three months from the date of termination of the Fellowship.

Dated: 07.08.2023

Signature of the Mentor:

Pradyut Bhattacharya
Prof. Pradyut Bhattacharya, Professor

Name & Designation:

University School of Environment Management

GGS Indraprastha University

Block-A, Sector-16C, Dwarka, New Delhi-110078

Dated:

Sanjukta

Signature of the Registrar of University/Head of Institute

Seal of the Institution

Registrar
Guru Gobind Singh Indraprastha University
Sector-16C, Dwarka, New Delhi-110078



No.

1200

Enrolment No. 16/20/ME/008

जवाहरलाल नेहरू विश्वविद्यालय
नई दिल्ली

JAWAHARLAL NEHRU UNIVERSITY

NEW DELHI - 110067

PROVISIONAL CERTIFICATE

DOCTOR OF PHILOSOPHY

THIS IS TO CERTIFY THAT Pardeep Kumar

having successfully completed the requirements in terms of the ordinance relating to Ph.D degree has been declared eligible for the award of the Degree of **DOCTOR OF PHILOSOPHY**, notification No. 298/P/2023 dated 27-05-2023 of the University in the year 2023

The title of the
Ph.D Thesis is :

“Aquifer mapping of Middle Andaman using Geospatial,
Geophysical and Machine learning approach”

New Delhi

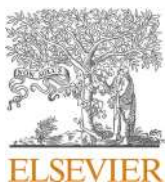
Date : 29.05.2023

Valid till the original degree is issued

Pardeep Kumar
Section Officer/Asstt./Dy. Registrar (Eval.)

 Section Officer (Evaluation Br-i)
Room No. 31, Admin. Block
Jawaharlal Nehru University
New Delhi-110067

*AKS
29/05/2023*



Impact of limestone caves and seawater intrusion on coastal aquifer of middle Andaman



Pardeep Kumar, Saumitra Mukherjee*

School of Environmental Sciences, Jawaharlal Nehru University, New Delhi, India

ARTICLE INFO

Keywords:

Limestone caves
Seawater intrusion
Hydrogeochemical investigation
Middle Andaman
Ionic ratios

ABSTRACT

Seawater intrusion has become a common problem in coastal and island aquifers with the rise in climate change that greatly affects the majority of developing countries. The island hydrology is very complex and associated with a unique set of environmental characteristics with the dynamic interaction of groundwater, surface water, and seawater. Further, Sea level rise, erratic rainfall, and over-extraction of groundwater triggered salt-water intrusion. A study on seawater intrusion and the effect of limestone caves on groundwater was carried out in middle Andaman using a combination of ionic ratios of major ions. A total of 24 samples and a reference sample from the sea were collected and analysed using ICP, spectrophotometer, and flame photometer. A combination of 10 ionic ratios Cl/HCO_3 , $\text{Ca}/(\text{HCO}_3 + \text{SO}_4)$, $(\text{Ca} + \text{Mg})/\text{Cl}$, Ca/Mg , Ca/Na , $\text{Cl}/(\text{SO}_4 + \text{HCO}_3)$, Ca/SO_4 , K/Cl , Mg/Cl , and SO_4/Cl was used to assess the dissolution of limestone minerals and the level of saltwater intrusion into groundwater. The geospatial method was used to extract and combine all the hydrogeochemical parameters and ionic ratios in the GIS platform. Durov plot was used for the interpretation of groundwater chemistry and the identification of natural processes controlling the hydrogeochemistry of the area. The dominance of $\text{Ca}-\text{HCO}_3$ and $\text{Na}-\text{HCO}_3$ was confirmed in 48% and 24% of the sample respectively. The equiline graph of chloride with other major ions showed the enrichment of alkali and alkaline earth metal salt in groundwater. Schoeller's diagram depicted the dominance of Cl , Ca , and the sum of CO_3 and HCO_3 in seawater near Mayabunder. The lower concentration of Na with respect to Cl (64%) and Ca (100%) showed the presence of a reverse ion exchange process. Further, the correlation matrix showed a strong relationship between Cl , K , Ca , and Na . The analysis of X-ray diffraction of the rock samples confirmed the presence of limestones such as Aragonite, Calcite, Chlorite, Chromite, Dolomite, Magnetite, and Pyrite in the study area. The integration of ionic ratios showed moderately affected and slightly affected saline regions in 44% and 54% of the region respectively. Finally, the role of tectonic activities and active lineaments connected to the sea was found to play a major role in the intrusion of seawater where interconnected faults created an opening for surface water to recharge groundwater leading to the deep aquifer.

1. Introduction

Groundwater is a prominent source of water for drinking, domestic, irrigation, and industrial usage in villages and cities in major countries (Adimalla et al., 2020; Gill et al., 2017; Subramani et al., 2005). The quantity and quality of groundwater are two significant aspects that sustain life on Earth. The insufficient availability of surface water to meet the increased water requirement has led to more dependency on groundwater to fulfil the demand for potable water supply. Therefore, quality of groundwater quality has become an important concern in many parts of the country. The source of groundwater contamination is

mainly through interaction with minerals, atmospheric precipitation, recharging water quality along with anthropogenic pollution coming from domestic, agricultural, and industrial activities (Li et al., 2021; Selvakumar et al., 2017; Tamta, 2003; Srivastava et al., 2012).

Seawater intrusion is one of the most common and widespread sources of groundwater contamination in Islands and coastal region of the world (Akshitha et al., 2021; Naily, 2018; Abdalla et al., 2015; Ahmed et al., 2013; Allow, 2012; Abdollahi-Nasab et al., 2010; Lee and Song, 2007; Post, 2005; Chidambaram et al., 2014). The identification and assessment of seawater intrusion are very important for the prevention and mitigation of contamination in aquifers. The seawater

* Corresponding author at: School of Environmental Sciences, Jawaharlal Nehru University, New Delhi 110067, India.
E-mail address: saumitramukherjee3@gmail.com (S. Mukherjee).

intrusion of an aquifer in island areas is a product of multiple salinization processes with different sources of water. Climate change such as erratic rainfall, accelerated sea-level rise, and the over-extraction of groundwater, increases the lateral movement of seawater into groundwater (Werner, 2010; Dragoni and Sukhija, 2008). Natural occurring rocks containing minerals like halite and anthropogenic effluents from households, agriculture, and industries are other possible causes of groundwater contamination (Rena et al., 2022; Singh et al., 2018; Rajkumar et al., 2010; Milnes, 2011; Jones et al., 1999; Custodio, 2010). The interaction of island aquifer with seawater is associated with several processes such as mineral dissolution or precipitation of salt/s, reverse ion exchange, and the reduction of sulphate which indicate the intensity of salinization in groundwater (Rani et al., 2021; Sakram et al., 2013; Elango and Kannan, 2007; Appelo and Postma, 2005). The groundwater intrusion is further controlled by several parameters like the difference in the rate of recharge and rate of discharge of freshwater in the aquifer, distance from the shoreline, hydraulic conductivity, aquifer depth, and the confining units in the aquifer which prevents the movement of saltwater vertically upward or inside the aquifer (Saidi et al., 2013; Barlow and Reichard, 2010).

The groundwater quality can be deteriorated by mixing only 2% of saltwater, studies have shown that 4% of mixing can lead to significant impairment of groundwater quality causing adverse environmental conditions. If the mixing of saltwater increases to 6%; it becomes unsuitable for human consumption but can be used by some industries (Srinivasamoorthy et al., 2013; Mondal et al., 2011; Custodio, 2010; Darnault and Godinez, 2008).

Since seawater intrusion is so complex and geochemically connected, it further requires a combination of indicators to study its occurrences in the islands (Bhagat et al., 2021; Sajil Kumar, 2016; Kazakis et al., 2016; Rajmohan and Elango, 2004).

Seawater intrusion has been investigated or monitored using approaches like geophysical, geochemistry, and groundwater flow models. Age, transport pathways, and seawater wedge theory can be identified through isotopes and water chemistry (Mohanty and Rao, 2019; Ganyaglo et al., 2017; Werner and Simmons, 2009; Vengosh, 2003; Louvat et al., 1999; Naidu et al., 2013). Since these above-stated studies are very costly, the study of ratios of major ion concentration is the only feasible way for saline water delineation.

Studies have shown that freshwater has a dominance of major ions such as calcium, magnesium, bicarbonates, sulphates, chloride, sodium, and potassium while seawater majorly contains chloride and sodium ions only, thus, intrusion of seawater inland aquifers may be detected by analyzing the increase in these ions in the aquifers (Srinivasamoorthy et al., 2013; Mondal et al., 2011; Todd and Mays, 2004; Bear et al., 1999). The concentration of these ions changes from the recharging area to discharging area of aquifers connected to the sea and the ionic ratios of major ions change at the interaction of groundwater and seawater through ion-exchange processes and oxidation-reduction reactions (Naily, 2018; Marimuthu et al., 2005; Stoessell, 1997; Gimenez and Morell, 1997). As a result, a lot of ionic ratios have been proposed to identify salinization in coastal areas; such as Na/Cl, Ca/Mg, Ca/Na, and Cl/(HCO₃ + SO₄) (Asare et al., 2021; Carol and Kruse, 2012; Marimuthu et al., 2005; Lee and Song, 2007; Panno et al., 2006; Gimenez and Morell, 1997; Vengosh, 2003). The change in the ratio of the molar concentration of ions associated with seawater intrusion may give dissimilar results. Therefore, an integration of their result is used to arrive at a consistent decision. The current research has also included the hydrogeological assessment of aquifer, spatial and statistical analysis of ionic ratios, correlation analysis of major ions, major hydro-chemical processes, X-ray diffraction of rocks, and finally inter-correlation of seawater intrusion with active faults and groundwater level of middle Andaman.

1.1. Study area

Middle Andaman is part of the Andaman and Nicobar group of islands system in the southeast part of the Indian subcontinent. The study area is a part of the Andaman series that lies between North Andaman and South Andaman connected through National Highway NH-223. The geographical extent of middle Andaman is 12°24'19.984" E to 12°55'38.788" E latitude and 92°48'15.417" N to 92°58'49.854" N longitude (Fig. 1). Most of the region (>80%) comprises a range of open to dense forests. The forest of the region is classified as moist deciduous and tropical evergreen forest. The vegetation of the Andaman Islands is similar to Malaysian islands and Burmese islands in comparison to the mainland of the Indian subcontinent. The biota species of the region belong to marine habitats. The island's beaches are the nesting sites of sea snakes and sea turtles (Ganeshaiah et al., 2019; Rao, 1996).

1.2. Geology of the area

Middle Andaman is part of the outer arc of the Arakan Yoma range that formed the main chain of Andaman and Nicobar Islands. It is made of sedimentary rocks mainly from marine deposits (Singha et al., 2019; Kumar, 1981; Jafri et al., 1993; Srinivasan, 1979). Limestone caves are formed in lithified rocks of aggregated particulate matter (Sankaran, 1998). The location of caves is controlled either by the source of sediments or their transformation into rocks (Gulam Rasool et al., 2022; Ford and Cullingford, 1976). Most limestone caves are formed by either underground drainage/erosion or sea cliffs or sea erosion of rocks (Challinor, 1967). Out of 384 caves found on the island, 61.5% are inland and 38.5% are sea shore, among inland caves 86% are underground, 1% are at the origin of streams, and the rest are above the ground either on inland cliffs or inland hills. They have very fragile ecosystems; their fauna is too sensitive to humidity, temperature, and light (Fig. 2).

The study area lies in earthquake and tsunami-prone areas which causes occasional damage to these caves. The impact on caves was first documented in 2004 earthquakes in both middle Andaman and North Andaman. It caused structural changes such as opening, closing, partial closing, narrowing, or widening of many existing caves. It was found that more damage had happened to caves that were above the ground than the caves below the ground (Manchi and Sankaran, 2009). The limestone in shallow water was found to be associated with the Mithakari mélange group of the Paleocene-Eocene age. Mélange itself is self-explanatory in indicating that there was a mixing of the lithological units due to tectonic activities. These mélanges when deposited as unconformity forms a suitable formation for groundwater exploration. Mithakari or Baratang Formation has two other members of the rock chain called Tugapur Limestone/ Berma Dera and Karmatang sandstone. Limestones i.e., lensoid and folded structures are in contact with sandstone units between Rangat and Mayabandar of middle Andaman. Berma Dera sector has an area of 4000 m² and a reservoir of approximately 10,000 tons per meter depth of limestone whereas the Tugapur sector has approximately 8500 tons per meter depth in a surface area of 3000 m². In the Buddha Nala, a reservoir of approximately 12,000 tons per meter depth of limestone is present on the surface of 5000 m² (Bandopadhyay and Carter, 2017).

1.3. Hydrology map of the area

Island receives abundant rainfall of approx. 3000 mm per annum but the undulating terrain with steep slopes, porous soil stratum, and its proximity to the sea leads to a loss of 75% of the annual rainfall. Also, the abundance of sedimentary rocks (70%) and the presence of clay minerals contribute to the unfavourable condition for rainfall percolation to sub-surface water (Fig. 3). Therefore, we are getting aquifers unsuitable for groundwater storage in both shallow and deep horizons. On the contrary, the presence of 15% coral rags or limestone formation

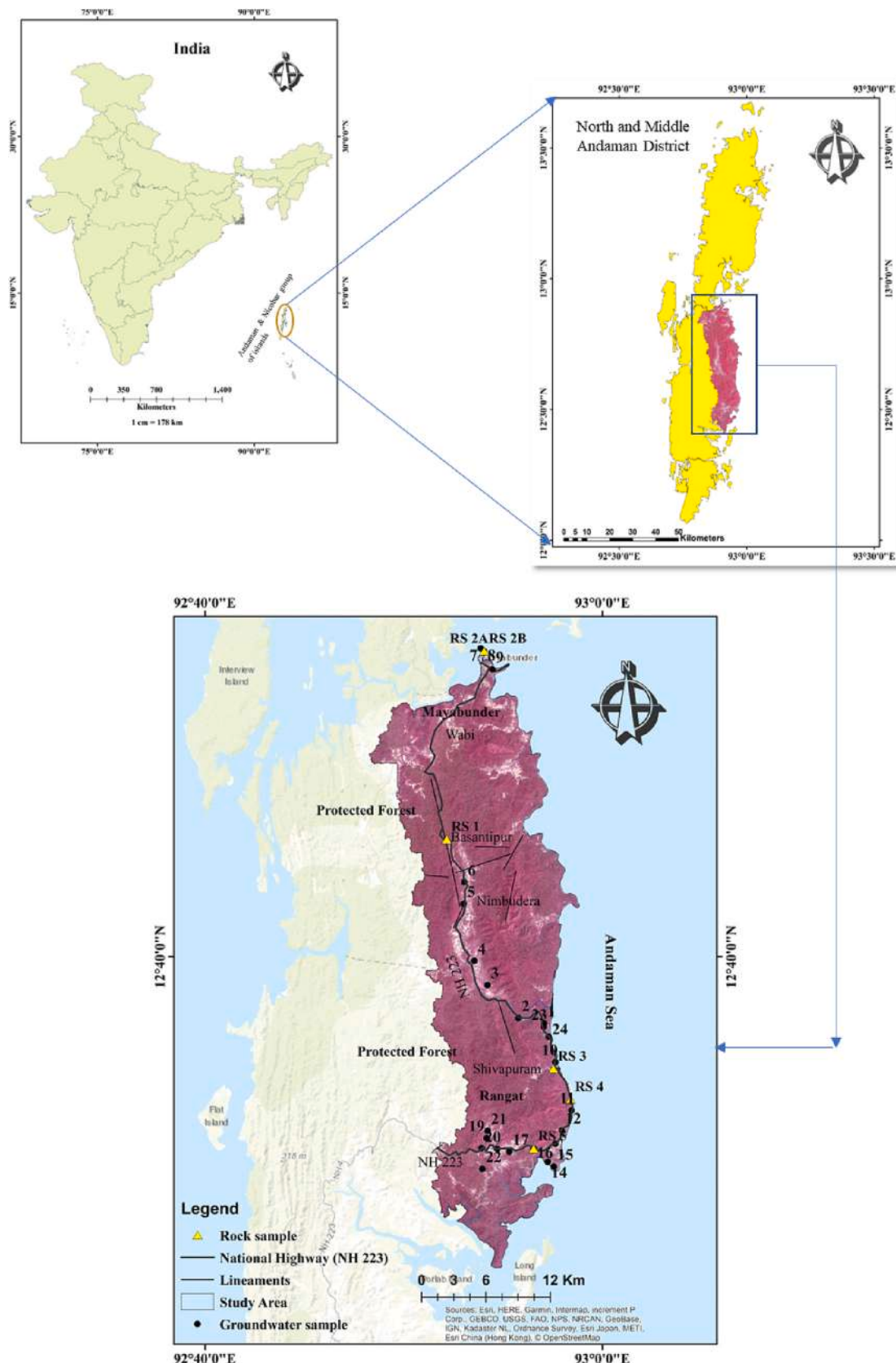


Fig. 1. Spatial map of the Study area showing the location of Rock and water sampling.

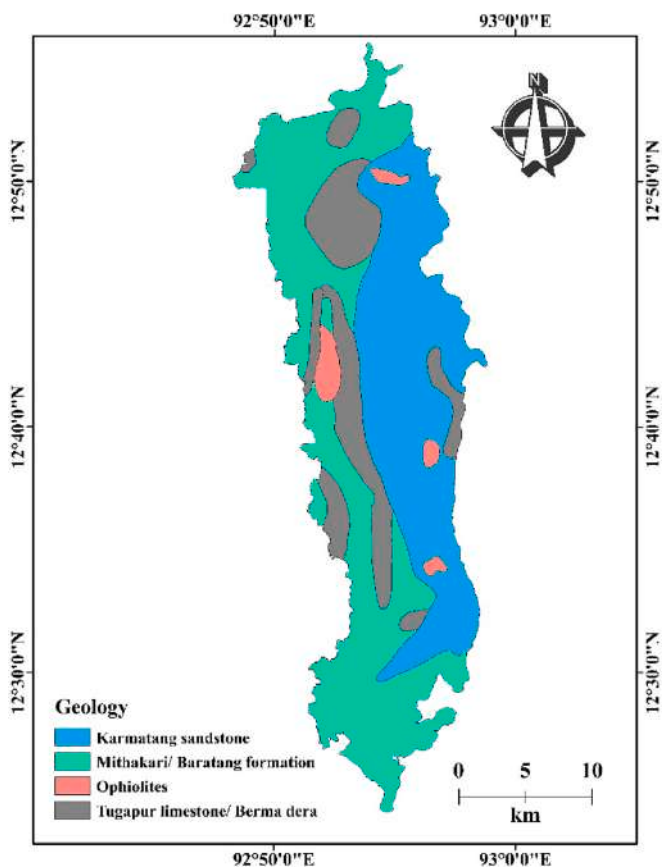


Fig. 2. Geology map of the area (Bandopadhyay and Ghosh, 2015).

and the remaining 15% of igneous rocks provide favourable conditions for a sustainable aquifer in the region (Mukherjee, 1986; Bandopadhyay and Carter, 2017). The ophiolite rocks of igneous origin (intruded in sandstone formation) have higher aerial fracture density than sedimentary rocks. The fracture density has greater control over drainage density for groundwater development and is associated with the presence of good aquifers. The weathered sandstone rocks may also be a source of water but of low transmissivity (Roy et al., 2005).

2. Methodology and data analyses

2.1. Groundwater sampling

Groundwater sampling points have been chosen based on surface manifestation from satellite images as well as the accessibility of the groundwater site. A total of 25 samples were collected from different parts of middle Andaman of which 24 samples were from groundwater and one sample from seawater as a reference. Most of the samples were collected from an open well except one sample from spring water (Sample no. 11).

The samples were collected in polypropylene plastic bottles for cation and anion analysis separately. The bottles were rinsed from the sampling water at least three times before the collection of samples. Also, precautions were taken to minimize the impact of the material of the pipe and biases on the representative sample. The groundwater samples were geolocated using Garmin GPS (global positioning system). The parameters like pH, electrical conductivity (EC), and total dissolved solids (TDS) were recorded using handheld probes. The water samples collected for cations were preserved by adding a few drops of Concentrated HNO_3 and stored at a cool temperature (4°C). Further, samples were filtered through 0.45 m-pore filter paper before analysis.

2.2. Groundwater parameter analysis

Major anions and major cations analysis were done in the laboratory using standard methods given by the American public health association (APHA, 2005) and (Diatloff and Rengel, 2001). Sodium, Potassium, and Calcium were measured using the Elico flame photometer (Elico CL-378) and Magnesium was measured using ICP-OES (Agilent 5110). Major anions such as Carbonate, Bicarbonate, and Chloride were analysed by using the titrimetric method whereas Nitrate, Phosphate, and Sulphate were analysed using UV/Vis spectrophotometer (Perkin Elmer-Lambda 35) with TRI method, Malachite Green method, and Barium Sulphate method respectively (APHA, 2005). pH, EC, and TDS were measured on the sampling site using a probe "multiparameter test 35 series".

The accuracy of groundwater parameters was calculated using charge balance error (CBE). It assumes the neutrality of charge in natural water (Domenico and Schwartz, 1997).

$$CBE = \frac{\sum C - \sum A}{\sum C + \sum A}$$

where $\sum C$ and $\sum A$ are the sums of cations and anions (meq/L) respectively.

The value of Charge Balance Error (CBE) was found in the range of $\pm 5\%$ in all the water samples. The Average, minimum, Maximum and standard deviation of CBE of all the samples was found to be 0.02, -0.42 , 0.24, and 0.19 respectively. As all the samples were within the acceptable limit, water parameters were assumed to be good for further analysis.

Firstly, major cations and major anions were converted from mg/L to meq/L to remove the effect of charge in the calculation. A total of ten ionic ratios were taken to estimate the seawater intrusion in the study area (Klassen and Allen, 2017; Lee and Song, 2007; Bear et al., 1999; Nadler et al., 1980; Rosenthal, 1988). These groundwater chemical ionic ratios were found to be Na/Cl , Na/Ca , Mg/Cl , Ca/Mg , $\text{Cl}/(\text{SO}_4 + \text{HCO}_3)$, K/Cl , SO_4/Cl , Cl/HCO_3 , $(\text{Ca} + \text{Mg})/\text{Cl}$, and $\text{Ca}/(\text{HCO}_3 + \text{SO}_4)$.

Further, the Base exchange index (BEX) was calculated to distinguish the undergoing process of salination or recharging/freshening (Stuyfzand, 2008). A positive value of BEX indicates refreshing water, a negative value represents salination and a zero value means the absence of base exchange.

$$\text{BEX} = \text{Na} + \text{K} + \text{Mg} - 1.0716 \times \text{Cl} \text{ (meq/L)}$$

The equiline graph is generated using MS-Excel 2019 whereas Durov and Schoeller's diagram was plotted using AqQA version 1.1.1. The earthquake data was taken from the USGS earth explorer from 1990 to 2022 with a Richter scale of >5 .

ArcGIS 10.8 was used for generating the spatial map of ionic ratios using the inverse distance weightage method (IDW). Further maps were integrated using the spatial overlay technique.

3. Result and discussion

3.1. Evaluation of water quality parameters

Table 1 is a summary of the water quality parameters (meq/L) comprised of the minimum, maximum, mean, median, and standard deviation of the major ions. It was observed that the electrical conductivity value of water samples varied from $100 \mu\text{S}/\text{cm}$ to $1500 \mu\text{S}/\text{cm}$ with an average value of $548 \mu\text{S}/\text{cm}$. 60% of samples were found above $500 \mu\text{S}/\text{cm}$. Chloride concentration varied between 0.98 meq/L to 270.55 meq/L with an average value of 12.47 meq/L . Cl and EC are two parameters that are universally accepted indicators of seawater intrusion. The high value of Cl and EC is indicative of seawater intrusion. In our study area, a high value of chloride and EC were found in the samples taken near the coast. Chloride is the single parameter found in seawater

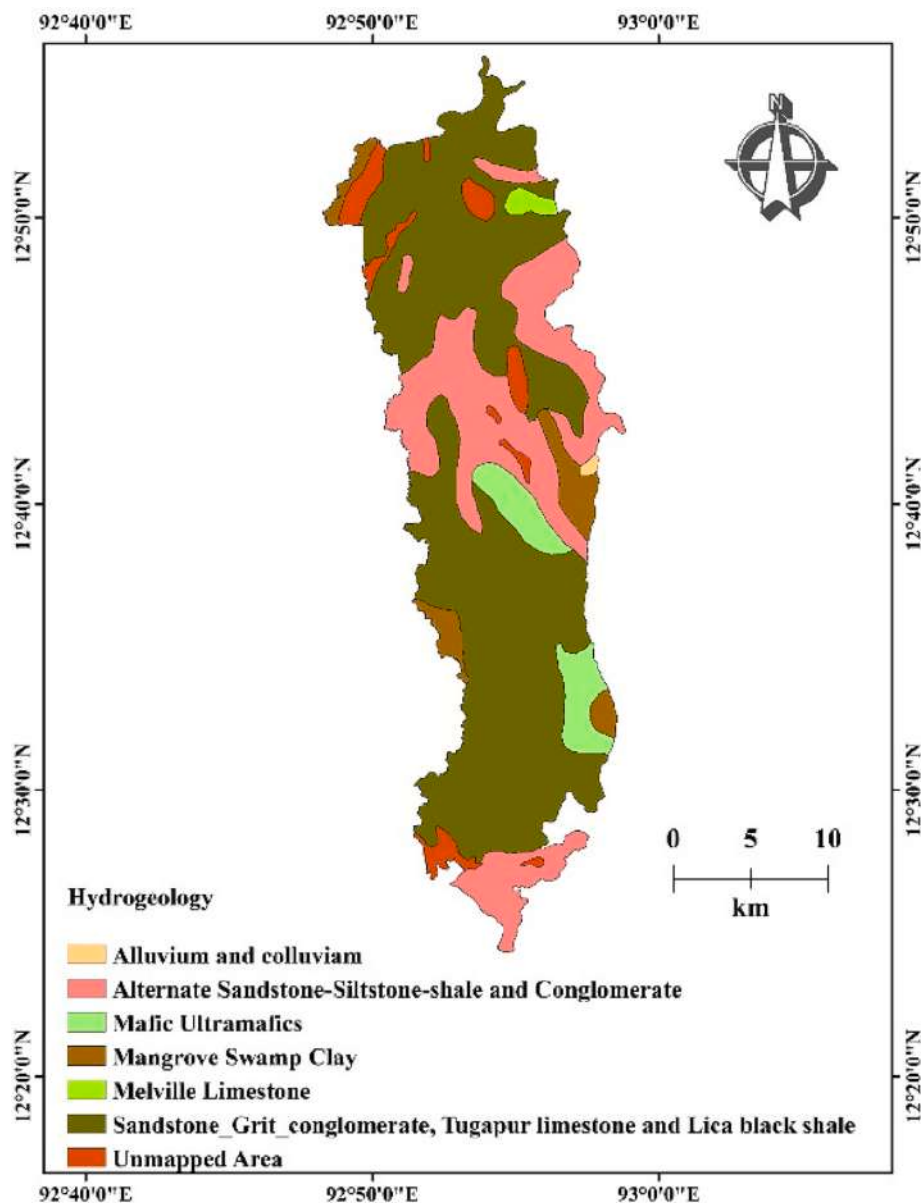


Fig. 3. Hydrology map of the study area.

Table 1
Statistical distribution concentration of major ions (meq/L) of middle Andaman.

	pH	EC	TDS	Na	K	Ca	Mg	CO ₃	HCO ₃	SO ₄	PO ₄	NO ₃	Cl	F
Mean	7.45	548	284.8	4.62	0.28	12	1.13	0.9	3.53	0.02	0.18	0.02	12.47	0.33
Min	6.2	100	30	0.13	0.01	0.5	0.29	0	1.28	0	0.01	0	0.98	0.07
Max	8.5	1500	740	87.45	5.09	175.12	2.09	1.7	5.53	0.14	0.38	0.05	270.55	1.43
S.D.	0.63	335.56	167.36	17.28	1	34.12	0.54	0.51	1.34	0.04	0.1	0.01	53.77	0.27

due to its conservative nature. It shares >55% of TDS in seawater and that makes it a very sensitive indicator of contamination of seawater in groundwater (Nadler et al., 1980; Moujabber et al., 2006; Jones et al., 1999; Panno et al., 2006).

It was found that the water sample taken from the sea, near Mayabunder Jatti (sample no. 25) also shown in Fig. 4 had a high concentration of Calcium (175.12 meq/L), Sodium (87.45 meq/L), Potassium (5.01 meq/L), Chloride (270 meq/L) and Sulphate (0.09 meq/L).

3.2. Schoeller diagram

In addition to the summarised data (Table 1), the Schoeller diagram illustrated the relative concentrations (meq/L) of major ions in each sample. It allowed to accommodate a large number of chemical constituents for comparison and investigation. As per Fig. 4, the pattern of ions obtained from different sources of groundwater indicated that the seawater sample (SEA1) showed the dominance of chloride and calcium ions. While the lower concentration of sodium with respect to chloride and calcium ions showed the presence of reverse ion exchange

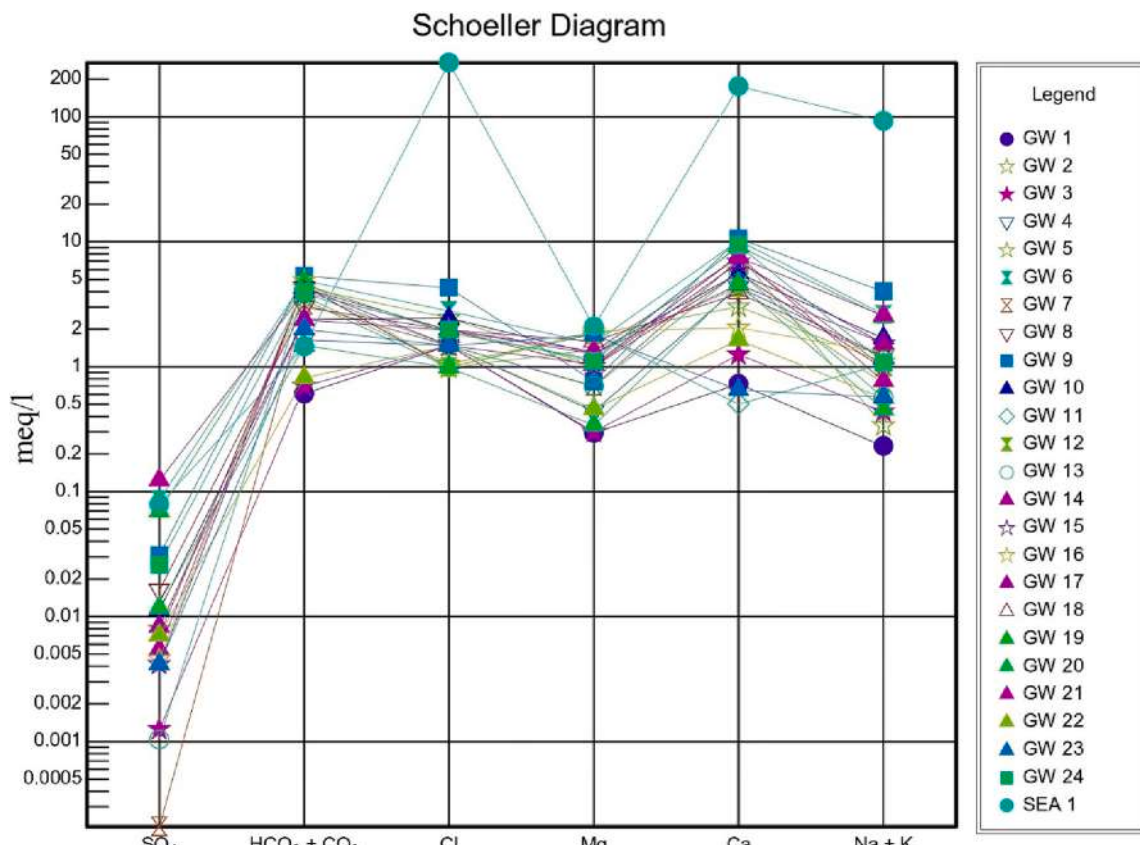


Fig. 4. Schoeller diagram of middle Andaman.

governing between sodium (from seawater) and calcium from limestone minerals. It was also found that bicarbonate has a higher value in all the samples except seawater whereas calcium was found dominant in all the samples including seawater. The chloride value (meq/L) was found higher value than sodium in 76% of the samples. The loss of sodium ions is probably due to the replacement of the sodium ion exchange process in groundwater. We may infer the possibility of seawater intrusion in the area.

3.3. Equiline graphs of Chloride with major ions

The concentrations of Chloride were plotted against the major ions (Na, Ca, Mg, K, SO₄, NO₃, HCO₃) and EC (Fig. 5), and the least r square value of linear regression was determined. Stoessell (1997) explained the good linear coefficient of determination between the Cl and major ions like Na, Ca, and K showed a possible mixing of freshwater with single-brine chemistry. The intrusion of seawater provided the replacement of Sodium with the same milliequivalent concentration of calcium and carbonate with chloride (Fig. 5a, f). Similarly, the analysis of seawater depicted a higher concentration of Potassium and chloride indicating the seawater influence in the aquifers. The equiline graphs (Fig. 5a, d, c) of potassium, calcium, and sodium showed a strong relation with chloride possibly due to the interaction of seawater with limestone and aquifers of the island. On the other hand, the equiline graph between EC and chloride did not show any linear correlation with each other. The dominance of EC over chloride and equal concentration (meq/L) of sodium and chloride suggested enrichment evaporation, NaCl aerosol, or direct mixing of seawater. The dominance of bicarbonate over chloride shows the weathering of carbonate minerals from limestone deposition in the study area. The dominance of chloride over nitrate and sulphate wipes out the possibility of anthropogenic influence in the aquifer. The highest value shown in the graph is the seawater

sample from the coast of Mayabunder in the middle Andaman (Umarrani et al., 2019; Lakshmanan et al., 2003).

3.4. Spatial map of ionic ratio

The summarised table of the mean, minimum, maximum, and standard deviation of the ionic ratios is shown in Table 2.

Equiline graphs and Schoeller showed that seawater intrusion is the major cause of low groundwater quality in most of the island's aquifers. The salinity caused by seawater intrusion has been associated with a lower value of sodium than chloride in groundwater compared to seawater (Vengosh, 2003). In the case of saltwater intrusion, the ratio of Na/Cl declines in saline groundwater, and that is lower than that of marine water (<0.86) (Schoeller, 1967). This is because when seawater intrudes into groundwater, a chemical exchange process takes place between rocks and seawater (Mercado, 1985; Nadler et al., 1980) and Calcium ions replace sodium ions resulting in depletion in sodium ion concentration but no change in chloride concentration. The ratio of Na/Cl ranges between 0.08 and 1.51 with an average value of 0.67. It was found that 68% of samples had Na/Cl ratio <0.86. It was also observed that the contamination zone of the groundwater was higher in the 5 km spatial range from the shoreline. Further, 24% of samples showed contamination which indicated the possibility of anthropogenic influences where the ratio of Na/Cl was >1 (Vengosh, 2003).

When seawater intrudes; the ion exchange process takes place between alkali and alkaline earth metals. Na ion replaces Ca and Mg ions in the aquifer from carbonate minerals leading to the enrichment of Calcium, Magnesium, and bicarbonate ions into aquifers. The ratio of the sum of alkaline earth metal to chloride was found higher in groundwater compared to seawater. The ratio (Ca + Mg)/Cl was found in the range of 0.65 to 7.99 and an average value of 3.68 and a standard deviation of 1.83 (Table 2). There was an enrichment of Sulphate in seawater, an

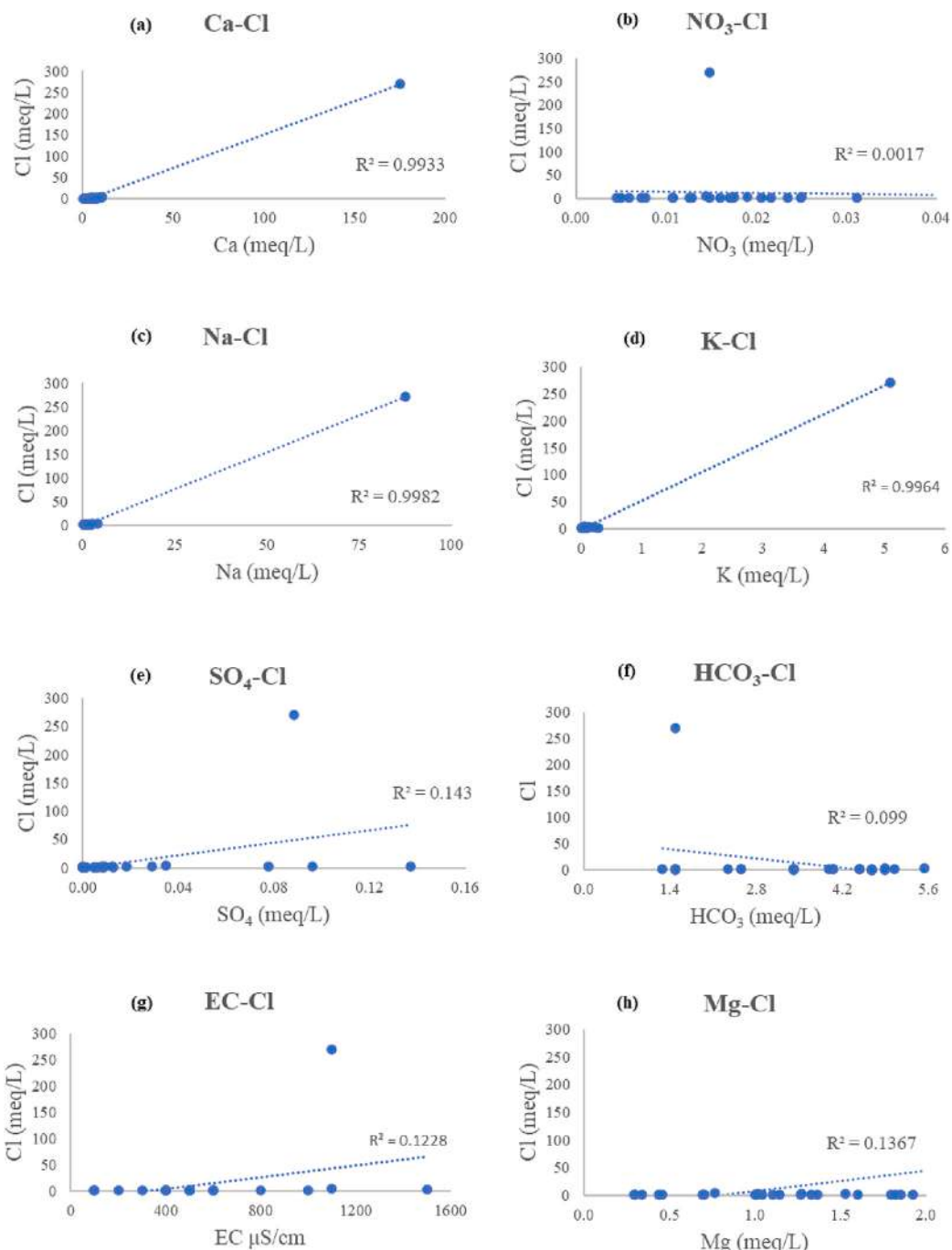


Fig. 5. Equiline graphs of chloride with major ions (a) Ca-Cl (b) NO₃-Cl (c) Na-Cl (d) K-Cl (e) SO₄-Cl (f) HCO₃-Cl (g) EC-Cl (h) Mg-Cl.

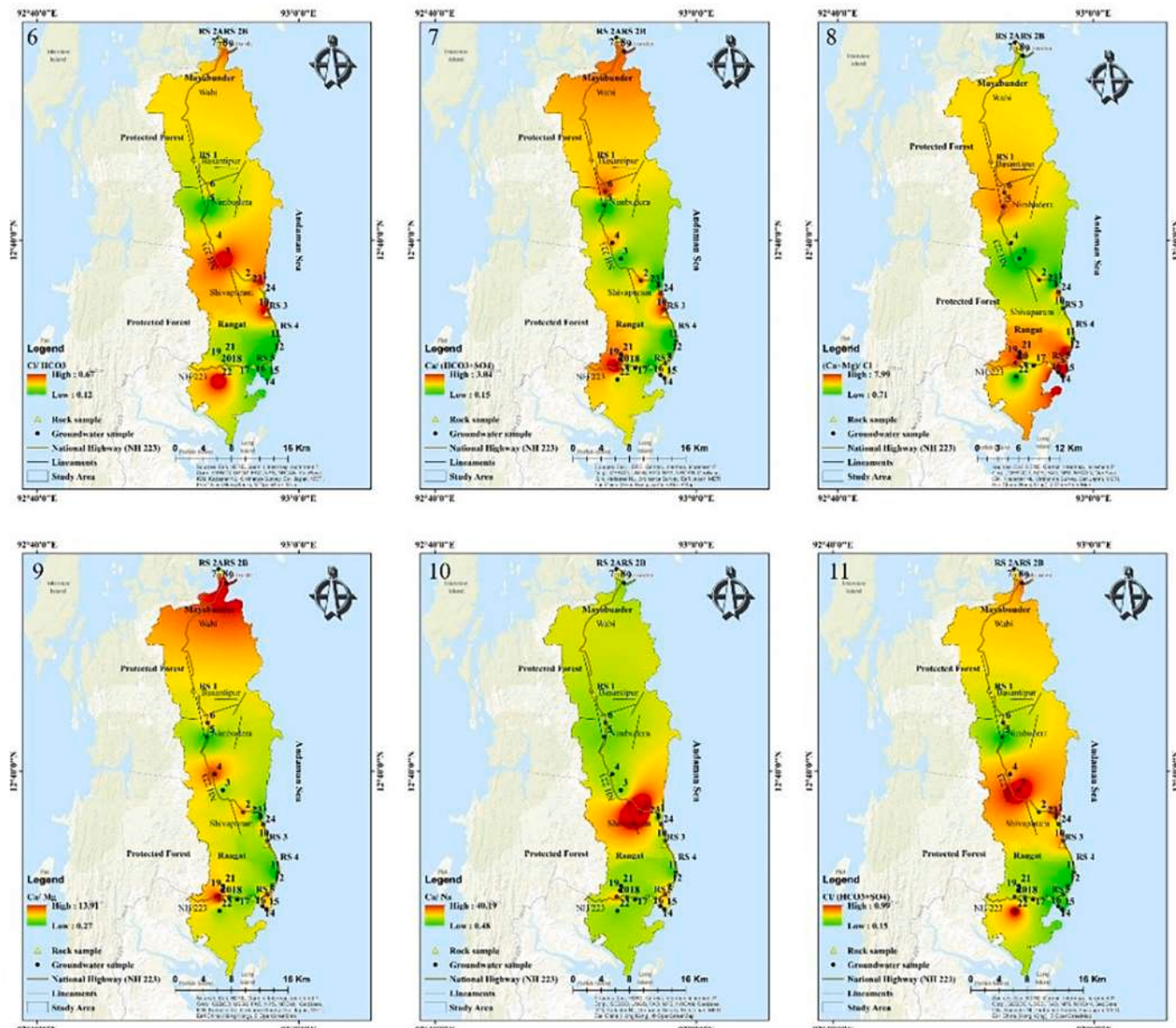
Table 2

Statistical distribution of ionic ratios of major ions of middle Andaman.

	EC	Ca/Mg	BEX	Cl/(HCO ₃ + CO ₃)	Ca/(HCO ₃ + SO ₄)	Mg/Cl	Ca/Na	Na/Cl	Cl/ HCO ₃	K/Cl	(Ca + Mg)/Cl	SO ₄ /Cl	Ca/SO ₄
Mean	548	8.92	-7.34	5.05	5.80	0.71	6.36	0.67	4.53	0.67	3.68	0.01	767.35
min	100	0.27	-195.3	0.15	0.15	0.01	0.48	0.08	0.12	0.08	0.65	0	54.31
max	1500	83.93	2.17	115.63	111.04	1.96	40.19	1.51	105.75	1.51	7.99	0.07	1490
SD	335.56	16.06	39.17	23.04	21.94	0.54	7.76	0.39	21.09	0.39	1.83	0.02	1123

interaction of seawater and groundwater may have led to the dissolution of calcium sulphate into the saline water. The higher concentration of ratio of calcium and sulphate indicates the seawater intrusion in the coastal aquifer (Fig. 12). For the ratio of Ca/SO₄, ratio values varied

between 54.31 and 1490 with a standard deviation of 1123. A ratio >1 indicates the intrusion of seawater into groundwater. EC is also a good indicator of saltwater intrusion and 16% percent of samples have found EC value >1000 (Lee and Song, 2007). This also confirmed the



Figs. 6–15. Represent the spatial map of ionic ratios: Cl/HCO_3 , $\text{Ca}/(\text{HCO}_3 + \text{SO}_4)$, $(\text{Ca} + \text{Mg})/\text{Cl}$, Ca/Mg , Ca/Na , $\text{Cl}/(\text{SO}_4 + \text{HCO}_3)$, Ca/SO_4 , K/Cl , Mg/Cl , and SO_4/Cl respectively.

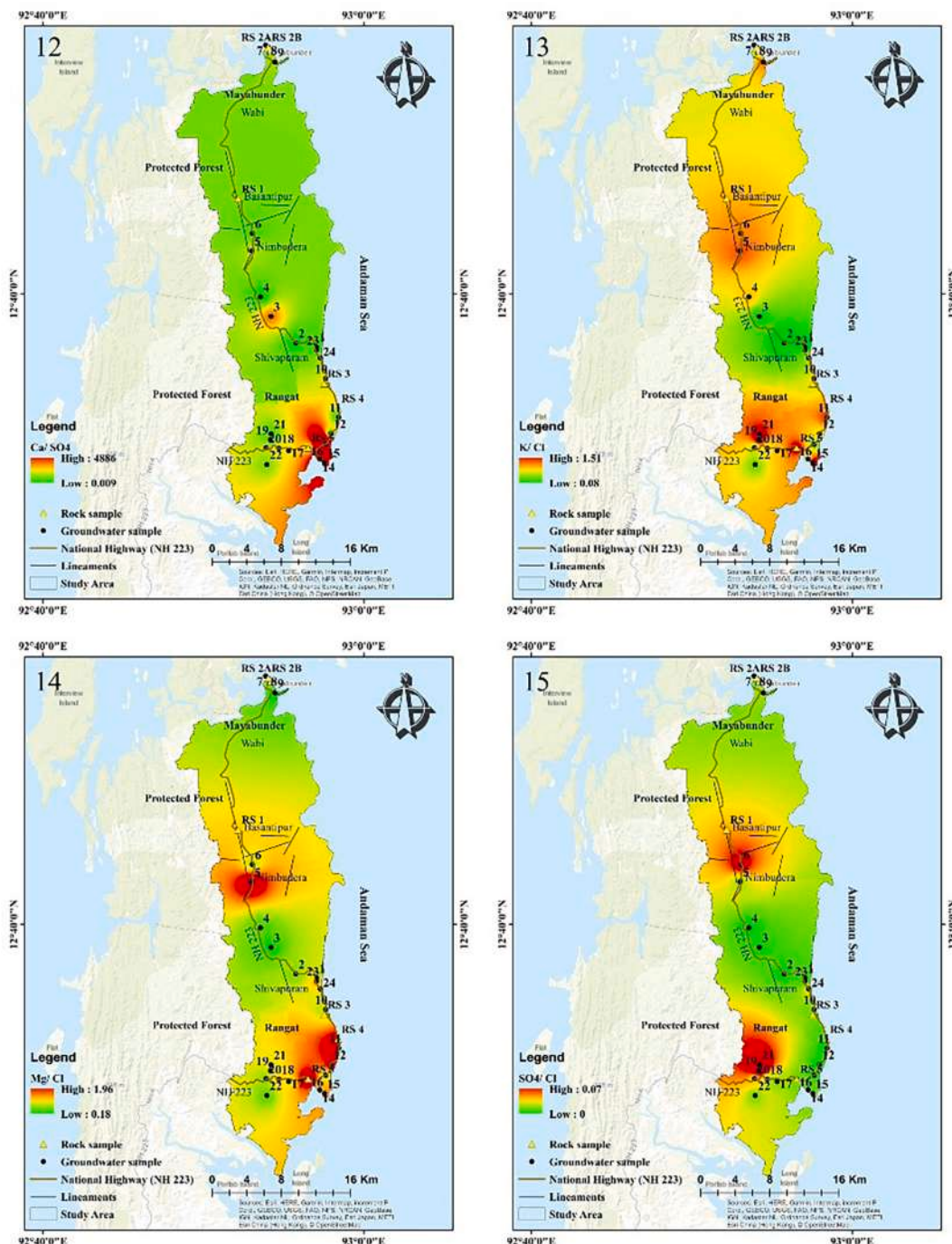
possibility of calcium dissolution from limestone caves and governs calcium enrichment in the coastal aquifer through to ion exchange process.

Fresh groundwater is usually abundant with both carbonate and bicarbonate ions and a small number of chloride ions as compared to seawater (Bear et al., 1999; Todd and Mays, 2004). Simpson ratio ($\text{Cl}/(\text{HCO}_3 + \text{CO}_3)$) can also be used to delineate the seawater contamination zone, as more chloride ions in groundwater contributed to the higher value of Simpson's ratio value. Freshwater is abundant with carbonate and bicarbonate ions giving a lower value of Simpson's ratio. In this way, the groundwater is classified into five classes; a ratio value <0.5 indicates good quality fresh water (0%), a value from 0.5 to 1.3 indicates slightly contaminated (36%), from 1.3 to 2.8 is moderately contaminated (60%), from 2.8 to 6.6 is injuriously contaminated (0%), and >6.6 is highly contaminated (0%). In the study area, no samples have values <0.5 and >2.8 which indicated slightly to moderately contaminated groundwater.

In coastal aquifers, the interaction of seawater-freshwater causes the

loss of sodium ions as it was replaced by calcium ions. The enrichment of calcium is a clear indicator of seawater intrusion. The source of calcium can be either leaching from surface soil or the dissolution of limestone occurring in the study area (Naily, 2018; Carol and Kruse, 2012; Mousjabber et al., 2006; Klassen et al., 2014). The value of $\text{Ca}/(\text{HCO}_3 + \text{SO}_4)$ lied between 0.15 and 111.04 with an average value of 5.80 (Fig. 7). The variation for K/Cl , Mg/Cl , and SO_4/Cl was found between 0.08 and 1.51, 0.01–1.96, and 0–0.07 respectively (Figs. 13, 14 & 15).

The value of $\text{Ca}/(\text{HCO}_3 + \text{SO}_4) > 1$ with low K/Cl , Mg/Cl , and SO_4/Cl also demarcated seawater intrusion in the coastal aquifer (Jones et al., 1999). 72% of the samples have found the ratio of $\text{Ca}/(\text{HCO}_3 + \text{SO}_4) > 1$ whereas 68% of the samples had a lower Na/Cl ratio (<0.86). Not a single sample was found to have a low ratio of K/Cl (<0.02). As seawater intrudes into groundwater, the absorption of K^+ on clay particles occurs due to silicate weathering, which decreases the concentration of K^+ in groundwater (Vengosh, 2003). The ratio of Mg/Cl varies from 0.01 to 1.96. Both sulphate and bicarbonates have a higher concentration in groundwater than in seawater. It was observed that 76% of the samples



Figs. 6-15. (continued).

had $\text{Ca}/(\text{HCO}_3 + \text{SO}_4) > 1$ and also had an Mg/Cl ratio < 1 . This indicated the increase in Cl concentrations in coastal aquifers. Similarly, the ratio of $\text{SO}_4/\text{Cl} < 1$ also indicates the intrusion of seawater in groundwater aquifer, it was observed that the samples having a ratio of $\text{Ca}/(\text{HCO}_3 + \text{SO}_4) > 1$ also had a ratio of $\text{SO}_4/\text{Cl} < 1$ (Abdalla, 2016).

The ratio of $\text{Ca}/\text{Na} > 1$ indicates the saltwater intrusion in groundwater (Gimenez and Morell, 1997) (Fig. 10). For the study area, the value of Ca/Na is distributed between 0.48 and 40.19 with an average value of 6.36; 96% of the samples may be contaminated with saltwater intrusion ($\text{Ca}/\text{Na} < 1$). The cation exchange process between seawater and calcium-rich rocks is the main cause of the enrichment of calcium ions in coastal aquifers. The Ca/Mg ratio varies from 0.27 to 80.93 with an average value of 8.92 and a standard deviation of 16.06 (Fig. 9). The

higher ratio of Ca/Mg again indicates the enrichment of calcium ions during the interaction of aquifers with seawater.

3.5. Correlation matrix of major ions

As per Table 3, a correlation matrix of major cations and anions was generated to understand the correlation of ions with each other. The green and red colors denote positive correlation and negative correlation. The dark and light shades represented strong correlation or weak correlation respectively.

The correlation matrix has shown that Total Dissolved Solid (TDS) was strongly correlated with EC. Carbonate, bicarbonate, and sulphate are positively correlated to EC and TDS. Carbonate was strongly

Table 3

Correlation matrix of major ions.

	pH	EC	TDS	Na	K	Ca	Mg	CO ₃	HCO ₃	SO ₄	PO ₄	NO ₃	Cl	F
pH	1.000													
EC	0.581	1.000												
TDS	0.577	0.995	1.000											
Na	0.100	0.381	0.405	1.000										
K	0.084	0.346	0.370	0.997	1.000									
Ca	0.119	0.402	0.427	0.997	0.996	1.000								
Mg	0.466	0.515	0.529	0.381	0.356	0.364	1.000							
CO ₃	0.626	0.502	0.513	-0.011	-0.037	-0.006	0.744	1.000						
HCO ₃	0.455	0.533	0.532	-0.291	-0.317	-0.264	0.359	0.469	1.000					
SO ₄	0.375	0.782	0.764	0.404	0.380	0.416	0.293	0.165	0.153	1.000				
PO ₄	0.352	0.056	0.062	-0.274	-0.258	-0.259	0.167	0.171	0.283	-0.034	1.000			
NO ₃	0.047	0.072	0.072	-0.043	-0.019	-0.025	0.038	-0.029	0.281	-0.073	0.269	1.000		
Cl	0.085	0.350	0.375	0.999	0.998	0.997	0.370	-0.019	-0.315	0.378	-0.278	-0.042	1.000	
F	0.167	0.534	0.548	0.858	0.860	0.877	0.266	0.036	-0.111	0.455	-0.089	0.016	0.853	1.000

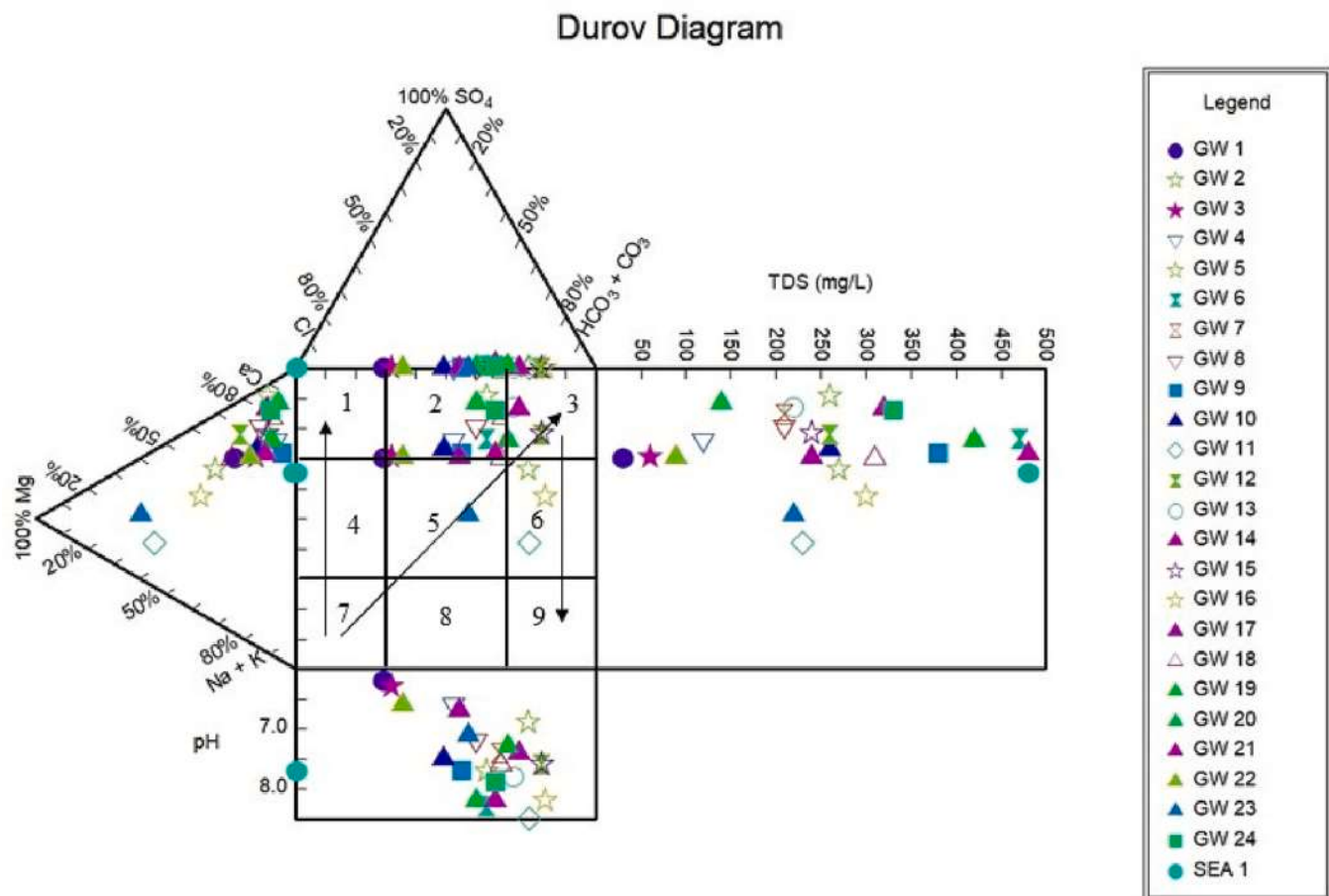


Fig. 16. Durov plot of the area.

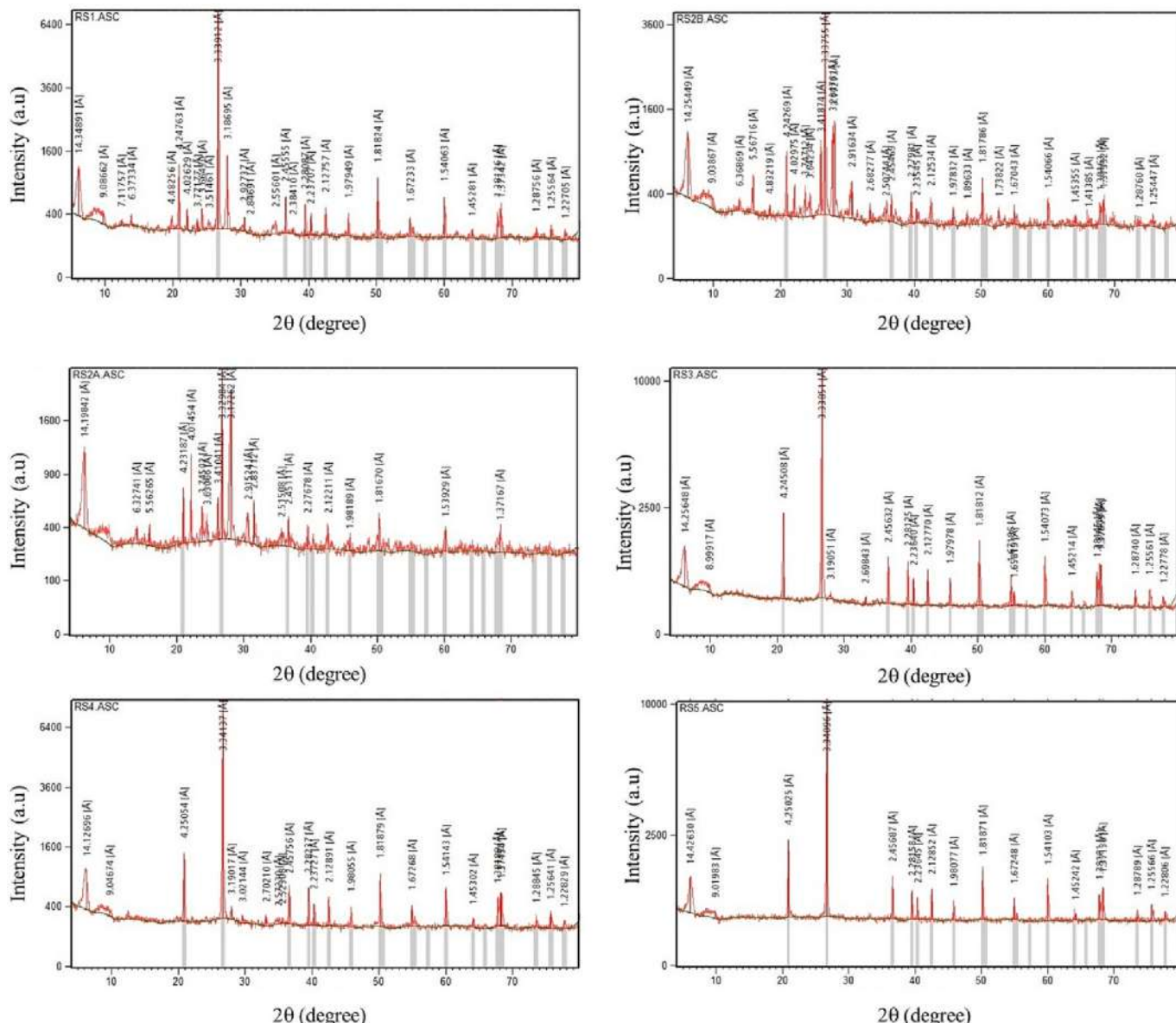
positively correlated to magnesium; and sodium, potassium, and calcium are strongly correlated to each other. This may confirm the dissolution of limestone with the interaction of Na from seawater intrusion and the release of K ions from weathering of rocks containing potassium.

Both chloride and fluoride are strongly correlated to sodium, potassium, calcium, and with each other. This strongly advocates the interaction of seawater with limestone minerals releasing calcium, potassium, and fluoride in the groundwater. The strongly correlated ions also revealed the same source or process (seawater and limestone) for their enrichment in groundwater.

3.6. Durov plot

The Durov diagram is another graph used to depict the water chemistry of water samples (Fig. 16). In advance of the Piper diagram, it uses other parameters pH and TDS for the water chemistry interpretation. Similar to the piper plot, it also uses the percentage of major cations and anions (meq/L) in the water samples. It calculates the percentage of

each cation group to the whole sum of the concentration of major cations- calcium, magnesium, and the sum of sodium and potassium. The percentage of each anion group is calculated with the summation of the concentration of sulphate, chloride, and the sum of both carbonate and bicarbonate. Lloyd and Heathcoat (1985) classified water into three major processes, ion exchange, simple dissolution or mixing, and reverse ion exchange. These processes are represented with the arrows (7 to 1) for ion exchange, (7 to 3) for simple dissolution or mixing, and (3 to 9) for reverse ion exchange. Most of the samples depicted an ion exchange process and simple dissolution or mixing at pH above 7 and TDS > 200. A few samples showed weak ion exchange processes in the aquifer. The dominant water type Ca-HCO₃ with significant Magnesium influence was observed in 48% of the samples. Na-HCO₃ indicating an ion exchange process was found in 24%, and non-dominating cations and anions were found in 12% of samples showing simple mixing and dissolution. Calcium and bicarbonate ions dominated in 56% and 76% of the samples respectively.



Figs. 17–23. XRD plot of rock samples (RS1, RS2A, RS2B, RS3, RS4, RS5) in the region, where the X-axis represents 2θ value and Y- the axis represents intensity value.

3.7. X-ray diffraction (XRD) data of the area

The mineralogical study for the rock samples found in the area was carried out using X-ray diffraction. The data obtained after XRD analysis provided a d-spacing value that was matched with the inventory of known minerals to confirm the presence of the minerals in the sample. The parent peak and a subordinate peak of d-spacing were compared with standard reference values given by (Lindholm, 1987) for the identification of minerals present in the samples. The graph in Figs. 17–23 was plotted using the software Xpert high score version 1.0a. The locations of rock samples are shown in Fig. 1.

The carbonate minerals found in middle Andaman after the analysis of rock samples were Aragonite found in rock samples (RS2A, RS2B)

having common Intensity peak values 3.396, 2.870, 2.484, 2.481, 2.410, Calcite found only in RS4 with an intensity peak value 3.030, 2.495, Chlorite was identified in RS1 with an intensity peak value 7.150, 2.870, 2.550, 2.475, 2.390, Chromite was observed in (RS1& RS4) with a common intensity peak value 2.950, 2.520, 2.400, Dolomite was observed in (RS1, RS2A, RS2B) with a common intensity peak value 4.030, 3.690, 2.886, 2.405, Magnetite was found in (RS1 & RS4) with a common intensity peak value 2.530, 2.419, Pyrite was confirmed in (RS2B, RS3, RS4) with a common intensity peak value 2.709, 2.423, 2.212. These minerals confirmed the presence of limestone deposits in the area. The presence of Aragonite showed evidence of burial and metamorphism of the rocks of the Mithakari formation.

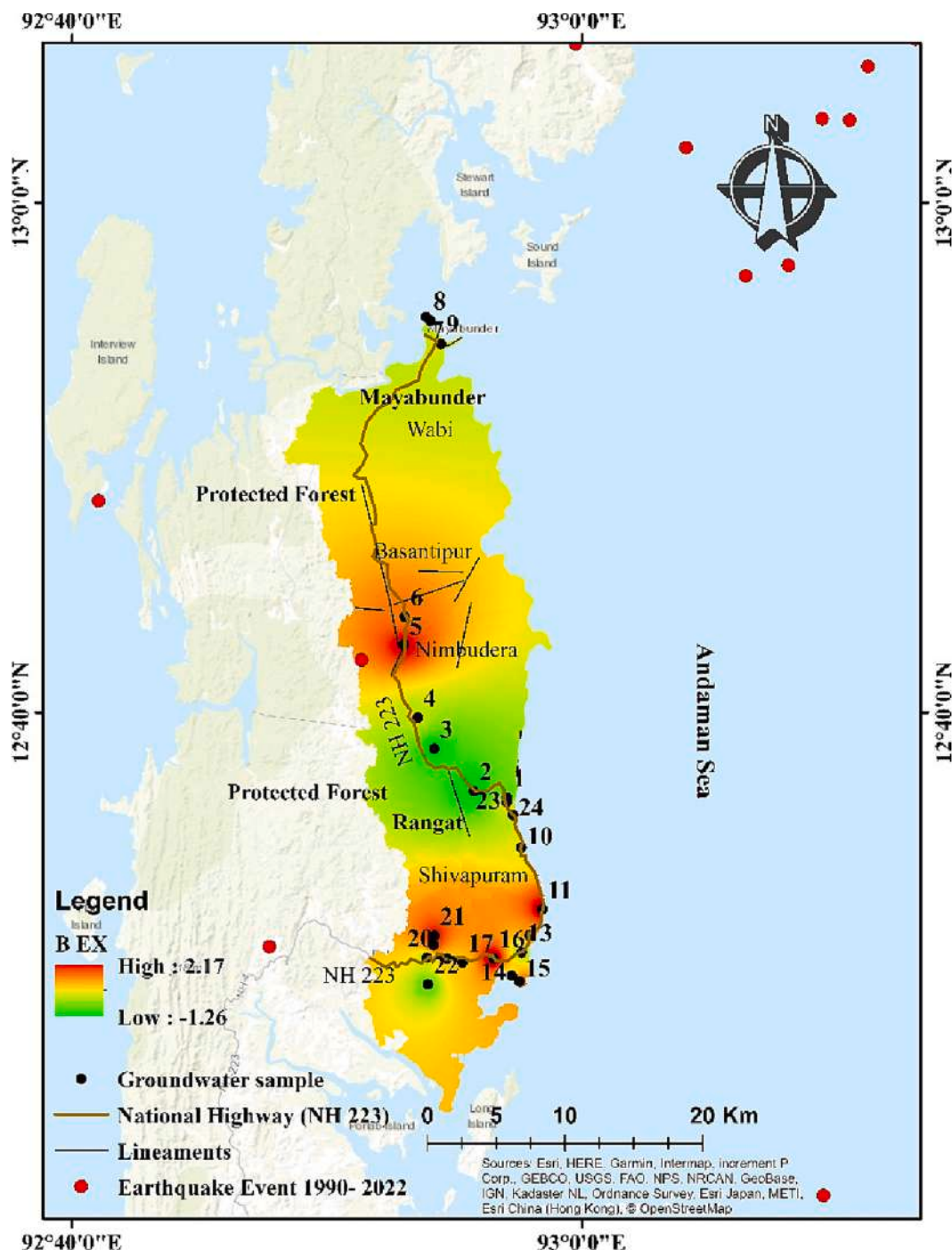


Fig. 24. BEX map of middle Andaman.

3.8. Base exchange index (BEX)

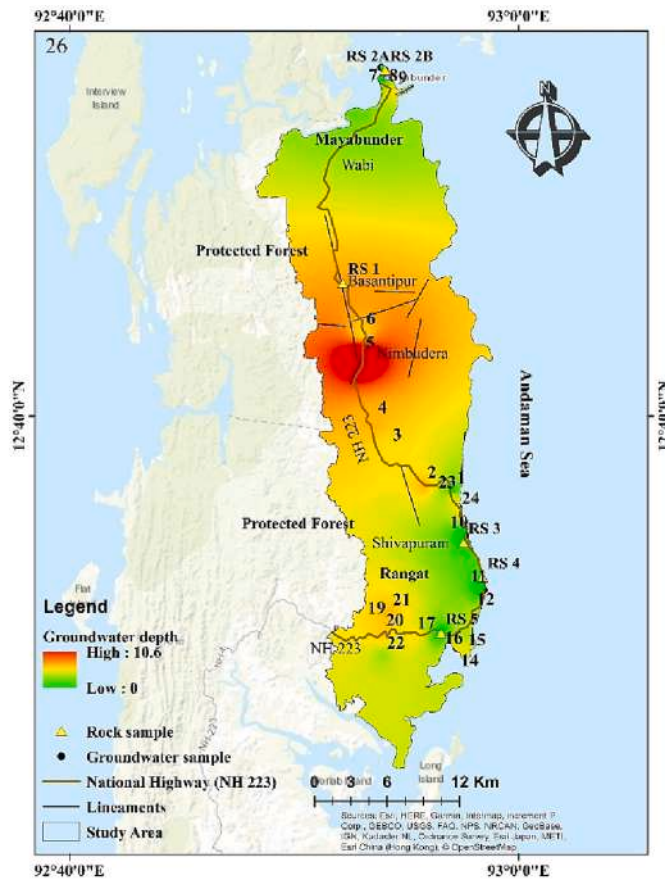
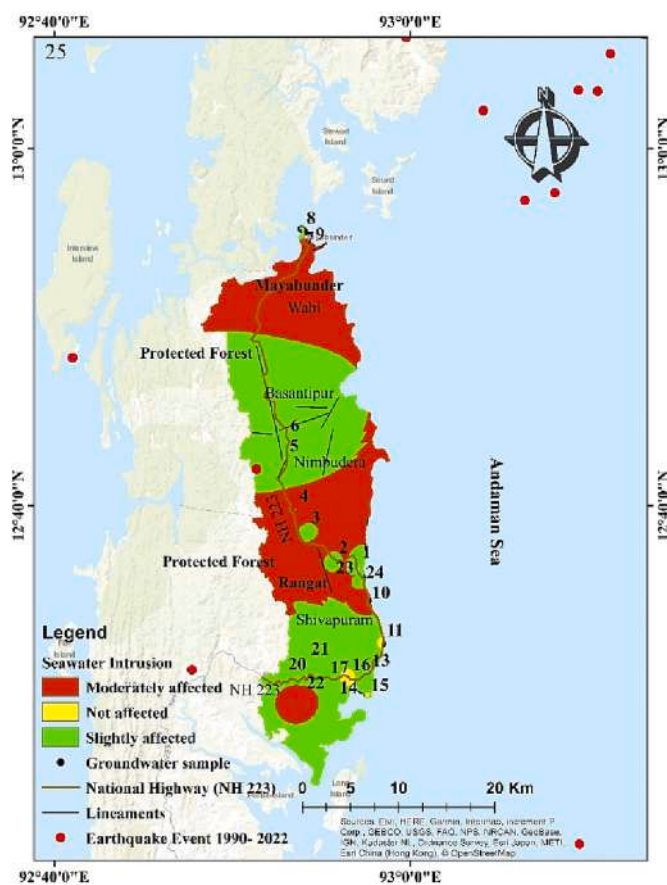
The base exchange index is an index of salinization that shows the negative value for seawater intrusion and positive values for the freshwater aquifer. It was observed that the BEX values were between -195.30 and 2.17 , with a mean value of -7.34 . The negative value of BEX indicated a higher concentration of $(\text{Na} + \text{Mg} + \text{K})$ relative to chloride ions. A zero value of BEX indicated the absence of base ion exchange in the area (Stuyfzand, 1989). The spatial map of BEX (Fig. 24) showed the effect of saltwater intrusion: a large portion in middle below Numbudera, a few spots in the southern region, and some parts of the northern region of the study area. BEX index showed that about 32% of groundwater samples are under the effect of seawater intrusion.

3.9. Integrated seawater intrusion

The integrated seawater intrusion diagram was made after the integration of all the ratio parameters on ArcGIS 10.8. It was classified based on the sum of the ionic ratios; strongly affected (≥ 8), Moderately affected (6, 7), Slightly affected (4, 5), and not affected (< 4). Fig. 25 showed the Moderately affected (44%), slightly affected (54%), and not affected (2%) saline groundwater in the area (Asare et al., 2021). Not a single sample was found strongly affected by seawater influences. The effect of seawater intrusion was found in the North and Middle with a small spot in the southern part as a moderately affected area. In comparison to groundwater depth (Fig. 26), the deep aquifers of Numbudera and Basantipur are less affected by seawater intrusion possibly due to groundwater recharge through interconnected fractures preventing seawater intrusion through the hydraulic gradient. The shallow aquifers of Mayabunder and Rangat were found moderately affected by seawater intrusion. The seashore extension of seawater intrusion was found above

Nimbudera and above Basantipur.

The integration map of Ionic ratio with earthquakes, active faults/fractured zone/ deep lineaments (Fig. 25). As the area already falls in earthquake zone V, seismic activities are very common in the study area. The earthquake shockwave also triggered the structural change in limestone deposits. Manchi and Sankaran (2009) studied the impact of the 2004 earthquakes on limestone caves and stated the impact caused the narrowing, widening, fractional, or complete shutting of present cave openings, (2) collapsed rocks inside caves, and (3) advanced existing cracks and fissures. The combination of active faults with earthquakes can be beneficial and disastrous for groundwater development. The connected fault found in the Nimbudera and Basantipur is found to be a good zone for groundwater recharge. The fault perpendicular to the sea provides an opening for seawater intrusion resulting in the dissolution of limestone as well. The seawater sample taken from Mayabunder was near the fault opening which lies perpendicular to the seashore that showed a higher amount of calcium ions than sodium. Generally, seawater usually contains NaCl dominance but the study area reported calcium chloride dominance in the sea. The higher value of bicarbonate in seawater again confirmed the limestone weathering in the study area. Similar to Mayabunder, Govindpur, and Monsdera are also having active faults perpendicular to seawater. The limestone minerals were present in all the rock samples in varied quantities. The middle of the study area has ophiolite group exposure overlying Mithakari and Bhartang formations. Geologically, the Mithakari formation has associated with a good aquifer zone with a good source of groundwater recharge zone. Sedimentary formation does not support the infiltration of surface water into the subsurface zone. Therefore, the sea level rise or extraction of groundwater may have developed a hydraulic gradient to infiltrate seawater in island aquifers. Similar way, seismic activities have created an explosion of the fracture within



Figs. 25–26. Integrated water intrusion and groundwater depth map of middle Andaman.

ophiolite that further provoked the Mithakari as well as Bhartang formations to develop a more interconnected fracture. Since some of the fractures have an opening in the sea, seawater can intrude through them. So, a precautionary measure must be taken so that the existing quality of the groundwater of the aquifer does not deteriorate over time.

4. Conclusion

The ionic ratio data showed the relative abundance of various constituents of water in the aquifer. The intrusion of seawater in freshwater changes the relative abundance of water parameters. We could successfully differentiate freshwater from seawater based on these ionic ratios. The Schoeller diagram aided in understanding the relative milli-equivalent proportion of each ion present in water and depicted limestone dissolution (higher concentration of calcium and bicarbonate) with a higher concentration of chloride than sodium (seawater effect). The GIS platform was found useful in the spatial visualization of BEX, ionic ratios, active faults, and geological formation. Bivariate plots have provided data on the enrichment of alkali metal salt and alkaline earth metal salts. The correlation matrix has depicted the strong relationships of chloride ions with major ions such as Na, K, Ca, and F (strongly correlated). Durov plots described the major water types (Ca-HCO₃ (48%) and Na-HCO₃ (24%)) and the processes (reverse ion exchange (56%) or mixing of seawater (12%) of the samples) taking place in the aquifer.

The shallow aquifer's proximity to the sea was found to be affected by seawater intrusion. The influence of seawater was found to be as follows: SO₄/Cl (100%) > Ca/SO₄ (100%) > Ca/Na (96%) > Mg/Cl (76%) > Ca/(HCO₃ + SO₄) (64%) > Cl/(HCO₃ + CO₃) (36%) > Cl/HCO₃ (16%) > (Ca + Mg)/Cl (2%) > Ca/Mg (0%) > K/Cl (0%). The integrated result has shown that the study area was found to be moderately affected (44%), slightly affected (54%), and not affected in 2% samples only.

Further X-ray diffraction plots of rock samples confirmed the presence of limestone minerals (Calcite, Aragonite Chlorite, Chromite, Dolomite, Magnetite, and Pyrite) in the area. The presence of limestone was indicative due to the dominance of calcium ions in coastal seawater. Further, the tectonic-metamorphic changes have been instrumental in the development of unconformity and lineament. These linear features needed to be monitored with utmost care to infer the possibility of seawater intrusion, especially in those areas where the openings of these fractures are associated with the coastal terrain. The current research has demarcated the salt-affected region of the coastal aquifer but it has not incorporated the effect of groundwater flow with an accurate hydraulic gradient. Even though the current research has described little about the role of earthquakes through active fault, data is still limited to understanding the role of tides, tsunamis, and disastrous events in the movement of seawater into aquifers of islands. There is a future possibility of studying groundwater modeling using geophysical data, time series analysis through machine learning techniques with accurate real-time weather data, tides movement, and groundwater flow detection using isotopes and age dating for understanding the lateral movement of seawater through the hydraulic gradient.

Declaration of Competing Interest

The authors declare that they have no known competing financial interests or personal relationships that could have appeared to influence the work reported in this paper.

Data availability

Data will be made available on request.

Acknowledgment

Authors show sincere gratitude to Lab 211, SES-JNU, AIRF-JNU, and

IUAC-New Delhi for instrumentation facilities and UGC for the scholarship.

References

- Abdalla, F., 2016. Ionic ratios as tracers to assess seawater intrusion and to identify salinity sources in Jazan coastal aquifer, Saudi Arabia. *Arab. J. Geosci.* 9 (1), 1–12.
- Abdalla, F., Al-Turki, A., Al Amri, A., 2015. Evaluation of groundwater resources in the southern Tihama plain, Saudi Arabia. *Arab. J. Geosci.* 8 (5), 3299–3310.
- Abdollahi-Nasab, A., Boufadel, M.C., Li, H., Weaver, J.W., 2010. Saltwater flushing by freshwater in a laboratory beach. *J. Hydrol.* 386 (1–4), 1–12.
- Adimalla, N., Dhakate, R., Kasarla, A., Taloor, A.K., 2020. Appraisal of groundwater quality for drinking and irrigation purposes in central Telangana, India. *Groundw. Sustain. Dev.* 10, 100334.
- Ahmed, M.A., Abdel Samie, S.G., Badawy, H.A., 2013. Factors controlling mechanisms of groundwater salinization and hydrogeochemical processes in the quaternary aquifer of the Eastern Nile Delta, Egypt. *Environ. Earth Sci.* 68 (2), 369–394.
- Akshitha, V., Balakrishna, K., Udayashankar, H.N., 2021. Assessment of hydrogeochemical characteristics and saltwater intrusion in selected coastal aquifers of southwestern India. *Mar. Pollut. Bull.* 173, 112989.
- Allow, K.A., 2012. The use of injection wells and a subsurface barrier in the prevention of seawater intrusion: a modeling approach. *Arab. J. Geosci.* 5 (5), 1151–1161.
- APHA, 2005. Standard Methods for the Examination of Water and Wastewater, 21st ed. American Public Health Association, Washington D.C.
- Appelo, C.A.J., Postma, D., 2005. Geochemistry, Groundwater, and Pollution, 2nd. ed. Balkema, Rotterdam.
- Asare, A., Appiah-Adjei, E.K., Ali, B., Owusu-Nimo, F., 2021. Assessment of seawater intrusion using ionic ratios: the case of coastal communities along the Central Region of Ghana. *Environ. Earth Sci.* 80, 1–14.
- Bandopadhyay, P.C., Carter, A., 2017. Introduction to the geography and geomorphology of the Andaman-Nicobar Islands. *Geol. Soc. Lond. Mem.* 47 (1), 9–18.
- Bandopadhyay, P.C., Ghosh, B., 2015. Provenance analysis of the Oligocene turbidites (Andaman Flysch), south Andaman Island: a geochemical approach. *J. Earth Syst. Sci.* 124, 1019–1037.
- Barlow, P.M., Reichard, E.G., 2010. Saltwater intrusion in coastal regions of North America. *Hydrogeol. J.* 18 (1), 247–260.
- Bear, J., Cheng, A.H.D., Sorek, S., Ouazar, D., Herrera, I. (Eds.), 1999. Seawater Intrusion in Coastal Aquifers: Concepts, Methods, and Practices, vol. 14. Springer Science & Business Media.
- Bhagat, C., Puri, M., Mohapatra, P.K., Kumar, M., 2021. Imprints of seawater intrusion on groundwater quality and evolution in the coastal districts of South Gujarat, India. *Case Stud. Chem. Environ. Eng.* 3, 100101.
- Carol, E.S., Kruse, E.E., 2012. Hydrochemical characterization of the water resources in the coastal environments of the outer Río de la Plata estuary, Argentina. *J. S. Am. Earth Sci.* 37, 113–121. <https://doi.org/10.1016/j.jsames.2012.02.009>.
- Challinor, J., 1967. Dictionary of Geology. University Press, Oxford/Great Britain, p. 39.
- Chidambaram, S., Anandhan, P., Prasanna, M.V., Thiyya, C., Thilagavathi, R., Sarathidasan, J., 2014. Hydrochemistry of groundwater in a coastal region and its repercussion on quality, a case study—Thoothukudi district, Tamil Nadu, India. *Arab. J. Geosci.* 7 (3), 939–950.
- Custodio, E., 2010. Coastal aquifers of Europe: an overview. *Hydrogeol. J.* 18 (1), 269–280.
- Darnault, C.J., Godinez, I.G., 2008. Coastal aquifers and saltwater intrusion. Overexploitation and contamination of shared groundwater resources: management. In: (Bio) Technological, and Political Approaches to Avoid Conflicts, pp. 185–201.
- Diatloff, E., Rengel, Z., 2001. Compilation of simple spectrophotometric techniques for the determination of elements in nutrient solutions. *J. Plant Nutr.* 24 (1), 75–86.
- Domenico, P.A., Schwartz, F.W., 1997. Physical and Chemical Hydrogeology. John Wiley & sons.
- Dragoni, W., Sukhija, B.S., 2008. Climate change and groundwater: a short review. *Geol. Soc. Lond., Spec. Publ.* 288 (1), 1–12.
- Elango, L., Kannan, R., 2007. Rock–water interaction and its control on chemical composition of groundwater. *Dev. Environ. Sci.* 5, 229–243.
- Ford, T.D., Cullingford, C.H.D., 1976. Science of Speleology. Academic Press.
- Ganeshiaha, K.N., Sanjappa, M., Rao, R., Murugan, C., Shivaprakash, K.N., 2019. Spatial distribution pattern of taxonomic and phylogenetic diversity of woody flora in Andaman and Nicobar Islands, India. *Forest Ecosyst.* 6, 1–14.
- Ganyaglo, S.Y., Osae, S., Akiti, T., Armah, T., Gourcy, L., Vitvar, T., Otoo, I.A., 2017. Application of geochemical and stable isotopic tracers to investigate groundwater salinity in the Ochi–Narkwa Basin, Ghana. *Hydrog. Sci. J.* 62 (8), 1301–1316.
- Gill, B., Webb, J., Stott, K., Cheng, X., Wilkinson, R., Cossens, B., 2017. Economic, social and resource management factors influencing groundwater trade: evidence from Victoria, Australia. *J. Hydrol.* 550, 253–267.
- Gimenez, E., Morell, I., 1997. Hydrogeochemical analysis of salinization processes in the coastal aquifer of Oropesa (Castellon, Spain). *Environ. Geol.* 29 (1), 118–131.
- Gulam Rasool, Bhat, Balaji, S., Ganai, M.Y., 2022. Tectonic Geomorphology and Seismic Hazard of the East Boundary Thrust in Northern Segment of the Sunda-Andaman Subduction Zone.
- Jafri, S.H., Balaram, V., Govil, P.K., 1993. Depositional environments of cretaceous radiolarian cherts from Andaman-Nicobar Islands, northeastern Indian Ocean. *Mar. Geol.* 112 (1–4), 291–301.
- Jones, B.F., Vengosh, A., Rosenthal, E., Yechiel, Y., 1999. Geochemical investigations. In: Seawater Intrusion in Coastal Aquifers—Concepts, Methods and Practices. Springer, Dordrecht, pp. 51–71.

- Kazakis, N., Pavlou, A., Vargemezis, G., Voudouris, K.S., Soulios, G., Pliakas, F., Tsokas, G., 2016. Seawater intrusion mapping using electrical resistivity tomography and hydrochemical data. An application in the coastal area of eastern Thermaikos Gulf, Greece. *Sci. Total Environ.* 543, 373–387.
- Klassen, J., Allen, D.M., 2017. Assessing the risk of saltwater intrusion in coastal aquifers. *J. Hydrol.* 551, 730–745.
- Klassen, J., Allen, D.M., Kirste, D., 2014. Chemical indicators of saltwater intrusion for the Gulf Islands. British Columbia. Final Report, Department of Earth Sciences, Simon Fraser University.
- Kumar, S., 1981. Geodynamics of Burma and Andaman-Nicobar region, based on tectonic stresses and regional seismicity. *Tectonophysics* 79 (1–2), 75–95.
- Lakshmanan, E., Kannan, R., Kumar, M.S., 2003. Major ion chemistry and identification of hydrogeochemical processes of ground water in a part of Kancheepuram district, Tamil Nadu, India. *Environ. Geosci.* 10 (4), 157–166.
- Lee, J.Y., Song, S.H., 2007. Groundwater chemistry and ionic ratios in a western coastal aquifer of Buan, Korea: implication for seawater intrusion. *Geosci. J.* 11 (3), 259–270.
- Li, P., Karunandhi, D., Subramani, T., Srinivasamoorthy, K., 2021. Sources and consequences of groundwater contamination. *Arch. Environ. Contam. Toxicol.* 80, 1–10.
- Lindholm, R.C., 1987. Mineral identification using X-ray diffraction. In: *A Practical Approach to Sedimentology*, pp. 124–153.
- Lloyd, J.W., Heathcoat, J.A., 1985. *Natural Inorganic Hydrochemistry in Relation to Groundwater: An Introduction*. Clarendon Press, Oxford.
- Louvat, D., Michelot, J.L., Aranyossy, J.F., 1999. Origin and residence time of salinity in the Åspö groundwater system. *Appl. Geochem.* 14 (7), 917–925.
- Manchi, S., Sankaran, R., 2009. Impact of the 2004 earthquake on the limestone caves in North and Middle Andaman Islands. *Curr. Sci.* 1230–1234.
- Marimuthu, S., Reynolds, D.A., La Salle, C.I.G., 2005. A field study of hydraulic, geochemical and stable isotope relationships in a coastal wetlands system. *J. Hydrol.* 315 (1–4), 93–116.
- Mercado, A., 1985. The use of hydrogeochemical patterns in carbonate sand and sandstone aquifers to identify intrusion and flushing of saline water. *Groundwater* 23 (5), 635–645.
- Milnes, E., 2011. Process-based groundwater salinisation risk assessment methodology: application to the Akrotiri aquifer (southern Cyprus). *J. Hydrol.* 399 (1–2), 29–47.
- Mohanty, A.K., Rao, V.G., 2019. Hydrogeochemical, seawater intrusion and oxygen isotope studies on a coastal region in the Puri District of Odisha, India. *Catena* 172, 558–571.
- Mondal, N.C., Singh, V.S., Saxena, V.K., Singh, V.P., 2011. Assessment of seawater impact using major hydrochemical ions: a case study from Sadras, Tamilnadu, India. *Environ. Monit. Assess.* 177 (1–4), 315–335.
- Moujabber, M.E., Samra, B.B., Darwish, T., Atallah, T., 2006. Comparison of different indicators for groundwater contamination by seawater intrusion on the Lebanese coast. *Water Resour. Manag.* 20 (2), 161–180.
- Mukherjee, S., 1986. Land subsidence in middle Andaman: A case study. *Hydrol. J.* 13 (3), 150–156.
- Nadler, A., Magaritz, M., Mazor, E., 1980. Chemical reactions of sea water with rocks and freshwater: experimental and field observations on brackish waters in Israel. *Geochim. Cosmochim. Acta* 44 (6), 879–886.
- Naidu, L.S., Rao, G., Rao, G., Mahesh, J., Padalu, G., Sarma, V.S., Prasad, P.R., Rao, S.M., Rao, B.M., 2013. An integrated approach to investigate saline water intrusion and to identify the salinity sources in the Central Godavari delta, Andhra Pradesh, India. *Arab. J. Geosci.* 6 (10), 3709–3724.
- Naily, W., 2018. Ratio of major ions in groundwater to determine saltwater intrusion in coastal areas. In: *IOP Conference Series: Earth and Environmental Science*, vol. 118. IOP Publishing, p. 012021. No. 1.
- Panno, S.V., Hackley, K.C., Hwang, H.H., Greenberg, S.E., Krapac, I.G., Landsberger, S., O'Kelly, D.J., 2006. Characterization and identification of na-cl sources in ground water. *Ground Water* 44 (2), 176–187.
- Post, V.E.A., 2005. Fresh and saline groundwater interaction in coastal aquifers: is our technology ready for the problems ahead? *Hydrogeol. J.* 13 (1), 120–123.
- Rajkumar, N., Subramani, T., Elango, L., 2010. Ground water contamination due to municipal solid waste disposal—A GIS based study in Erode City. *Int. J. Environ. Sci.* 1 (1), 39–55.
- Rajmohan, N., Elango, L.J.E.G., 2004. Identification and evolution of hydrogeochemical processes in the groundwater environment in an area of the Palar and Cheyyar River Basins, Southern India. *Environ. Geol.* 46, 47–61.
- Rani, N.S., Satyanarayana, A.N.V., Bhaskaran, P.K., Rice, L., Kantamaneni, K., 2021. Assessment of groundwater vulnerability using integrated remote sensing and GIS techniques for the West Bengal coast, India. *J. Contam. Hydrol.* 238, 103760.
- Rao, P.S.N., 1996. Phytogeography of the Andaman and Nicobar Islands, India. *Nat. J.* 50 (2), 56–79.
- Rena, V., Vishwakarma, C.A., Singh, P., Roy, N., Asthana, H., Kamal, V., Mukherjee, S., 2022. Hydrogeological investigation of fluoride ion in groundwater of Ruparail and Banganga basins, Bharatpur district, Rajasthan, India. *Environ. Earth Sci.* 81 (17), 430.
- Rosenthal, E., 1988. Hydrochemical changes induced by overexploitation of groundwater at common outlets of the bet Shean-Harod multiple-aquifer system, Israel. *J. Hydrol.* 97 (1–2), 107–128.
- Roy, P.S., Padalia, H., Chauhan, N., Porwal, M.C., Gupta, S., Biswas, S., Jagdale, R., 2005. Validation of geospatial model for biodiversity characterization at landscape level—A study in Andaman & Nicobar Islands, India. *Ecol. Model.* 185 (2–4), 349–369.
- Saidi, S., Bouri, S., Dhia, H.B., 2013. Groundwater management based on GIS techniques, chemical indicators and vulnerability to seawater intrusion modelling: application to the Mahdia-Ksour Essaf aquifer, Tunisia. *Environ. Earth Sci.* 70 (4), 1551–1568.
- Sajil Kumar, P.J., 2016. Deciphering the groundwater-saline water interaction in a complex coastal aquifer in South India using statistical and hydrochemical mixing models. *Model. Earth Syst. Environ.* 2 (4), 1–11.
- Sakram, G.S., Bhoopathi, R.V., Saxena, P.R., 2013. The impact of agricultural activity on the chemical quality of groundwater. Karanavagu watershed, Medak district. *Andhra Pradesh Int. J. Adv. Scientific Tech. Res.* 3.
- Sankaran, R., 1998. An annotated list of the endemic avifauna of the Nicobar Islands. *Forktail* 17–22.
- Schoeller, H., 1967. *Geochemistry of groundwater—an international guide for research and practice*, 15. Chap, pp. 1–18.
- Selvakumar, S., Chandrasekar, N., Kumar, G., 2017. Hydrogeochemical characteristics and groundwater contamination in the rapid urban development areas of Coimbatore, India. *Water Resour. Industry* 17, 26–33.
- Singh, P., Asthana, H., Rena, V., Kumar, P., Kushawaha, J., Mukherjee, S., 2018. Hydrogeochemical processes controlling fluoride enrichment within alluvial and hard rock aquifers in a part of a semi-arid region of Northern India. *Environ. Earth Sci.* 77, 1–15.
- Singha, P., Dewangan, P., Kamesh Raju, K.A., Aswini, K.K., Ramakrushna Reddy, T., 2019. Geometry of the subducting Indian plate and local seismicity in the Andaman region from the passive OBS experiment. *Bull. Seismol. Soc. Am.* 109 (2), 797–811.
- Srinivasamoorthy, K., Vasanthaigar, M., Vijayaraghavan, K., Sarathidasan, R., Gopinath, S., 2013. Hydrochemistry of groundwater in a coastal region of Cuddalore district, Tamilnadu, India: implication for quality assessment. *Arab. J. Geosci.* 6, 441–454.
- Srinivasan, M.S., 1979. *Geology and mineral resources of the Andaman and Nicobar Islands*. Andaman Nicobar Informa. 1979, 44–52.
- Srivastava, P.K., Gupta, M., Mukherjee, S., 2012. Mapping spatial distribution of pollutants in groundwater of a tropical area of India using remote sensing and GIS. *Appl. Geomatics* 4, 21–32.
- Stoessell, R.K., 1997. Delineating the chemical composition of the salinity source for saline ground waters: an example from East-Central Concordia Parish, Louisiana. *Groundwater* 35 (3), 409–417.
- Stuyfzand, P.J., 1989. A new hydrochemical classification of water types. *Iahs Publ* 182, 89–98.
- Stuyfzand, P.J., 2008. Base exchange indices as indicators of salinization or freshening of (coastal) aquifers. In: *20th Salt Water Intrusion Meeting*, Naples, Florida, USA.
- Subramani, T., Elango, L., Damodarasamy, S.R., 2005. Groundwater quality and its suitability for drinking and agricultural use in Chithar River Basin, Tamil Nadu, India. *Environ. Geol.* 47, 1099–1110.
- Tamta, S.R., 2003. Groundwater contamination in India. *Ind. J. Public Admin.* 49 (3), 578–584.
- Todd, D.K., Mays, L.W., 2004. *Groundwater Hydrology*. John Wiley & Sons.
- Umarani, P., Ramu, A., Kumar, V., 2019. Hydrochemical and statistical evaluation of groundwater quality in coastal aquifers in Tamil Nadu, India. *Environ. Earth Sci.* 78, 1–14.
- Vengosh, A., 2003. Salinization and saline environments. *Treat. Geochem.* 9, 612.
- Werner, A.D., 2010. A review of seawater intrusion and its management in Australia. *Hydrogeol. J.* 18 (1), 281–285.
- Werner, A.D., Simmons, C.T., 2009. Impact of sea-level rise on seawater intrusion in coastal aquifers. *Groundwater* 47 (2), 197–204.

Hydrogeochemical processes controlling fluoride enrichment within alluvial and hard rock aquifers in a part of a semi-arid region of Northern India

Priyadarshini Singh¹ · Harshita Asthana¹ · Vikas Rena¹ · Pardeep Kumar¹ · Jyoti Kushawaha¹ · Saumitra Mukherjee¹ 

Received: 15 May 2017 / Accepted: 19 June 2018
© Springer-Verlag GmbH Germany, part of Springer Nature 2018

Abstract

Rock–water interaction along with mineral dissolution/ precipitation plays a profound role in the control of fluoride ion concentration within the alluvial groundwater in a part of semi-arid northern India. In the premonsoon season, the alluvial region experiences evaporative processes leading to increase in Na^+ ions which through reverse ion exchange processes are adsorbed onto suitable sites within the aquifer matrix in exchange for Ca^{2+} ion in solution. Increase in Ca^{2+} ions in solution inhibits fluorite mineral dissolution, thereby controlling premonsoon fluoride ion concentration within alluvial groundwaters ($1.40 \pm 0.5 \text{ mg/l}$). In the postmonsoon season, however, higher average fluoride ion concentration within the alluvial aquifer samples ($2.33 \pm 0.80 \text{ mg/l}$) is observed mainly due to increase in silicate weathering of fluoride-bearing rocks and direct ion exchange processes enabling Ca^{2+} ion uptake from solution accompanied with the release of fluoride ions. Combined effect of these processes results in average fluoride ion concentration falling above the WHO drinking water permissible limit (1.5 mg/l). Alternatively, the hard rock aquifer samples within the study area have an average fluoride ion concentration falling below the permissible limit in both the seasons.

Keywords Geochemistry · Ion exchange · Rock–water interaction · Mineral dissolution · Weathering

Introduction

The groundwater chemistry of a particular region reflects the chemical characteristics of the aquifer through which it flows (Maya and Loucks 1995; Daniele et al. 2013). Changes in the chemical properties of groundwater elucidate the geochemical processes taking place within the aquifer over time. Apodaca et al. (2002) inferred that hydrogeochemical processes such as dissolution, precipitation, ion exchange, evaporation, and the residence time along the flow path of

groundwater control its chemical composition within shallow alluvial aquifers. Groundwater quality is also influenced by the presence of different mineral phases derived from either atmospheric deposition or through weathering and erosion of the sediments and rocks (Saleh et al. 1999). Complexity in the groundwater aquifer system further arises due to local lithological diversity, geological structures as well as seasonal influences. Several geochemical processes which determine the presence of minerals derived from soluble fractions from rock weathering and dissolution/dilution process upon rock–water interaction have also been described (Chenini et al. 2010).

Fluoride-bearing mineral dissolution is considered to be the primary source of fluoride in groundwater; therefore, its occurrence is usually attributed to regional geo-genic sources (Jagadeshan et al. 2015; Brindha and Elango 2013). Within the Indian subcontinent, high groundwater fluoride is associated with igneous and metamorphic rocks such as granite and gneisses (Fawell et al. 2006). Fluoride is also known to have anthropogenic point sources of contamination, e.g., agro-chemicals and brick industries

Electronic supplementary material The online version of this article (<https://doi.org/10.1007/s12665-018-7656-3>) contains supplementary material, which is available to authorized users.

✉ Saumitra Mukherjee
saumitra@mail.jnu.ac.in; saumitramukherjee3@gmail.com
<http://www.jnu.ac.in/Faculty/smukherjee>

¹ Remote Sensing Applications Laboratory, School of Environmental Sciences, Jawaharlal Nehru University, New Delhi 110067, India

(Datta and Tyagi 1996). Furthermore, weathering of primary rocks rich in fluoride-bearing minerals and leaching of the fluoride ion from soil and clay sediments under alkaline conditions also lead to fluoride-rich groundwater, marked by high bicarbonate ion concentration (Daniel and Karuppasamy 2012). This is enhanced once calcite precipitation takes place under alkaline conditions (Mrazovaca et al. 2013).

While low levels of fluoride (< 0.1 mg/l) may cause dental decay, high fluoride concentration in drinking water is known to cause adverse health effects. WHO standards for safe drinking water show that fluoride concentrations of up to 10 mg/l were associated with dental fluorosis (Fawell et al. 2006; Schoeller 1967). Alternatively, a concentration ranging from 0.5 to 1 mg/l is considered safe for drinking purposes. Dental mottling, mostly affecting children aged up to 12 years takes place when the concentrations range between 1.5 and 2 mg/l, while skeletal fluorosis is known to occur when the concentrations exceed 4–8 mg/l (Raju et al. 2012). The rural to semi-rural populations within the study region which primarily depend on groundwater resource for a majority of domestic purposes including drinking water supply, therefore, may face serious threats due to the high concentration of groundwater fluoride.

Aquifer material and the origin of the mineralization can be identified by geochemical modeling and by analyzing the behavior of several graphical plots of ionic concentrations and their ratios (Kumari et al. 2013; Subramani et al. 2010). Presence of fluoride, dissolved silica, and alkalinity predominantly suggests the influence of rock–water interaction, mineral dissolution, and ion exchange processes (Subramani et al. 2005). Most of the districts of Haryana and Delhi have bed rock of quartzite, mica, clay as well as gneisses and schists which sets the primary conditions for fluoride existence in groundwater. Precipitation of evaporates termed as soil salt efflorescence due to high temperatures and low rainfall and subsequent re-dissolution during flooding events causes further increase in ionic concentration of Ca^{2+} , Mg^{2+} , Na^+ , HCO_3^- , Cl^- , etc (Bowles et al. 1982). Previous studies have briefly explored hydrogeochemical processes involved in fluoride ion contamination of groundwater within the study area (Gupta and Mishra 2014; Datta and Tyagi 1996). They, however, do not address in detail the interplay of various factors and processes responsible for the increase in fluoride ion concentration. The present study, therefore, examines in detail major processes responsible for the seasonal fluctuations in fluoride ion concentration within alluvial and hard rock aquifers in the semi-arid region of Northern India.

Moreover, a comprehensive understanding of the spatial distribution of groundwater types in different aquifers can be achieved, which could help to identify appropriate techniques to mitigate fluoride contamination of groundwater useful for drinking and other domestic purposes.

Study area

The study area lies in the old alluvial and hard rock region within the districts of Rohtak, Sonipat, Jhajjhar, Gurugram, Faridabad, and some parts of NCT of Delhi (Fig. 1). It is bounded by $29^{\circ}08'18.57''\text{N}$ and $76^{\circ}28'34.90''\text{E}$ in the west to $28^{\circ}11'27.27''\text{N}$ and $77^{\circ}21'50.63''\text{E}$ in the East.

Hydrogeology

The hard rock region of Faridabad and Gurugram consists of the quartzite ridge which forms the north extension of the Aravalli Fold Belt trending NNW-SSW with the groundwater occurring in fractures, joints, and crevices. Sandy layers at different depths also form the water bearing zones (Shekhar et al. 2015; CGWB Reports for Gurgaon and Faridabad 2007a, b). The hydrogeology of the alluvial region consists of clay group of formations dominating the sand group. The groundwater occurs in alluvial sand, silt, and gravel forming the potential aquifer zones. Granular zones which are interbedded with clays and sand form the principal groundwater reservoirs (Supplementary Table 1). The salinity of the groundwater increases with depth, with the deepest groundwater aquifer present at a depth of 200–350 m (CGWB 2007c, d, e Report for Rohtak, Jhajjhar and Sonipat).

The study area within Rohtak region lies in the Indo-Gangetic alluvial plain of quaternary age with the permeable zones comprising fine-to-medium-grained sand and occasional coarse sand and gravel. Groundwater in the alluvial region occurs within semi confined to confined conditions (Shekhar et al. 2015). The soils of the alluvial region are alkaline in nature with the deeper soils being more alkaline compared to surface soils (Chopra 1990).

The hard rock area is dominated by sandy soils, whereas soils of the alluvial zone consist of mainly fine-to-coarse-loamy alkaline soil ($\text{pH} > 7$) (Supplementary Fig. 3). The hard rock regions of Gurugram, Faridabad, and Delhi are surrounded by agricultural land along with scattered built-up land. The alluvial region has agriculture as the dominant landuse along with (Supplementary Fig. 2) scattered brick industries. Canal irrigation is highly prevalent in the region with the western Yamuna canal system feeding the minor canals.

Methodology

The ground water samples were collected from the alluvial and hard rock aquifers for premonsoon (April–May 2015) and postmonsoon season (Nov–Dec 2015) in pre-washed polypropylene plastic bottles rinsed 2–3 times

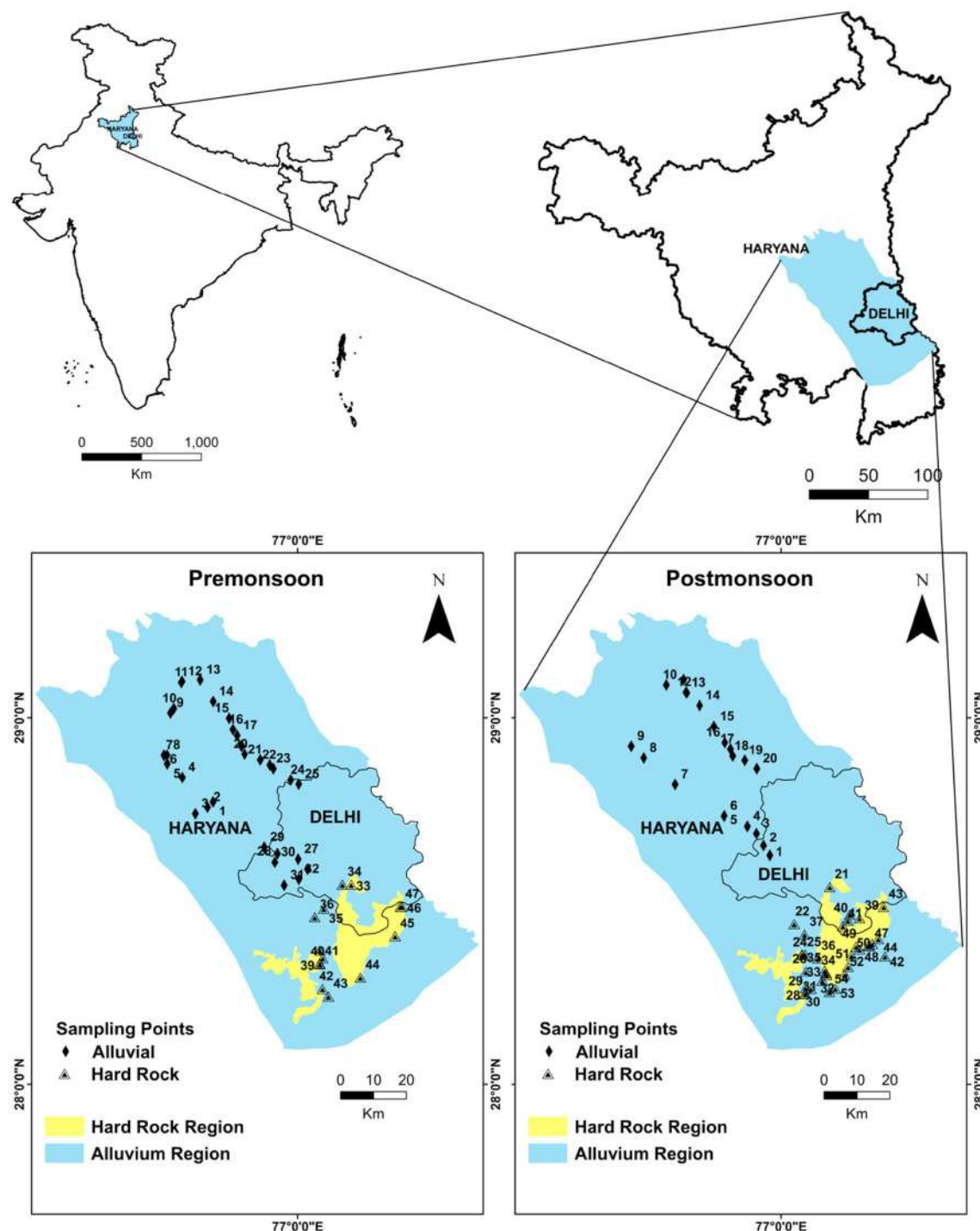


Fig. 1 Study area with sampling locations

with the water being sampled. Water was collected from hand pumps after pumping 20–25 strokes to minimize the impact of iron pipes. In case of borewells, the water was allowed to run for approximately 10 min before collecting the sample. Coordinates of each sampling location was recorded by Garmin global positioning system (GPS).

Temperature, pH, electrical conductivity (EC), and total dissolved solids (TDS) measurements were done in the field using thermometer and handheld probes (thermo Fischer multi-parameter TESTR 35 series). In the premonsoon season, 16 samples were collected from the hard rock aquifers and 32 samples were collected from the alluvial

aquifers. In the postmonsoon season, 33 samples were collected from the hard rock aquifers and 20 samples were collected from the alluvial aquifers. The samples collected for cation analysis were preserved using conc. HNO_3 ($\text{pH} < 2$). All samples were filtered using $0.45 \mu\text{m}$ Millipore filter paper and stored at 4°C until analysis was done.

Soil samples were collected in polyethylene bags from the alluvial and hard rock aquifer regions. The soils were air dried and homogenized by coning and quartering method after which the samples were gently crushed in a mortar and pestle and sieved through $200 \mu\text{m}$ mesh. Soil pH was also measured using pH meter. Mineralogical analysis of sediment samples was carried out using X-ray diffraction (XRD; PANalytical X'Pert PRO) at the Advanced Instrumentation Research Facility, Jawaharlal Nehru University, New Delhi.

Samples were analyzed for major ions (Na^+ , K^+ , Ca^{2+} , Mg^{2+} , CO_3^{2-} , HCO_3^- , NO_3^- , PO_4^{3-} , SO_4^{2-} , Cl^-), dissolved silica, and minor ions (Zn^{2+} , F^-) using the standard methods described in APHA (1995). Sulfate, nitrate, phosphate, fluoride, and silica were analyzed using UV/visible spectrophotometer (Lambda 35, Perkin Elmer); sodium, potassium, and calcium using flame photometer (Elico CL-378); magnesium and zinc using Atomic Absorption Spectrometer and chloride and Alkalinity ($\text{HCO}_3 + \text{CO}_3$) by titration technique (Subramani et al. 2010). All the laboratory analyses were done at the School of Environmental Sciences, Jawaharlal Nehru University.

The spatial distribution maps of the fluoride ion concentration were prepared using inverse distance weighted (IDW) technique on ArcGIS 10.2 software. Major processes governing the overall chemistry of the region were analyzed using Gibbs plot and several bivariate plots (using Microsoft Excel 2010).

For speciation analysis, the saturation index (SI) was calculated using PHREEQC 3.1.2. The chemical equilibrium for a particular mineral can be explained by the Saturation Index which is represented by the equation below:

$$\text{SI} = \log \left(\text{IAP}/K_t \right),$$

where IAP = Ion activity product of the dissociated mineral, K_t = equilibrium solubility at mineral temperature.

$\text{SI} < 0$ indicates undersaturation of groundwater with respect to a particular mineral present in the geological formations in the area and, therefore, indicates that mineral will further dissolve or that the groundwater has short residence time. Alternately, $\text{SI} > 0$ indicates that the groundwater is oversaturated with respect to a particular mineral and, therefore, the mineral will not dissolve further or that the groundwater has had a sufficient residence time to reach equilibrium. When the groundwater is in thermodynamic equilibrium with respect to a particular mineral, $\text{SI} = 0$.

Results and discussion

(i) Spatial and temporal variability of groundwater parameters

For the premonsoon samples from both the alluvial and the hard rock aquifers, the abundance of the major cations was $\text{Ca}^{2+} > \text{Na}^+ > \text{Mg}^{2+} > \text{K}^+$, whereas for the postmonsoon samples from both aquifers the abundance for major cations was $\text{Na}^+ > \text{Ca}^{2+} > \text{Mg}^{2+} > \text{K}^+$. For anions, the abundance in the premonsoon samples from the hard rock aquifer was $\text{HCO}_3^- > \text{Cl}^- > \text{SO}_4^{2-} > \text{NO}_3^- > \text{PO}_4^{3-}$, whereas for the samples from the alluvial aquifer, it was $\text{Cl}^- > \text{HCO}_3^- > \text{SO}_4^{2-} > \text{NO}_3^- > \text{PO}_4^{3-}$. The major anionic abundance for the postmonsoon samples from both the hard rock and the alluvial aquifers was $\text{HCO}_3^- > \text{Cl}^- > \text{SO}_4^{2-} > \text{NO}_3^- > \text{PO}_4^{3-}$. High concentration of bicarbonate ion indicates the contribution from carbonate weathering and silicate weathering present in the geological formations within the study region (Freeze and Cherry 1979). High value of EC in the premonsoon (warmer months) suggests enrichment of various ions in the groundwater due to enhanced evaporation and soil salt efflorescence (Bowles et al. 1982). Some samples both from the hard rock and the alluvial aquifers show the presence of moderately saline water ($\text{EC} \sim 4000 \mu\text{S}/\text{cm}$). The temperature of the samples collected ranged from 19.9 – 29.3°C . The mean, range, and standard deviation values for the analyzed ions from the hard rock aquifers, for the pre and postmonsoon seasons are presented in Table 1. Except for sodium and potassium, there is no major fluctuation in the major ion concentration between the pre and the postmonsoon samples.

Table 2 represents the pre and postmonsoon ionic concentrations for the alluvial aquifer samples. The EC, sodium, potassium, magnesium, sulfate, and bicarbonate ionic concentration show large fluctuation from the pre to the postmonsoon samples within the alluvial aquifers.

The spatial interpolation maps for the fluoride ion concentration show that in the premonsoon season (Fig. 2a), the alluvial aquifers have a lower fluoride concentration range compared to the hard rock aquifers, whereas in the postmonsoon season (Fig. 2b) the reverse is observed. In the premonsoon season, samples from both aquifers show fluoride ion concentrations below the WHO permissible limit for drinking water ($< 1.5 \text{ mg/l}$) in majority of the samples (Supplementary Table 2). However in the postmonsoon season, 85% of alluvial aquifer samples and ~21% of the hard rock aquifer samples have fluoride concentration higher than the permissible limit.

Table 1 Statistical summary of analyzed data for the hard rock aquifer samples

Parameters	Premonsoon		Postmonsoon	
	Mean \pm SD	Range	Mean \pm SD	Range
pH	6.59	5.9–7.9	7.15	6.7–7.8
EC	$1233.13 \pm 624.61 \mu\text{S}/\text{cm}$	308–2500 $\mu\text{S}/\text{m}$	$1368.94 \pm 573.48 \mu\text{S}/\text{cm}$	600–3000 $\mu\text{S}/\text{cm}$
HCO_3^-	$299.61 \pm 122.75 \text{ mg/l}$	61–480.38 mg/l	$368.93 \pm 80.81 \text{ mg/l}$	200.49–546.92 mg/l
Cl^-	$281.52 \pm 211.11 \text{ mg/l}$	67.48–852.15 mg/l	$236.75 \pm 156.22 \text{ mg/l}$	33.75–656.21 mg/l
NO_3^-	$38.48 \pm 46.97 \text{ mg/l}$	ND–135.02 mg/l	$41.57 \pm 38.55 \text{ mg/l}$	ND–130.62 mg/l
PO_4^{3-}	$0.43 \pm 0.12 \text{ mg/l}$	0.13–0.63 mg/l	$0.43 \pm 0.13 \text{ mg/l}$	0.09–0.62 mg/l
SO_4^{2-}	$50.79 \pm 43.86 \text{ mg/l}$	ND–135.73 mg/l	$60.98 \pm 52.48 \text{ mg/l}$	ND–213.48 mg/l
Na^+	$102.13 \pm 53.02 \text{ mg/l}$	11.2–191.7 mg/l	$230.61 \pm 57.9 \text{ mg/l}$	25.90–296.2 mg/l
K^+	$5.28 \pm 3.81 \text{ mg/l}$	0.8–13.8 mg/l	$16.51 \pm 23.67 \text{ mg/l}$	0.9–140.9 mg/l
Ca^{2+}	$143.71 \pm 113.19 \text{ mg/l}$	31.2–453.5 mg/l	$125.38 \pm 74.02 \text{ mg/l}$	49–395 mg/l
Mg^{2+}	$35.17 \pm 4.08 \text{ mg/l}$	28.39–43.96 mg/l	$34.59 \pm 5.97 \text{ mg/l}$	15.62–47.4 mg/l
Zn^{2+}	$0.40 \pm 0.94 \text{ mg/l}$	ND–2.94 mg/l	$0.29 \pm 0.66 \text{ mg/l}$	ND–3.07 mg/l
Silica	$28.80 \pm 6.86 \text{ mg/l}$	7.27–36.33 mg/l	$30.89 \pm 6.35 \text{ mg/l}$	18.07–43.56 mg/l
F [−]	$1.60 \pm 1.21 \text{ mg/l}$	0.09–4.68 mg/l	$1.15 \pm 0.55 \text{ mg/l}$	0.29–2.47 mg/l

ND not detected

Table 2 Statistical summary of analyzed data for the alluvial aquifer samples

Parameters	Premonsoon		Postmonsoon	
	Mean \pm SD	Range	Mean \pm SD	Range
pH	7.21	6.7–8	7.29	6.80–8.3
EC	$2062.31 \pm 1486.98 \mu\text{S}/\text{cm}$	365–5760 $\mu\text{S}/\text{cm}$	$1715.05 \pm 1194.96 \mu\text{S}/\text{cm}$	240–4630 $\mu\text{S}/\text{cm}$
HCO_3^-	$264.75 \pm 145.5 \text{ mg/l}$	90.79–620.92 mg/l	$368.51 \pm 135.61 \text{ mg/l}$	135.61–682.4 mg/l
Cl^-	$359.42 \pm 367.31 \text{ mg/l}$	42.38–1421.42 mg/l	$319.97 \pm 320.43 \text{ mg/l}$	42.19–1181.77 mg/l
NO_3^-	$31.66 \pm 32.28 \text{ mg/l}$	1.30–106.94 mg/l	$31.69 \pm 41.59 \text{ mg/l}$	ND–97.87 mg/l
PO_4^{3-}	$0.53 \pm 0.19 \text{ mg/l}$	0.17–1.02 mg/l	$0.20 \pm 0.13 \text{ mg/l}$	ND–0.53 mg/l
SO_4^{2-}	$81.52 \pm 82.86 \text{ mg/l}$	6.24–306.99 mg/l	$120.86 \pm 66.99 \text{ mg/l}$	ND–285 mg/l
Na^+	$79 \pm 55.01 \text{ mg/l}$	6.20–206.7 mg/l	$144.06 \pm 108.05 \text{ mg/l}$	9–384.4 mg/l
K^+	$19.08 \pm 34.53 \text{ mg/l}$	1.50–170.8 mg/l	$30.19 \pm 54.02 \text{ mg/l}$	1.40–211.2 mg/l
Ca^{2+}	$121.05 \pm 91.18 \text{ mg/l}$	16.20–347.1 mg/l	$139.74 \pm 117.74 \text{ mg/l}$	27.20–517.9 mg/l
Mg^{2+}	$70.80 \pm 48.43 \text{ mg/l}$	13.53–188.5 mg/l	$38.04 \pm 7 \text{ mg/l}$	22.89–54.22 mg/l
Zn^{2+}	$0.38 \pm 0.95 \text{ mg/l}$	0–5.14 mg/l	$0.19 \pm 0.36 \text{ mg/l}$	ND–138 mg/l
Silica	$28.74 \pm 6.53 \text{ mg/l}$	13.02–43.27 mg/l	$20.57 \pm 6.39 \text{ mg/l}$	5.76–27.92 mg/l
F [−]	$1.40 \pm 0.5 \text{ mg/l}$	0.38–2.12 mg/l	$2.33 \pm 0.80 \text{ mg/l}$	0.80–3.39 mg/l

ND not detected

(ii) Geochemical modeling and graphical representation of hydrochemical data

Graphical plots such as Gibbs plot and other bivariate scatter plots of ionic ratios are made to understand the hydrochemical processes which lead to the observed ionic values and the respective variation over space and time.

The Gibbs plot shows that several points from both aquifers have their chemical composition derived from rock–water interaction with a few falling in the evaporation dominance field in the premonsoon season (Gibbs 1970). This suggests that rock–water interaction in this region

controls the major ion groundwater chemistry (Fig. 3 a, b). More points from the alluvial aquifer samples fall in the evaporation dominance field compared to the hard rock samples in the premonsoon season (Fig. 3b). It is therefore estimated that the process of soil salt efflorescence due to evaporation leads to leaching of salts when soil water percolates to the groundwater. This influences major ion groundwater chemistry primarily in the premonsoon alluvial aquifers.

For the postmonsoon season, a greater number of points from the alluvial aquifer samples fall in the rock–water dominance zone suggesting that rock–water interaction majorly influences the groundwater chemistry (Fig. 3 c, d).

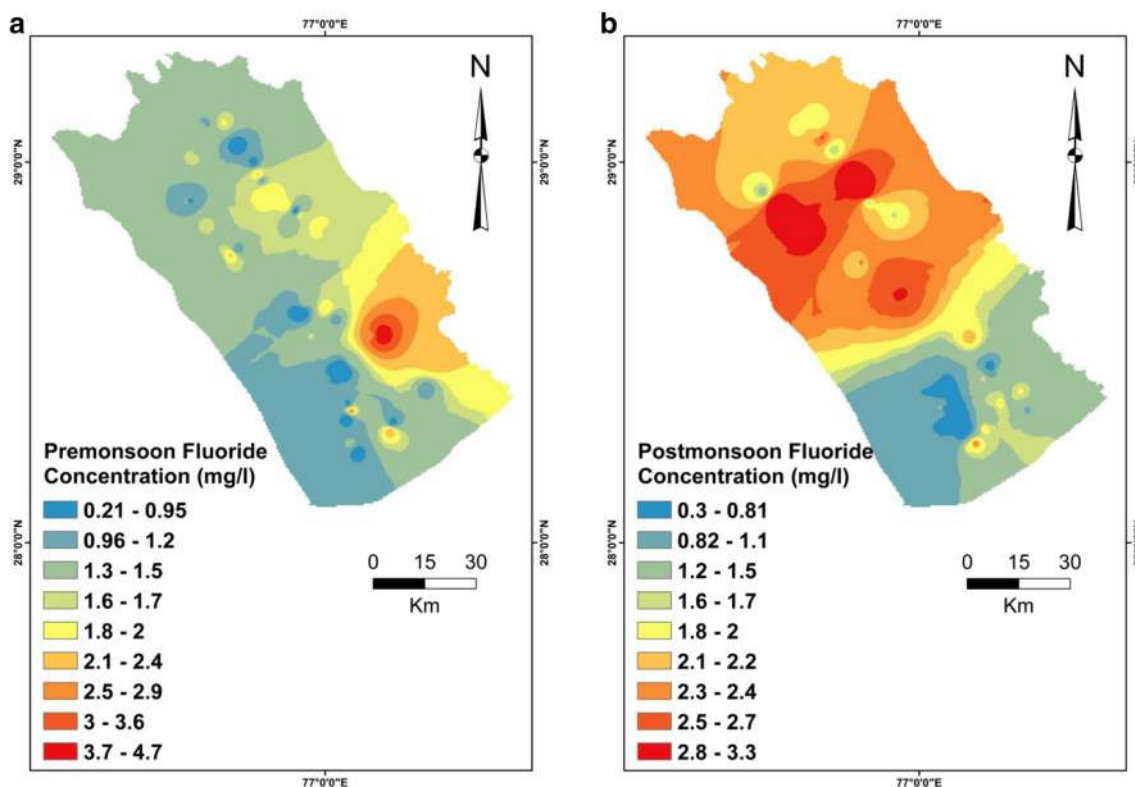


Fig. 2 Spatial interpolation of fluoride ion concentration (mg/l) in **a** premonsoon and **b** postmonsoon

The increase in the concentration of fluoride ions in alluvial postmonsoon samples, therefore, seems to be influenced by rock–water interaction primarily.

(iii) Sediment mineralogy and saturation index of water

The chemical concentration of different ions within the groundwater is largely influenced by the geochemistry of the soil through which water flows prior to reaching the aquifers. Therefore, the mineral composition of the soil sediments would elucidate the origin of various ions in groundwater of the region. X-ray diffraction was carried out for 20 representative soil samples from the hard rock and the alluvial aquifer region. The XRD diffractogram for several samples from the alluvial region indicated the presence of fluorite and calcite along with other major minerals such as quartz (Fig. 4a). The mineral composition suggests a geogenic origin of fluoride ion in the groundwater samples. For the hard rock samples also, fluorite was found along with calcite and quartz (Fig. 4b).

The mineral saturation indices for the groundwater samples show that calcite and dolomite are dominant carbonate minerals, whereas quartz is the primary silicate mineral present within the groundwater of the aquifers sampled. For the hard rock aquifers (Fig. 5a), all the

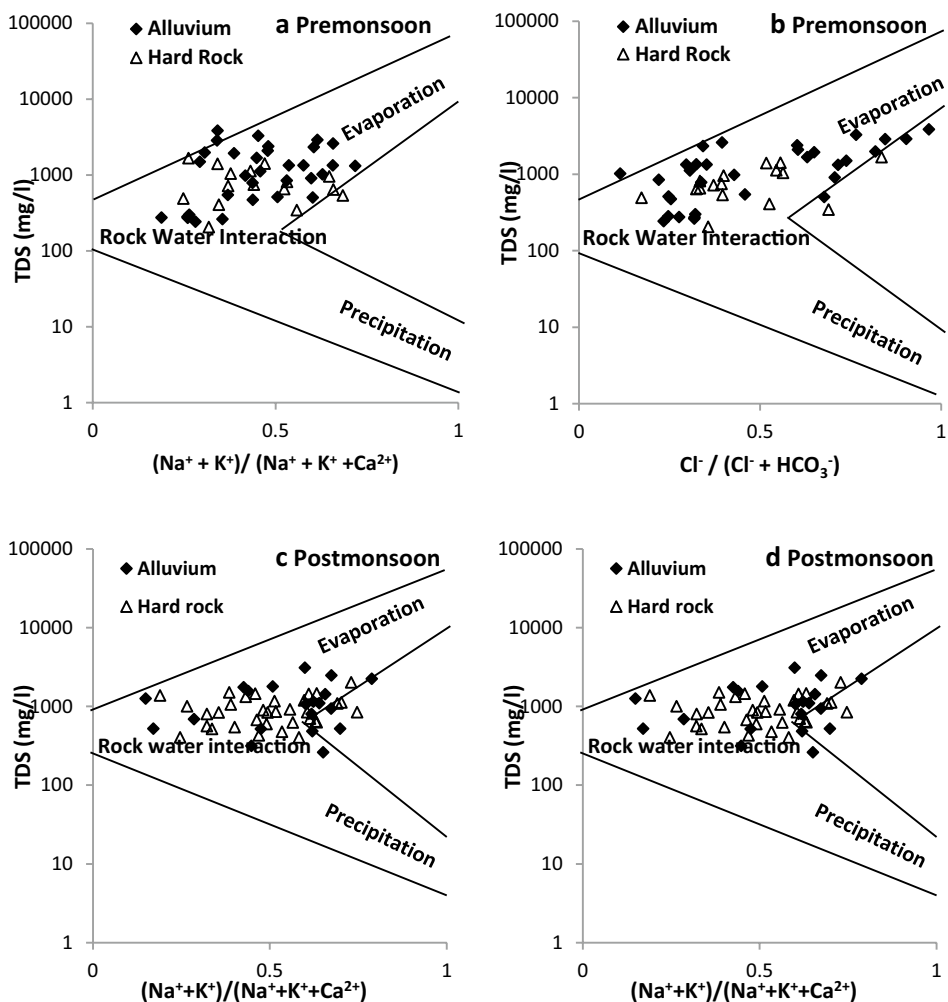
premonsoon samples show undersaturation for anhydrite and halite while five samples show undersaturation for dolomite and calcite only. 75% of samples show undersaturation for fluorite suggesting that mineral dissolution can be contributing to the high concentration of fluoride ion.

For the postmonsoon hard rock aquifer samples, a positive SI value for calcite and dolomite was observed for ~90% of samples whereas halite SI value indicates undersaturation for all the samples (Fig. 5b). Undersaturation of anhydrite in all the postmonsoon samples from both aquifers also suggests that dissolution of anhydrite would likely occur.

Almost all the alluvial premonsoon samples are oversaturated in terms of calcite, dolomite and chrysotile and undersaturated for fluorite, halite, quartz, and anhydrite (Fig. 6a). The oversaturation of calcite and dolomite suggests that high concentration of Ca^{2+} is not from mineral dissolution since calcite and dolomite are oversaturated in the premonsoon samples and, therefore, would not dissolve further. Therefore, the observed dominance of Ca^{2+} and HCO_3^- ions in groundwater in the alluvial aquifer samples could be the result of other processes like evaporation or ion exchange in the alluvial aquifers.

For the postmonsoon alluvial samples (Fig. 6b), 80% show undersaturation for fluorite suggesting that the mineral will dissolve further. Calcite and dolomite, although

Fig. 3 Gibbs plots: premonsoon **a, b** and postmonsoon **c, d** for alluvial and hard rock aquifer samples



oversaturated in majority of samples, show a lower positive SI index as compared to the premonsoon SI values.

(iv) Hydrochemical processes controlling fluoride ion concentration

(a) Carbonate and Silicate weathering

Chemical weathering leads to dissolution of fluoride species controlled by calcium and governed by thermodynamic principles. Calcium is the dominant cation in the premonsoon samples from both alluvial and hard rock aquifers along with bicarbonate ions. Weathering of rocks such as calcite, crystalline limestone, dolomite limestone, calc-granulite, and kankar (lime-rich weathered mantle overlying carbonate rocks) is the major sources of carbonates in groundwater (Subramani et al. 2010).

The scatter plot of $\text{Ca}^{2+} + \text{Mg}^{2+}$ vs $\text{HCO}_3^- + \text{SO}_4^{2-}$ represents the weathering pattern within the two aquifer types. Points falling along the 1:1 equiline show that these ions have resulted from calcite, dolomite, and

gypsum dissolution (Datta and Tyagi 1996). If reverse ion exchange or carbonate weathering is the dominant process, the points would shift to the left of the equiline due to an excess of $\text{Ca}^{2+} + \text{Mg}^{2+}$ over $\text{SO}_4^{2-} + \text{HCO}_3^-$ (Rajmohan and Elango 2004; Datta et al. 1980). Alternatively, if direct ion exchange processes are in play along with silicate weathering, the points shift to the right due to an excess of $\text{SO}_4^{2-} + \text{HCO}_3^-$ over $\text{Ca}^{2+} + \text{Mg}^{2+}$ (Cerling et al. 1989; Fisher and Mulcahy 1997). ~60% of samples from the hard rock aquifers and ~72% of the alluvial aquifer samples for premonsoon fall above the equiline with a few lying along and below the equiline (Fig. 7a) suggestive of carbonate weathering and reverse ion exchange processes as major contributors of calcium and bicarbonate ions in the groundwater apart from mineral dissolution.

In the postmonsoon period, the number of samples from both the hard rock and alluvial aquifers falling below the equiline increases (Fig. 7b). This suggests that the occurrence of silicate weathering is also controlling the major ion groundwater chemistry apart from carbonate weathering. The postmonsoon alluvial aquifer points also show a greater

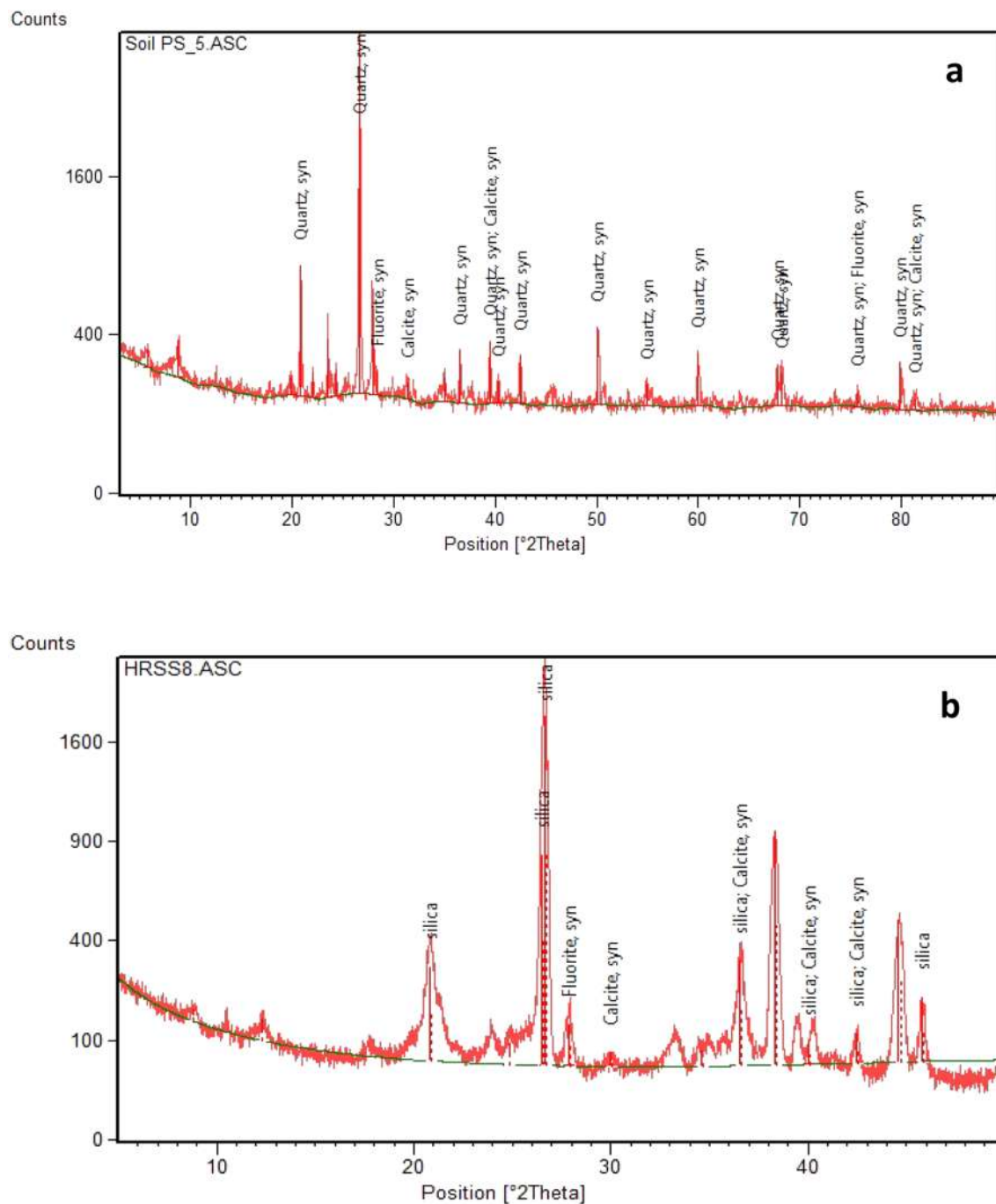


Fig. 4 XRD diffractogram of soil samples from **a** alluvial region and **b** hard rock region

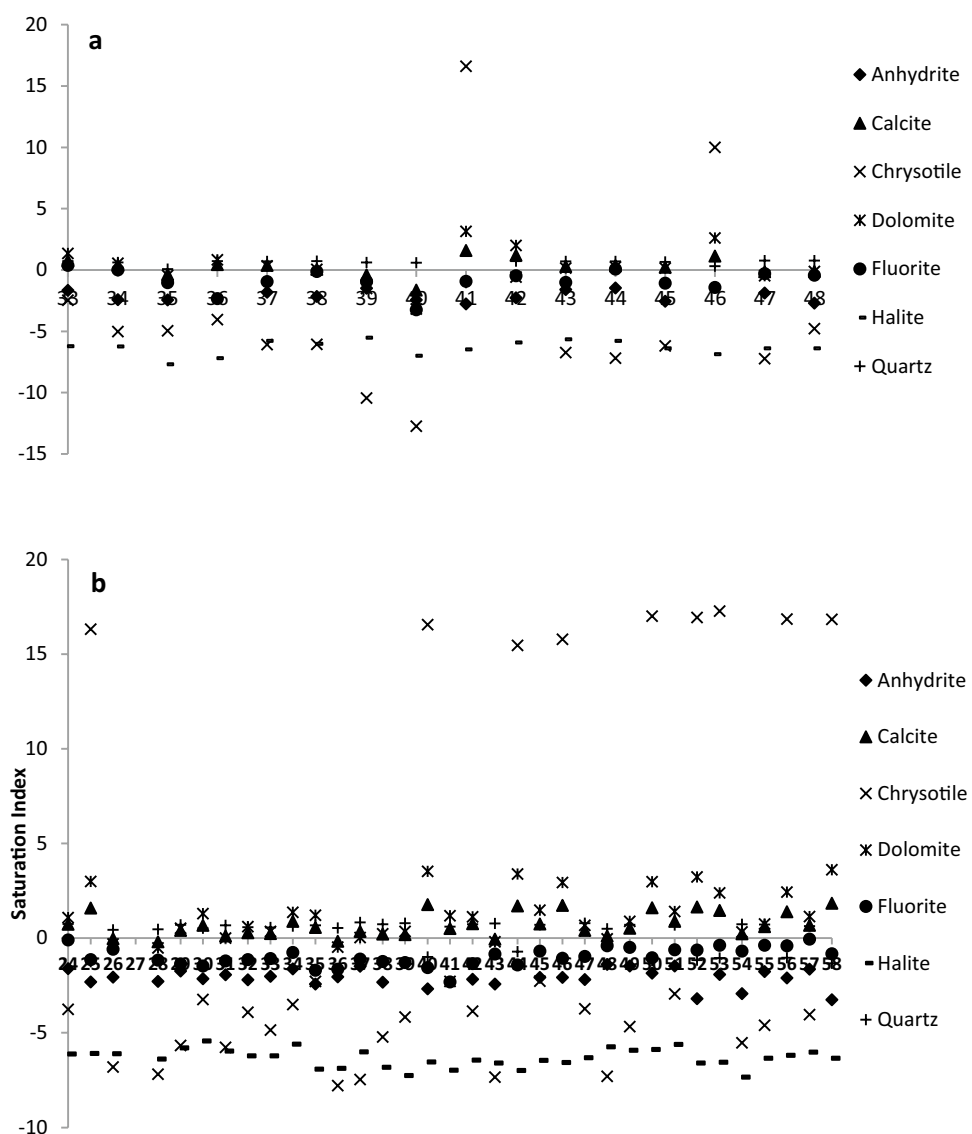
shift from carbonate to silicate weathering as compared to the hard rock samples.

This can further be validated through the $(\text{Na}^+ + \text{K}^+)$ vs Cl^- ion scatter plot (Fig. 8a) which shows ~63% of the points from the alluvial aquifers and 70% of points from the hard rock aquifers falling below the 1:1 equiline suggesting the prevalence of carbonate weathering in the premonsoon season. This explains the dominance of Ca^{2+} ion concentration

in the samples. For the postmonsoon samples (Fig. 8b), a comparatively greater number of points fall close to or on the equiline with a few falling below the equiline indicating contribution of silicate weathering at a few locations in both the aquifer samples.

Weathering of silicate mineral bearing rocks such as quartzite, schist, and gneissic complexes (represented by the equation below) present in the study area may be responsible

Fig. 5 Mineral saturation indices for hard rock samples from **a** pre and **b** postmonsoon



for the dominance of Ca^{2+} and Na^+ ions in the groundwater samples. This also contributes to HCO_3^- ions in the groundwater according to the following equation (Kumar et al. 2006):



Since silicate weathering is higher in the postmonsoon alluvial samples compared to the hard rock samples, it may have contributed to the increase in Na^+ and HCO_3^- ion concentration (Kumari et al. 2013; Elango et al. 2003).

The estimation of silicate weathering is difficult because the degradation of silicates is highly variable, giving a range of solid phases and dissolved species (Subramani et al. 2010). Therefore, silicate weathering can also be understood by comparing the ratio between $\text{Na}^+ + \text{K}^+$ and

total cations (TZ^+). The relationship between $\text{Na}^+ + \text{K}^+$ and total cations (TZ^+) shows a majority of points falling close to or on the $\text{Na}^+ + \text{K}^+ = 0.5 \text{ TZ}^+$ line in the postmonsoon samples from both aquifers (Fig. 9b). In the pre-

monsoon samples, however, most of the points fall above the $\text{Na}^+ + \text{K}^+ = 0.5 \text{ TZ}^+$ line (Fig. 9a). This validates that silicate weathering contributes to sodium and potassium ions in the groundwater in the postmonsoon alluvium samples (Sarin et al. 1989; Stallard and Edmond 1983). In addition to this, silicate weathering in the postmonsoon season might also cause desorption of fluoride ions from soil and clay particles due to the prevailing alkaline conditions since an alkaline environment favorably dissolves

Fig. 6 Mineral saturation Indices for alluvium aquifer samples from **a** pre and **b** postmonsoon

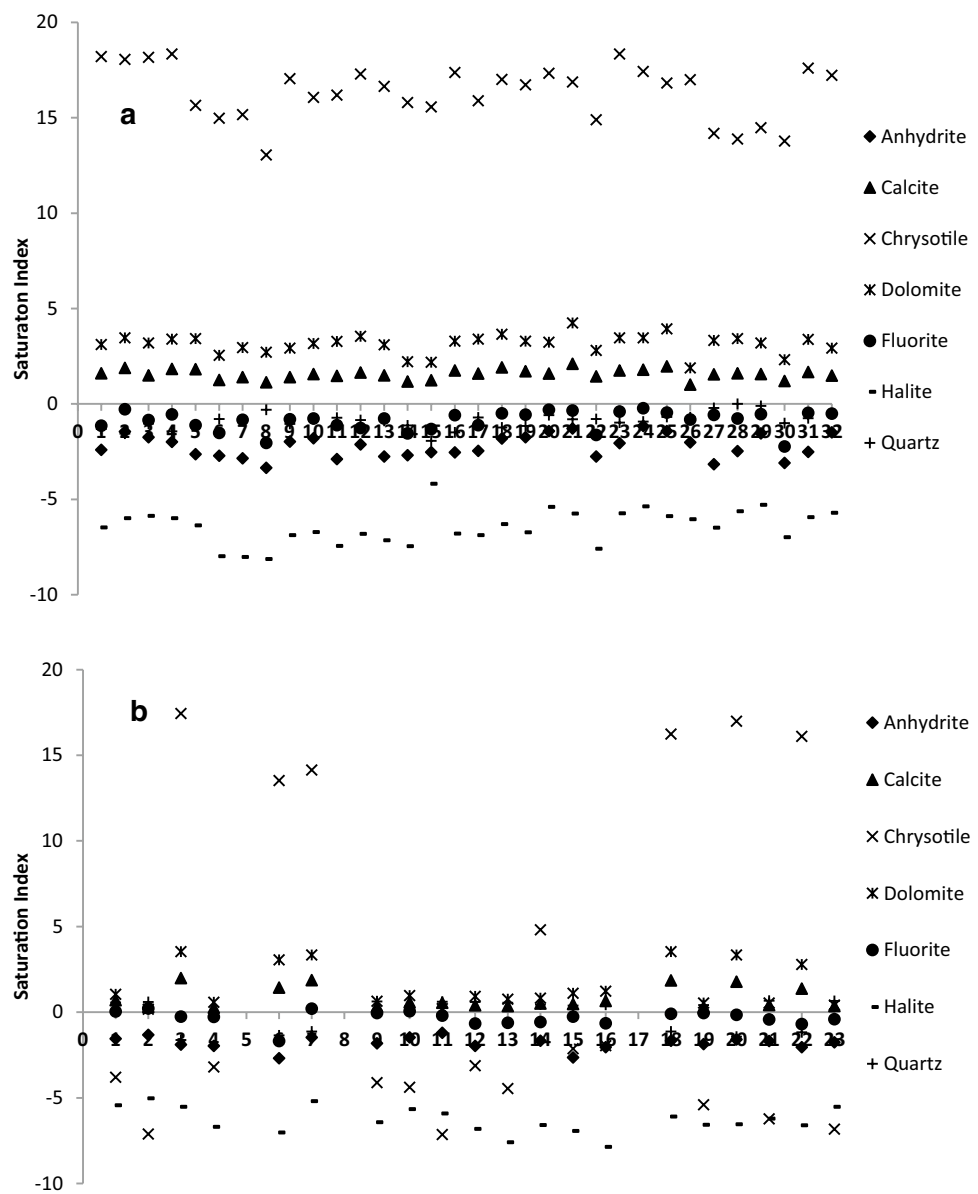


Fig. 7 Scatter plot of $(\text{Ca}^{2+} + \text{Mg}^{2+})$ vs $(\text{HCO}_3^- + \text{SO}_4^{2-})$ for **a** pre and **b** postmonsoon

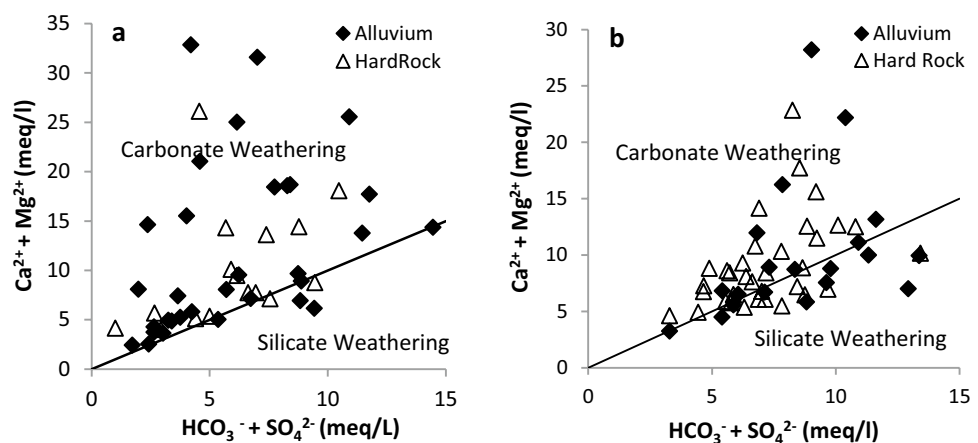


Fig. 8 Relationship between $\text{Na}^+ + \text{K}^+$ and Cl^- for **a** pre and **b** postmonsoon

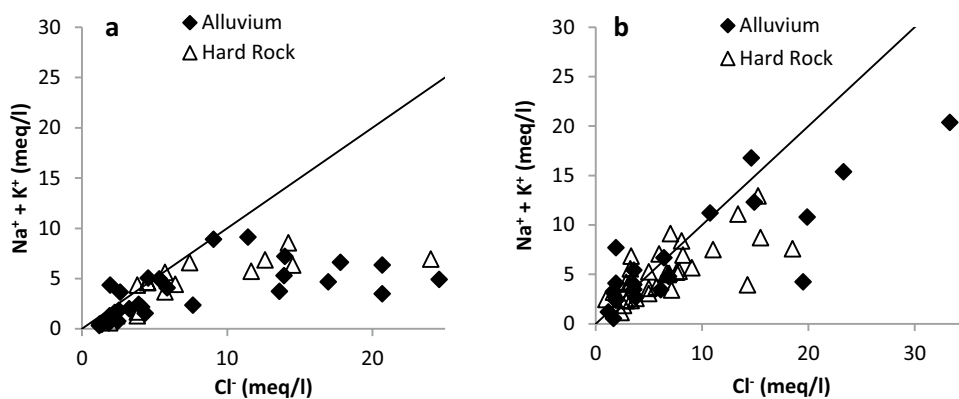
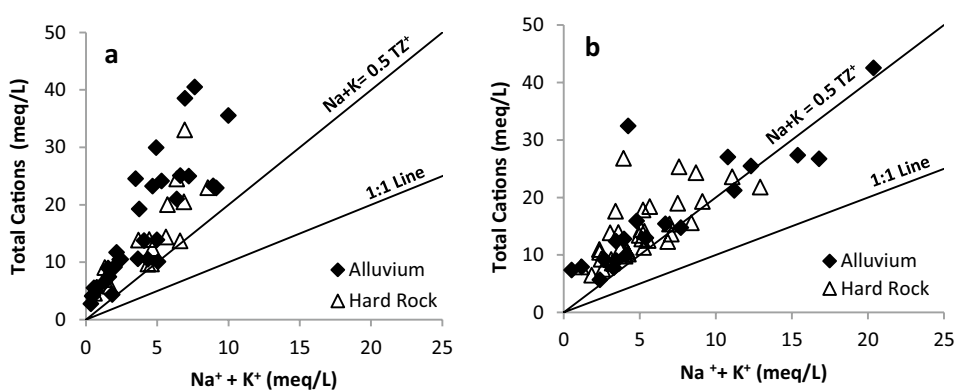


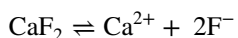
Fig. 9 Relationship between total cations and $\text{Na}^+ + \text{K}^+$ for **a** pre and **b** postmonsoon



fluoride ions from the aquifer material to groundwater (Jagadeshan et al. 2015).

(b) Rock–water interaction

(i) Mineral precipitation and dissolution Fluorite dissolution affects fluoride ion concentration according to the following equation (Brown and Roberson 1977) which also shows that the activities of calcium and fluoride are negatively correlated (Kumar and Singh 2015):



$$K_{\text{CaF}_2} = a(\text{Ca}^{2+})$$

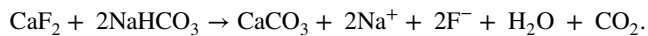
$$a(\text{F}^-)^2 = 10^{-10.58} \text{ at } 25^\circ\text{C},$$

where K = solubility product constant, a = activities of the corresponding ions.

A negative correlation between Ca^{2+} with F^- for the hard rock premonsoon samples Regression coefficient ($R^2 = 0.0267$) and positive correlation for the alluvium samples ($R^2 = 0.1287$) was observed from the Ca^{2+} vs F^- scatter plot (Fig. 10a). In the postmonsoon samples (Fig. 10b), however, a negative regression coefficient for both the alluvium ($R^2 = 0.0073$) and hard rock ($R^2 = 0.017$)

samples showing that increase in fluoride ion concentration might be linked to the decrease in calcium ion concentration in solution.

Decreasing Ca^{2+} concentrations are observed under alkaline conditions with a corresponding rise in Na^+ ions in regions having high fluoride concentrations. Furthermore, sodium carbonate type water in weathered rock formations allow precipitation of calcite from Ca^{2+} and CO_3^{2-} ions accelerating the dissolution of CaF_2 according to the following equation (Raju et al. 2012):



This positive correlation observed between sodium and fluoride in the postmonsoon (Fig. 11b) alluvium samples as well as the alkaline aquifer conditions suggests that the above reaction might be taking place. Removal of Ca^{2+} ions from groundwater through mineral precipitation in the postmonsoon alluvial samples, therefore, seems to cause enhanced dissolution of fluoride-bearing minerals (e.g., fluorite and fluorapatite), thereby increasing its concentration in the postmonsoon season. Also, Na^+ ion concentration increases from pre to postmonsoon season within both the aquifer samples. The reaction represented by the equation above may contribute to the increase in Na^+ ion apart from other processes such as ion exchange and evaporation.

Fig. 10 Relationship between Ca^{2+} and F^- concentration for **a** pre and **b** postmonsoon

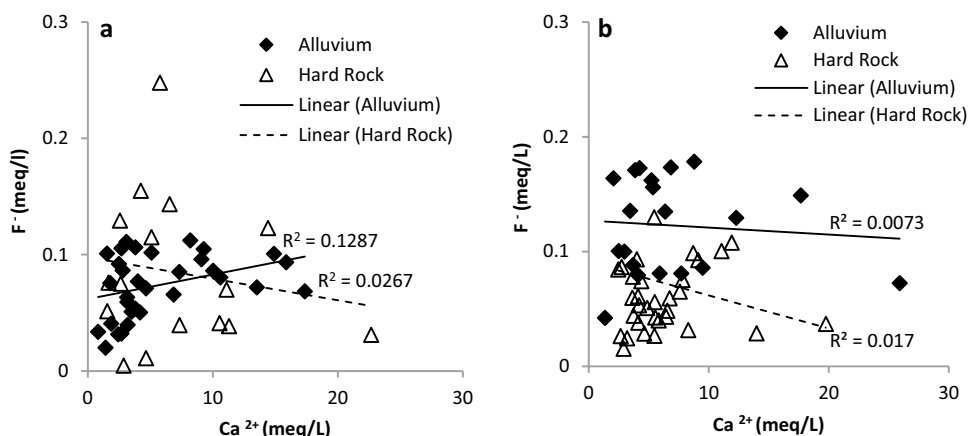
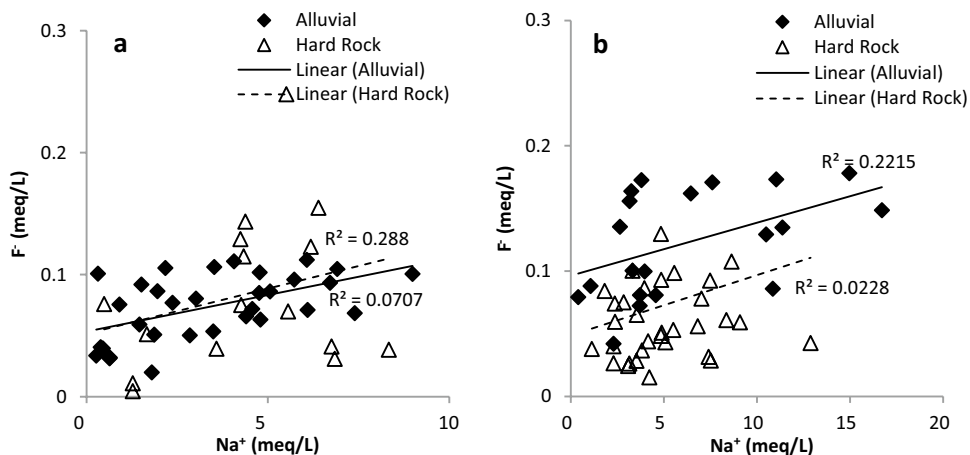


Fig. 11 Relationship between Na and F for **a** pre and **b** postmonsoon



Undersaturation of fluorite in the premonsoon and postmonsoon samples shows further dissolution of fluorite to take place. Moreover, when groundwater reacts with gneissic rocks bearing fluoride minerals for a prolonged period, it continuously gets enriched in the groundwater, even after the saturation of fluorite (Saxena and Ahmed 2003). This takes place due to the removal of Ca^{2+} ion through calcite (CaCO_3) precipitation which is evident from the presence of calcium carbonate gravels (kankars) in the soil of the alluvial region (Supplementary Fig. 6). The removal of Ca^{2+} ion would cause continuous fluorite mineral dissolution and therefore an increase in fluoride ion concentration is observed in the alluvial aquifer samples (Daniel and Karuppasamy 2012).

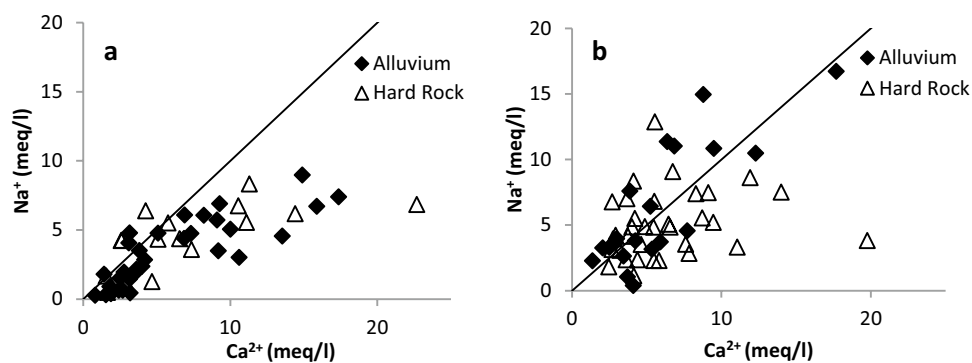
(ii) Ion exchange Apart from weathering and mineral dissolution/ precipitation, the increase in fluoride ion concentration seems to be enhanced by other geochemical processes such as ion exchange mainly in the postmonsoon season in the alluvial aquifers. The Chaddha plot (modified piper diagram) (Supplementary Fig. 4, Table 3) for the samples in both seasons within the alluvial and hard rock aquifers

shows that a major percentage of sample water is derived from reverse ion exchange processes.

This reverse ion exchange taking place on the surface of clay particles leads to the increase in Ca^{2+} ion concentration in the premonsoon season which is validated by plotting the Na^+ vs. Ca^{2+} scatter plot. In the premonsoon samples, 90% of points from the alluvial aquifer and 85% of points from the hard rock aquifers (Fig. 12a) fall close to and below the equiline suggesting the depletion of Na^+ ions with respect to Ca^{2+} and Mg^{2+} ions in solution. This occurs by the adsorption of Na^+ and K^+ at favorable sites within the aquifer matrix upon release of Ca^{2+} and Mg^{2+} ions into the groundwater (Zaidi et al. 2015). Although the affinity for Na^+ and K^+ ion is lower in comparison to Ca^{2+} and Mg^{2+} ions, the high concentration of Na^+ in solution, possibly due to their contribution from evaporative processes occurring simultaneously, facilitates their adsorption on the surface of clay particles (e.g., Kaolinite, illite, and montmorillonite) within the aquifer and soil sediments.

Alternatively, for the postmonsoon alluvial samples, 50% of points fall above the equiline (Fig. 12b) suggestive of direct ion exchange process also taking place causing uptake

Fig. 12 Relationship between Ca^{2+} and Na^+ for **a** pre and **b** postmonsoon



of Ca^{2+} ion upon release of Na^+ and K^+ ions into the groundwater. This uptake of calcium enhances fluorite mineral dissolution causing the increase in fluoride ion concentration.

(c) Effect of evaporation

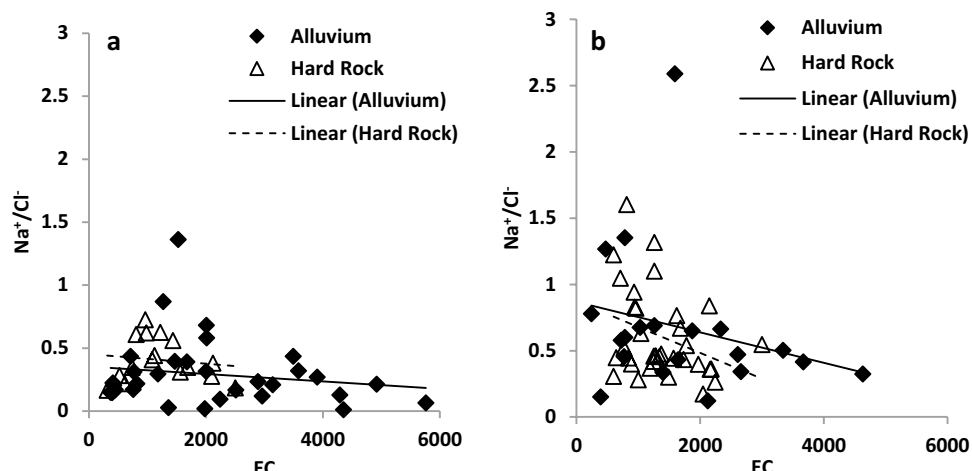
High temperatures in the summer season increase the solubility and the rate of dissolution of most soil minerals (Hem 1985). In the absence of surface drainage, slopes allowing natural water migration are limited. This along with local geomorphology leads to water accumulation/logging (Saini and Mujtaba 2002). Evaporation of accumulated irrigation water leads to precipitation of salts within the unsaturated soil layers in the hot summer months. This process termed as soil salt efflorescence leads to the subsequent leaching of the precipitated soil salts in the groundwater through percolation causing increase in ionic concentrations for Ca^{2+} , Na^+ , HCO_3^- , and Cl^- (Bowles et al. 1982). It is estimated that evaporation causes an increase in all ionic concentrations in the groundwater; however, prevalence of evaporation can be identified if the Na^+ versus Cl^- ratio remains constant with increase in EC, assuming that no mineral species is precipitated (Jankowski and Acworth 1997). Moreover, it has been observed in arid and semi-arid regions experiencing

high temperature and less rainfall that soil becomes alkaline in nature primarily due to evaporative processes. The alkaline condition of the soil enhances leaching of fluoride ions from clayey soils in the presence of high bicarbonate concentration, thereby increasing fluoride ion concentration in groundwater. This process seems to be prevalent in the alluvial soils of the region.

As seen from the Gibbs plot (Fig. 3b) for the premonsoon samples, evaporation process is active in the summer months (premonsoon) majorly for the alluvium samples along with rock–water interaction. The Na^+/Cl^- vs EC plot shows a horizontal trendline for both the aquifers for the premonsoon samples (Fig. 13a) further validating that the process of evaporation is also influencing the major ion groundwater chemistry. For the postmonsoon samples (Fig. 13b), the trendline shows a negative slope suggesting that evaporative processes are not predominant.

Evaporation leading to increase in Na^+ ion concentration in groundwater further influences the desorption of Ca^{2+} ion in solution through reverse ion exchange processes. Ca^{2+} ion release into solution inhibits fluorite mineral dissolution which explains the lower values of fluoride ion concentration in the premonsoon alluvial samples compared to the postmonsoon samples.

Fig. 13 Relationship between Na^+/Cl^- vs EC for **a** pre and **b** postmonsoon season



Alternatively, in the postmonsoon samples, it can be seen from the Gibbs plot from both alluvial and hard rock aquifers that rock–water interaction is dominant over evaporation. This might cause a comparative decrease in Na^+ ion contribution through evaporation within the alluvial aquifers. A lower Na^+ concentration in the groundwater would therefore lead to direct ion exchange processes occurring within the aquifer matrix causing the uptake of Ca^{2+} ion upon release of Na^+ ion in solution. Therefore, the Na^+ ion concentration is observed to be higher in the postmonsoon alluvial aquifer samples as compared to the premonsoon samples. The uptake of Ca^{2+} enhances fluorite mineral dissolution leading to increase in fluoride ion concentration in the postmonsoon alluvial aquifer samples.

(d) Effect of landuse

Concentration of ions primarily derived from anthropogenic sources such as nitrate may reflect contamination from anthropogenic point sources such as agriculture, surface runoff, and irrigation. Anthropogenic input of fluoride into groundwater acts as a point source of contamination as reported by Datta and Tyagi (1996) through fluoride containing agro-chemicals (e.g., phosphate fertilizer). Also, zones of agricultural and urban landuse experience high nitrate ion concentration in groundwater due to leaching of chemical fertilizers and farm manure from irrigation return flow as well as sewage and septic discharge (Subramani et al. 2010).

The landuse landcover map of the study area (Supplementary Fig. 5) shows that the region of the alluvial aquifers is dominated by agricultural cropland. The region of hard rock aquifers has both agricultural land nearby surrounded by barren scrubland. The data from the study area for both hard rock and alluvial aquifers (Supplementary Table 2) showed that values of nitrate ion concentration were both stable and below permissible limits from the pre to the postmonsoon season. This indicates that agricultural activity and canal irrigation although being prevalent in the alluvial as well as around the hard rock aquifers, do not adversely influence the groundwater quality of both aquifers and therefore agriculture is not a major source of fluoride contamination in the aquifer waters.

Datta and Tyagi (1996) reported that brick industries could act as point sources of fluoride contamination due to the use of fluoride salts. This leads to very high concentration of fluoride ion in the aquifer samples near to the brick kilns. In the study area, the higher concentration of fluoride ion concentration (2.71–4.68 ppm) in the premonsoon season is observed in the hard rock aquifers which do not have brick kilns located close by; therefore, anthropogenic influence of brick kilns can be ruled out for the hard rock aquifers sampled. Moreover, if brick kilns were the major sources of direct fluoride contamination of groundwater in the aquifers

sampled, the concentration of fluoride ion would be high in all seasons due to continuous input of fluoride salts. Hence, both agricultural activity and brick industries do not seem to be major sources of fluoride contamination of groundwater within the alluvial region.

Conclusion

The premonsoon hydrochemistry within the alluvial aquifers of the study area is largely influenced by evaporation, carbonate weathering, and rock–water interaction. These processes lead to the increase in Ca^{2+} ion concentration in groundwater which impedes fluorite mineral dissolution, thereby controlling the fluoride ion concentration in the premonsoon season. In the postmonsoon season, increase in fluoride ion concentration is brought about by fluorite mineral dissolution as well as uptake of Ca^{2+} ions from solution in exchange for Na^+ ion primarily through silicate weathering of fluorite bearing rocks and direct ion exchange processes.

Acknowledgements The authors are thankful to Advanced Instrumentation Research Facility at Jawaharlal Nehru University for providing XRD facility for soil XRD analysis. They are also thankful to the editor of Environmental Earth Sciences Journal and the anonymous reviewers for their valuable suggestions and comments which greatly helped to improve this manuscript.

Compliance with ethical standards

Conflict of interest All the co-authors declare that there are no conflicts of interest.

References

- APHA (1995) Standard methods for the examinations of water and waste water, 19th edn. American Public Health Association, Washington
- Apodaca LE, Jeffrey BB, Michelle CS (2002) Water quality in shallow alluvial aquifers, Upper Colorado River Basin, Colorado, 1997. *J Am Water Res Assoc* 38(1):133–143. <https://doi.org/10.1111/j.1752-1688.2002.tb01541.x>
- Bowles DS, Nezafati H, Bhasker RK, Riley JP, Wagenet RJ (1982) Salt LOADING FROM EFFLORESCENCE AND SUSPENDED SEDIMENTS IN the Price River Basin. Reports. Paper 585. http://digitalcommons.usu.edu/water_rep/585
- Brindha K, Elango L (2013) Geochemistry of fluoride rich groundwater in a weathered granitic rock region, Southern India. *Water Qual Exposure Health* 5(3):127–138. <https://doi.org/10.1007/s12403-013-0096-0>
- Brown DW, Roberson CE (1977) Solubility of natural fluorite at 25 °C. *US Geol Surv J Res* 5(4):506–517
- Cerling TE, Pederson BL, Damm KLV (1989) Sodium–calcium ion exchange in the weathering of shales: implications for global weathering budgets. *Geology* 17:552–554. [https://doi.org/10.1130/0091-7613\(1989\)017](https://doi.org/10.1130/0091-7613(1989)017)
- Chenini I, Farhat B, Mammou AB (2010) Identification of major sources controlling groundwater chemistry from a multilayered

- aquifer system. *Chem Spec Bioavail* 22(3):183–189. <https://doi.org/10.3184/095422910X12829228276711>
- Chopra S (1990) A geological cum geomorphological framework of Haryana and adjoining areas for landuse appraisal using LAND-SAT imagery. *J Indian Soc Remote Sens* 18(1):15–22. <https://doi.org/10.1007/BF03017813>
- Daniel J, Karuppasamy S (2012) Evaluation of fluoride contamination in groundwater using remote sensing and GIS techniques in Virudhunagar District. *Int J Adv Remote Sens GIS* 1:12–19
- Daniele L, Vallejos A, Corbella M, Molina L, Pulido-Bosch A (2013) Hydrogeochemistry and geochemical simulations to assess rock water interactions in complex carbonate aquifers: the case of Aguadulce (SE Spain). *Appl Geochem* 29: 43–54. <https://doi.org/10.1016/j.apgeochem.2012.11.011>
- Datta PS, Tyagi SK (1996) Major ion chemistry of groundwater Delhi area: chemical weathering processes and groundwater flow regime. *Geol Soc India* 47(2):179–188. <https://doi.org/10.12691/jgg-2-5A-4>
- Datta PS, Desai DI, Gupta SK (1980) Hydrological investigations in Sabarmati basin. I. Groundwater recharge estimation using tritium tagging method. *Proc Indian Nat Sci Acad Part A* 46(1):84–98
- Elango L, Kannan R, Kumar S (2003) Major ion chemistry and identification of hydrogeochemical processes of groundwater in a part of Kancheepuram district, Tamil Nadu, India. *J Environ Geosci* 10(4):157–166. <https://doi.org/10.1306/eg100403011>
- Fawell J, Bailey K, Chilton J, Dahi E, Fewtrell L, Magara Y (2006) Fluoride in drinking-water. World Health Organisation, IWA Publishing London, pp 5–24
- Fisher RS, Mulican WF III (1997) Hydrochemical evolution of sodium–sulphate and sodium–chloride groundwater beneath the Northern Chihuahuan desert, Trans-Pecos, Texas, USA. *Hydrogeol J* 10(4):455–474. <https://doi.org/10.1007/s100400050102>
- Freeze RA, Cherry JA (1979) Groundwater. Englewood Cliffs, Prentice Hall 604
- Gibbs RJ (1970) Mechanisms controlling world water chemistry. *Sci J* 170:795–840. <https://doi.org/10.1126/science.170.3962.1088>
- Groundwater Information Booklet – Faridabad District, Haryana (2007a) Central Groundwater Board, Ministry of Water Resources, Govt. of India
- Groundwater Information Booklet – Gurgaon District, Haryana (2007b) Central Groundwater Board, Ministry of Water Resources, Govt. of India
- Groundwater Information Booklet – Jhajjar District, Haryana (2007c) Central Groundwater Board, Ministry of Water Resources, Govt. of India
- Groundwater Information Booklet – Rohtak District, Haryana (2007d) Central Groundwater Board, Ministry of Water Resources, Govt. of India
- Groundwater Information Booklet – Sonipat District, Haryana (2007e) Central Groundwater Board, Ministry of Water Resources, Govt. of India
- Gupta R, Misra AK (2014) Groundwater Fluoride in Haryana State: a review on the status and its mitigation, study of civil engineering and architecture (SCEA), 3, pp 24–28
- Hem JD (1985) Study and interpretation of the chemical characteristics of natural water. US Geological Survey Water Supply paper, p 2254
- Jagadesan G, Kalpana L, Elango L (2015) Major ion signatures for identification of geochemical reactions responsible for release of fluoride from geogenic sources to groundwater and associated risk in Vaniyar River basin, Dharmapuri district, Tamil Nadu, India. *Environmental Earth Sciences*. <https://doi.org/10.1007/s12665-015-4250-9>
- Jankowski J, Acworth RI (1997) Impact of debris-flow deposits on hydrogeochemical processes and the development of dryland salinity in the Yass River catchment, New South Wales, Australia. *Hydrogeol J* 5(4):71–88. <https://doi.org/10.1023/A:1006352922219>
- Kumar A, Singh CK (2015) Characterization of hydrogeochemical processes and fluoride enrichment in groundwater of South-Western Punjab. *Water Qual Expo Health* 7:373–387. <https://doi.org/10.1007/s12403-015-0157-7>
- Kumar M, Ramanathan AL, Rao MS, Kumar B (2006) Identification and evaluation of hydrogeochemical processes in the groundwater environment of Delhi, India. *Environ Geol* 50:1025–1039. <https://doi.org/10.1007/s00254-006-0275-4>
- Kumari R, Singh CK, Datta PS, Singh N, Mukherjee S (2013) Geochemical modelling, ionic ratio and GIS based mapping of groundwater salinity and assessment of governing processes in Northern Gujarat, India. *Environ Earth Sci* 69:2377–2391. <https://doi.org/10.1007/s12665-012-2067-3>
- Maya AL, Loucks MD (1995) Solute and isotopic geochemistry and groundwater flow in the Central Wasatch Range, Utah. *J Hydrol* 172:31–59. [https://doi.org/10.1016/0022-1694\(95\)02748-E](https://doi.org/10.1016/0022-1694(95)02748-E)
- Mrazovaca S, Miloradov MV, Matic I, Maric N (2013) Multivariate statistical analysis of chemical parameters of groundwater in Vojvodina. *Chem Erde* 73:217–225. <https://doi.org/10.1016/j.chemer.2012.11.002>
- Rajmohan N, Elango L (2004) Identification and evolution of hydrogeochemical processes in the groundwater environment in an area of the Palar and Cheyyar River Basins, Southern India. *Environ Geol* 46:47–61. <https://doi.org/10.1007/s00254-004-1012-5>
- Raju NJ, Dey S, Gossel W, And Wycisk P (2012) Fluoride hazard and assessment of groundwater quality in the semi-arid upper Panda River basin, Sonbhadra district, Uttar Pradesh, India. *Hydrol Sci J* 57(7):1433–1452. <https://doi.org/10.1080/02626667.2012.715748>
- Saini HS, Mujtaba SAI (2002) Anatomy, crisis and management of flooding in Gurgaon District of Haryana. In: Dubey CS, Saklani PS (eds) *Geoindicator and related environmental studies focus on India*. Pilgrim publication, New Delhi, pp 153–162
- Saleh A, Al-Ruwaih F, Shehata M (1999) Hydrogeochemical processes operating within the main aquifers of Kuwait. *J Arid Environ* 42:195–209. <https://doi.org/10.1006/jare.1999.0511>
- Sarin MM, Krishnaswamy S, Dilli K, Somayajulu BLK, Moore WS (1989) Major ion chemistry of the Ganga-Brahmaputra river system: Weathering process and fluxes to the Bay of Bengal. *Geochim Cosmochim Acta* 53:997–1009. [https://doi.org/10.1016/0016-7037\(89\)90205-6](https://doi.org/10.1016/0016-7037(89)90205-6)
- Saxena VK, Ahmed S (2003) Inferring the chemical parameters for the dissolution of fluoride in groundwater. *Environ Geol* 43:731–736. <https://doi.org/10.1007/s00254-002-0672-2>
- Schoeller H (1967) *Geochemistry of groundwater- an international guide for research and practice*. UNESCO, Chap. 15, pp. 1–18
- Shekhar S, Purohit RR, Kaushik YB (2015) Groundwater management in NCT Delhi, Central Ground Water Board, pp 1–10
- Stallard RF, Edmond JM (1983) Geochemistry of the Amazon, the influence of geology and weathering environment on the dissolved load. *J Geophys Res* 88:9671–9688. <https://doi.org/10.1029/JC088iC14p09671>
- Subramani T, Elango L, Damodarasamy SR (2005) Groundwater quality and its suitability for drinking and agricultural use in Chithar River basin, Tamil Nadu, India. *J Environ Geol* 47:1099–1110. <https://doi.org/10.1007/s00254-005-1243-0>
- Subramani T, Rajamohan N, Elango L (2010) Groundwater geochemistry and identification of hydrogeochemical processes in a hard rock region, Southern India. *Environ Monit Assess* 162:123–137. <https://doi.org/10.1007/s10661-009-0781-4>
- Zaidi FK, Nazzal Y, Jafri MK, Naeem M, Ahmed I (2015) Reverse ion exchange as a major process controlling the groundwater chemistry in an arid environment: a case study from northwestern Saudi Arabia. *Environ Monit Assess* 187(10):607

PROFORMA FOR BIO-DATA (to be uploaded)

1. **Name and full correspondence address:** Dr. Prodyut Bhattacharya, Room no 102, Block A, University School of Environment Management, Guru Gobind Singh Indraprastha University, Sector-16- C; Dwarka, New Delhi-110078, India
2. **Email(s) and contact number(s):** prodyutbhattacharya@yahoo.com, 91-9560866868
3. **Institution:** University School of Environment Management, Guru Gobind Singh Indraprastha University, New Delhi
4. **Date of Birth:** 24 August 1964
5. **Gender (M/F/T):** Male
6. **Category:** Gen
7. **Whether differently abled:** No

8. Academic Qualification (Undergraduate Onwards)

	Degree	Year	Subject	University/Institution	% of marks
1.	Bachelor of Science	1986	Botany, Anthropology, Zoology	Calcutta University, Kolkata	62.8
2.	Masters of Science	1989	Botany (specialization in Forest Ecology)	Dr.H. S. Gour University, Sagar, MP	68.5
3.	Doctoral of Philosophy (PhD)	1992	Ethno-botany and Ecological status of Medicinal Plants	Dr.H. S. Gour University, Sagar, MP	N.A.
4.	Community Forestry Programme (Certificate course)	1999	Forestry, Livelihood, NTFP, Gender, Conflict, Policy	Kasetsart University, Thailand	N.A.

9. Ph.D thesis title, Guide's Name, Institute/Organization/University, Year of Award:

“Studies on medicinal plants in forest of chhindwara district with special reference to ethnobotanical aspect”, Professor GP Mishra, Department of Botany, Dr H.S. Gaur University, SAGAR, M.P. (1992)

10. Work experience (in chronological order).

S.No.	Positions held	Name of the Institute	From	To	Pay Scale
1	CSIR Research Fellow	State Forest Research Institute, Jabalpur and University of Sagar, M.P	July 1989	April 1992	NA
2	Senior Ecologist	Indian Institute of Social Research & Development (IBRAD), Calcutta	April 1992	July 1994	NA

3	Assistant Professor	Indian Institute of Forest Management, Bhopal	July 1994	Feb 2006	37000-57000/- HRD scale
4	Associate Professor	Indian Institute of Forest Management (IIFM), Bhopal	February 2006	19 th April 2010	37000-67000 +AGP 9500/-
5	Professor	University School of Environment Management, Guru Gobind Singh Indraprashtha University	20 th April 2010	Till Date	37000-67000+AGP 10000/-
6	Dean	University School of Environment management, GGS Indrprastha University	12 th Aug 2011	11 th Aug 2014	37000-67000 +AGP 10000/-
7	Controller of Examinations	Guru Gobind Singh Indraprastha University, Delhi	17 th March 2020	1 st May 2021	
8	Professor & Director, Coordination	Guru Gobind Singh Indraprastha University, Delhi	1 st May 2021	Till Date	144200-218200/-

11. Professional Recognition/ Award/ Prize/ Certificate, Fellowship received by the applicant.

S.No	Name of Award	Awarding Agency	Year
1.	Technical Committee Expert Group member for Asia Pacific Small holders	Forest Stewardship Council (FSC)	2020
2.	Member –Expert group of Planning commission	Planning Commission, Govt. of India	2011-2012.
3.	Fellow, Beahrs Environmental Leadership Programme	University of California, Berkeley, USA,	2005
4.	Convener of the Indian Forest Governance Learning Group	supported by IIED, UK	2007 to 2010
5.	Member	International Society of Tropical Foresters	2017 onwards.
6.	Membership awarded	FSC Hong Kong	2017
7	Editorial Committee Member	International and National Journals	
8	Awarded fellowship	Queensland University, Australia and Queensland Forestry Research Institute	1996.
9	Awarded Fellowship	Kasetsart University, Bangkok	1996
10	Awarded for Research Fellow	CSIR	1991
11	Awarded for Young Scientist Award	Council of Science & Technology, Government of Madhya Pradesh, Bhopal.	1992

12. Publications (List of papers published in SCI Journals, in year wise descending order (last 5 year).

S.No.	Author(s)	Title	Name of	Volume	Page	Year
-------	-----------	-------	---------	--------	------	------

			Journal			
1	Kumar, D., Velankar, A.D., Rao, N.V., Kumara, H.N., Mishra, P., Bhattacharya, P., & Raj, V.M.	Ecological determinants of occupancy and abundance of chinkara (<i>Gazella bennettii</i>) in Yadahalli Wildlife Sanctuary, Karnataka, India	<i>Current Science</i>	118 (2)	264-270	2020
2	Khosla, Ayesha & Bhattacharya, Prodyut.	Review of Various Initiatives for Tribal Development in Tripura within the purview of Forest Rights Act, 2006.	<i>International Journal of Research in Social Sciences</i>	10 (8)	15-29.	2020
3	Mishra, R., Dookia, S. & Bhattacharya, P.	Avenue Plantations as Biodiversity Havens: A Case Study of Population Status of the Indian Flying Fox, <i>Pteropus giganteus</i> Brunnich, 1782 and Implications for Its Conservation in the Urban Megacity, Delhi, India	Proc Zool Soc	73	127–136	2020
4	Khosla, A., & Bhattacharya, P.	Assessment of Socio-Economic and Livelihood Conditions Post Forest Rights Act: A comparative study of Two Tribal Districts in Tripura.	<i>Indian Journal of Social Work</i>	80(4).	477-500	2019
5	Yadav, Seema Prodyut Bhattacharya, Kuldeep Srivastava	Analysing long term seasonal and annual trends for precipitation and temperature in Central India. Mausam	Mausam	70	523-532	2019
6	Rajlakshmi Mishra, Sumit Dookia *, Manoj Kumar Singh, Aisha Sultana, Prodyut Bhattacharya	Ecological and Acoustic-call Characteristics of Blyth's Horseshoe bat, <i>Rhinolophus lepidus</i> in Delhi, India	<i>Ambient Science</i>	05	online	2018

13. Detail of patents. NO

14. Books/Reports/Chapters/General articles etc. (last 5 year)

S.No	Title	Author's Name	Publisher	Year of Publication
1.	REDD+ in the Indian Context: Planning and Implementation Scenario. In: <i>Climate Resilience and Environmental Sustainability Approaches Global</i>	Prodyut Bhattacharya and Swapan Mehera	Springer Nature	2021

	<i>Lessons and Local Challenges</i>			
2.	Predicting impact of climate change on geographical distribution of major NTFP species in the Central India Region. Modeling Earth Systems and Environment	Seema Yadav, Prodyut Bhattacharya, G. Areendran Mehebub Sahana, Krishna Raj, Haroon Sajjad	Springer Nature	2021
3.	Comparative Analysis of Different Vegetation Indices of Noida City Using Landsat Data	Sharma R., Pradhan L., Kumari M., Bhattacharya P	Springer Nature, Singapore	2021
4.	Assessment of Carbon Sequestration Potential of Tree speaces in Amity University Campus Noida. In Environmental Sciences Proceedings	Sharma, R., Pradhan, L, Kumari,M, & Bhattacharya, P.	Multidisciplinary Digital Publishing Institute.	2020
5.	Redefining Forestry for Effective Livelihoods	Prodyut Bhattacharya	TERI Press, New Delhi	2018

15. Any other Information (maximum 500 words)

Number of PhD Students 7

Number of Post doctoral students 0

SCHEDULED CASTE CERTIFICATE

This is to Certify that Shri/Smt./Km. **रामेश्वर**
 Shri/Smt./Km. **प्रिया**
 of Village/Town **मुमुक्षु**
 in District/Division/Hinor of the State of Haryana, belongs to the **रामेश्वर**
 Block - **मुमुक्षु** Caste which is registered as a scheduled caste under -
 The Constitution (Scheduled Castes) Order, 1950.
 The Constitution (Scheduled Tribes) Order, 1950.
 The Constitution (Schedule Caste Union Territories) order, 1951.
 The Constitution (Scheduled Tribes) Union Territory order, 1951.
 As amended by the Scheduled Castes and Scheduled Tribes modification order, 1964.
 The Homi-Bhabha (Amendment) Act, 1966 the Punjab reorganisation Act, 1966 the State of Haryana Act, 1971, the North Eastern area reorganisation Act, 1971 and the Scheduled Castes and Scheduled Tribes order (Amendment) Act, 1978.
 The Constitution (Maa & Kusum) Scheduled Caste order, 1956.
 The Constitution (Andaman and Nicobar Islands) Scheduled Tribes, 1959 as amended by the Scheduled Castes and Scheduled Tribes order (Amendment) Act, 1974.
 The Constitution (Maa & Nagara Hanuman) Scheduled Caste order, 1960.
 The Constitution (Andamans) Scheduled Caste order, 1964.
 The Constitution (Scheduled Tribes) Uttar Pradesh order, 1967.
 The Constitution (Maa, Dham & Hanuman) Scheduled Caste order, 1968.
 The Constitution (Maa, Dham & Didi) Scheduled Tribes order, 1968.
 The Constitution (Maa, Dham & Didi) Scheduled Tribes order, 1969.
 The Constitution (Maa & Kusum) Scheduled Caste order, 1970.
 The Constitution (Maa) Scheduled Caste order, 1972.
 The Constitution (Maa) Scheduled Tribes order, 1973.
 The Constitution (Maa & Kusum) Scheduled Tribes order, 1978.
 The Constitution (Maa & Kusum) Scheduled Tribes order, 1989.
 The Constitution (ST) Order (Amendment) Act, 1990.
 The Constitution (ST) Order (Amendment) ordinance, 1990.
 The Constitution (ST) Order (Second Amendment) Act, 1991.
 The Constitution (ST) Order (Amendment) ordinance, 1991.

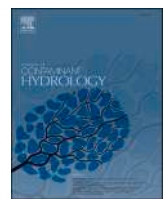
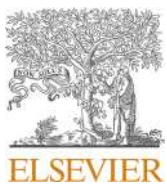
This Certificate is issued on the basis of the Scheduled Caste Certificate issued to
 Shri/Smt./Km. Father/Mother of
 Shri/Smt./Km. of Village/Town
 in Dist/Division of the State/Union Territory
 who belongs to the caste which is recognised as a Scheduled Caste in the State/Union Territory issued
 by the Dated

Shri/Smt./Km. and/or his/her family ordinary resides in
 Village/Town of Dist/Division/Hinor of the State of Haryana.

This Certificate is issued as per the Verification by the Tehsildar/Naib Tehsildar **रामेश्वर** **प्रिया**

No.
 Dated **10/10/16**
 Place

Sub Divisional Magistrate
रामेश्वर
 of **भीमानी**
 City Magistrate



Impact of limestone caves and seawater intrusion on coastal aquifer of middle Andaman



Pardeep Kumar, Saumitra Mukherjee*

School of Environmental Sciences, Jawaharlal Nehru University, New Delhi, India

ARTICLE INFO

Keywords:

Limestone caves
Seawater intrusion
Hydrogeochemical investigation
Middle Andaman
Ionic ratios

ABSTRACT

Seawater intrusion has become a common problem in coastal and island aquifers with the rise in climate change that greatly affects the majority of developing countries. The island hydrology is very complex and associated with a unique set of environmental characteristics with the dynamic interaction of groundwater, surface water, and seawater. Further, Sea level rise, erratic rainfall, and over-extraction of groundwater triggered salt-water intrusion. A study on seawater intrusion and the effect of limestone caves on groundwater was carried out in middle Andaman using a combination of ionic ratios of major ions. A total of 24 samples and a reference sample from the sea were collected and analysed using ICP, spectrophotometer, and flame photometer. A combination of 10 ionic ratios Cl/HCO_3 , $\text{Ca}/(\text{HCO}_3 + \text{SO}_4)$, $(\text{Ca} + \text{Mg})/\text{Cl}$, Ca/Mg , Ca/Na , $\text{Cl}/(\text{SO}_4 + \text{HCO}_3)$, Ca/SO_4 , K/Cl , Mg/Cl , and SO_4/Cl was used to assess the dissolution of limestone minerals and the level of saltwater intrusion into groundwater. The geospatial method was used to extract and combine all the hydrogeochemical parameters and ionic ratios in the GIS platform. Durov plot was used for the interpretation of groundwater chemistry and the identification of natural processes controlling the hydrogeochemistry of the area. The dominance of $\text{Ca}-\text{HCO}_3$ and $\text{Na}-\text{HCO}_3$ was confirmed in 48% and 24% of the sample respectively. The equiline graph of chloride with other major ions showed the enrichment of alkali and alkaline earth metal salt in groundwater. Schoeller's diagram depicted the dominance of Cl , Ca , and the sum of CO_3 and HCO_3 in seawater near Mayabunder. The lower concentration of Na with respect to Cl (64%) and Ca (100%) showed the presence of a reverse ion exchange process. Further, the correlation matrix showed a strong relationship between Cl , K , Ca , and Na . The analysis of X-ray diffraction of the rock samples confirmed the presence of limestones such as Aragonite, Calcite, Chlorite, Chromite, Dolomite, Magnetite, and Pyrite in the study area. The integration of ionic ratios showed moderately affected and slightly affected saline regions in 44% and 54% of the region respectively. Finally, the role of tectonic activities and active lineaments connected to the sea was found to play a major role in the intrusion of seawater where interconnected faults created an opening for surface water to recharge groundwater leading to the deep aquifer.

1. Introduction

Groundwater is a prominent source of water for drinking, domestic, irrigation, and industrial usage in villages and cities in major countries (Adimalla et al., 2020; Gill et al., 2017; Subramani et al., 2005). The quantity and quality of groundwater are two significant aspects that sustain life on Earth. The insufficient availability of surface water to meet the increased water requirement has led to more dependency on groundwater to fulfil the demand for potable water supply. Therefore, quality of groundwater quality has become an important concern in many parts of the country. The source of groundwater contamination is

mainly through interaction with minerals, atmospheric precipitation, recharging water quality along with anthropogenic pollution coming from domestic, agricultural, and industrial activities (Li et al., 2021; Selvakumar et al., 2017; Tamta, 2003; Srivastava et al., 2012).

Seawater intrusion is one of the most common and widespread sources of groundwater contamination in Islands and coastal region of the world (Akshitha et al., 2021; Naily, 2018; Abdalla et al., 2015; Ahmed et al., 2013; Allow, 2012; Abdollahi-Nasab et al., 2010; Lee and Song, 2007; Post, 2005; Chidambaram et al., 2014). The identification and assessment of seawater intrusion are very important for the prevention and mitigation of contamination in aquifers. The seawater

* Corresponding author at: School of Environmental Sciences, Jawaharlal Nehru University, New Delhi 110067, India.
E-mail address: saumitramukherjee3@gmail.com (S. Mukherjee).

intrusion of an aquifer in island areas is a product of multiple salinization processes with different sources of water. Climate change such as erratic rainfall, accelerated sea-level rise, and the over-extraction of groundwater, increases the lateral movement of seawater into groundwater (Werner, 2010; Dragoni and Sukhija, 2008). Natural occurring rocks containing minerals like halite and anthropogenic effluents from households, agriculture, and industries are other possible causes of groundwater contamination (Rena et al., 2022; Singh et al., 2018; Rajkumar et al., 2010; Milnes, 2011; Jones et al., 1999; Custodio, 2010). The interaction of island aquifer with seawater is associated with several processes such as mineral dissolution or precipitation of salt/s, reverse ion exchange, and the reduction of sulphate which indicate the intensity of salinization in groundwater (Rani et al., 2021; Sakram et al., 2013; Elango and Kannan, 2007; Appelo and Postma, 2005). The groundwater intrusion is further controlled by several parameters like the difference in the rate of recharge and rate of discharge of freshwater in the aquifer, distance from the shoreline, hydraulic conductivity, aquifer depth, and the confining units in the aquifer which prevents the movement of saltwater vertically upward or inside the aquifer (Saidi et al., 2013; Barlow and Reichard, 2010).

The groundwater quality can be deteriorated by mixing only 2% of saltwater, studies have shown that 4% of mixing can lead to significant impairment of groundwater quality causing adverse environmental conditions. If the mixing of saltwater increases to 6%; it becomes unsuitable for human consumption but can be used by some industries (Srinivasamoorthy et al., 2013; Mondal et al., 2011; Custodio, 2010; Darnault and Godinez, 2008).

Since seawater intrusion is so complex and geochemically connected, it further requires a combination of indicators to study its occurrences in the islands (Bhagat et al., 2021; Sajil Kumar, 2016; Kazakis et al., 2016; Rajmohan and Elango, 2004).

Seawater intrusion has been investigated or monitored using approaches like geophysical, geochemistry, and groundwater flow models. Age, transport pathways, and seawater wedge theory can be identified through isotopes and water chemistry (Mohanty and Rao, 2019; Ganyaglo et al., 2017; Werner and Simmons, 2009; Vengosh, 2003; Louvat et al., 1999; Naidu et al., 2013). Since these above-stated studies are very costly, the study of ratios of major ion concentration is the only feasible way for saline water delineation.

Studies have shown that freshwater has a dominance of major ions such as calcium, magnesium, bicarbonates, sulphates, chloride, sodium, and potassium while seawater majorly contains chloride and sodium ions only, thus, intrusion of seawater inland aquifers may be detected by analyzing the increase in these ions in the aquifers (Srinivasamoorthy et al., 2013; Mondal et al., 2011; Todd and Mays, 2004; Bear et al., 1999). The concentration of these ions changes from the recharging area to discharging area of aquifers connected to the sea and the ionic ratios of major ions change at the interaction of groundwater and seawater through ion-exchange processes and oxidation-reduction reactions (Naily, 2018; Marimuthu et al., 2005; Stoessell, 1997; Gimenez and Morell, 1997). As a result, a lot of ionic ratios have been proposed to identify salinization in coastal areas; such as Na/Cl, Ca/Mg, Ca/Na, and Cl/(HCO₃ + SO₄) (Asare et al., 2021; Carol and Kruse, 2012; Marimuthu et al., 2005; Lee and Song, 2007; Panno et al., 2006; Gimenez and Morell, 1997; Vengosh, 2003). The change in the ratio of the molar concentration of ions associated with seawater intrusion may give dissimilar results. Therefore, an integration of their result is used to arrive at a consistent decision. The current research has also included the hydrogeological assessment of aquifer, spatial and statistical analysis of ionic ratios, correlation analysis of major ions, major hydro-chemical processes, X-ray diffraction of rocks, and finally inter-correlation of seawater intrusion with active faults and groundwater level of middle Andaman.

1.1. Study area

Middle Andaman is part of the Andaman and Nicobar group of islands system in the southeast part of the Indian subcontinent. The study area is a part of the Andaman series that lies between North Andaman and South Andaman connected through National Highway NH-223. The geographical extent of middle Andaman is 12°24'19.984" E to 12°55'38.788" E latitude and 92°48'15.417" N to 92°58'49.854" N longitude (Fig. 1). Most of the region (>80%) comprises a range of open to dense forests. The forest of the region is classified as moist deciduous and tropical evergreen forest. The vegetation of the Andaman Islands is similar to Malaysian islands and Burmese islands in comparison to the mainland of the Indian subcontinent. The biota species of the region belong to marine habitats. The island's beaches are the nesting sites of sea snakes and sea turtles (Ganeshaiah et al., 2019; Rao, 1996).

1.2. Geology of the area

Middle Andaman is part of the outer arc of the Arakan Yoma range that formed the main chain of Andaman and Nicobar Islands. It is made of sedimentary rocks mainly from marine deposits (Singha et al., 2019; Kumar, 1981; Jafri et al., 1993; Srinivasan, 1979). Limestone caves are formed in lithified rocks of aggregated particulate matter (Sankaran, 1998). The location of caves is controlled either by the source of sediments or their transformation into rocks (Gulam Rasool et al., 2022; Ford and Cullingford, 1976). Most limestone caves are formed by either underground drainage/erosion or sea cliffs or sea erosion of rocks (Challinor, 1967). Out of 384 caves found on the island, 61.5% are inland and 38.5% are sea shore, among inland caves 86% are underground, 1% are at the origin of streams, and the rest are above the ground either on inland cliffs or inland hills. They have very fragile ecosystems; their fauna is too sensitive to humidity, temperature, and light (Fig. 2).

The study area lies in earthquake and tsunami-prone areas which causes occasional damage to these caves. The impact on caves was first documented in 2004 earthquakes in both middle Andaman and North Andaman. It caused structural changes such as opening, closing, partial closing, narrowing, or widening of many existing caves. It was found that more damage had happened to caves that were above the ground than the caves below the ground (Manchi and Sankaran, 2009). The limestone in shallow water was found to be associated with the Mithakari mélange group of the Paleocene-Eocene age. Mélange itself is self-explanatory in indicating that there was a mixing of the lithological units due to tectonic activities. These mélanges when deposited as unconformity forms a suitable formation for groundwater exploration. Mithakari or Baratang Formation has two other members of the rock chain called Tugapur Limestone/ Berma Dera and Karmatang sandstone. Limestones i.e., lensoid and folded structures are in contact with sandstone units between Rangat and Mayabandar of middle Andaman. Berma Dera sector has an area of 4000 m² and a reservoir of approximately 10,000 tons per meter depth of limestone whereas the Tugapur sector has approximately 8500 tons per meter depth in a surface area of 3000 m². In the Buddha Nala, a reservoir of approximately 12,000 tons per meter depth of limestone is present on the surface of 5000 m² (Bandopadhyay and Carter, 2017).

1.3. Hydrology map of the area

Island receives abundant rainfall of approx. 3000 mm per annum but the undulating terrain with steep slopes, porous soil stratum, and its proximity to the sea leads to a loss of 75% of the annual rainfall. Also, the abundance of sedimentary rocks (70%) and the presence of clay minerals contribute to the unfavourable condition for rainfall percolation to sub-surface water (Fig. 3). Therefore, we are getting aquifers unsuitable for groundwater storage in both shallow and deep horizons. On the contrary, the presence of 15% coral rags or limestone formation

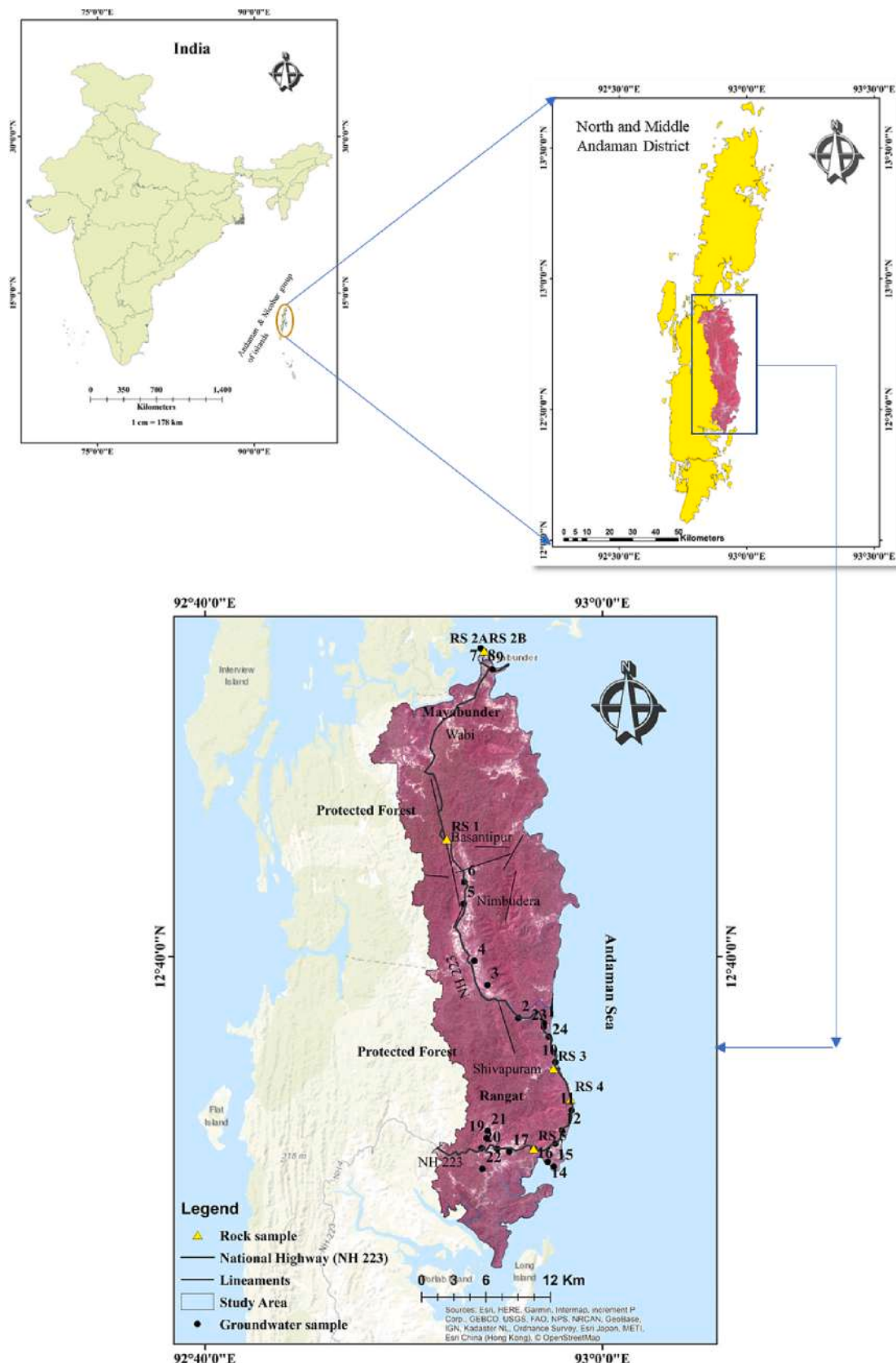


Fig. 1. Spatial map of the Study area showing the location of Rock and water sampling.

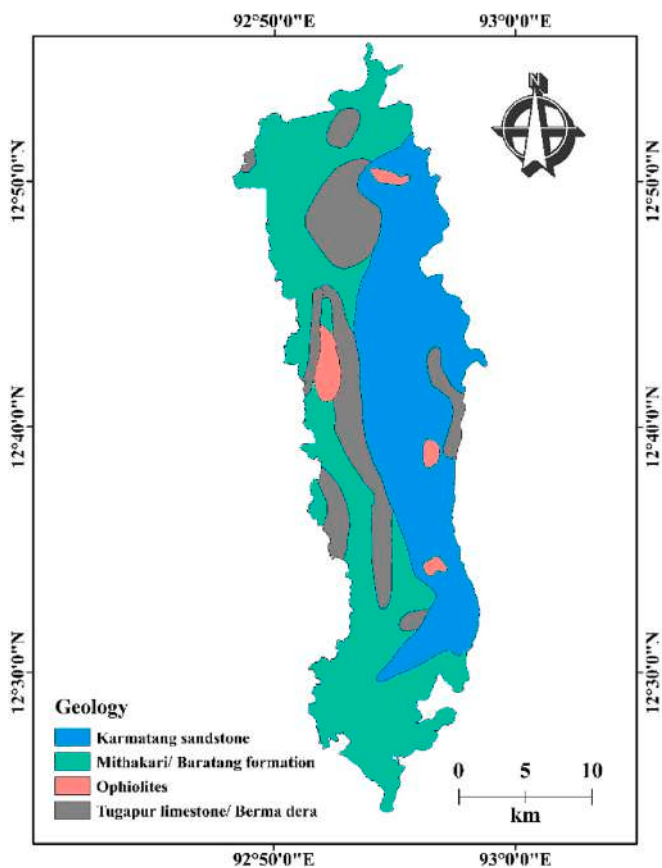


Fig. 2. Geology map of the area (Bandopadhyay and Ghosh, 2015).

and the remaining 15% of igneous rocks provide favourable conditions for a sustainable aquifer in the region (Mukherjee, 1986; Bandopadhyay and Carter, 2017). The ophiolite rocks of igneous origin (intruded in sandstone formation) have higher aerial fracture density than sedimentary rocks. The fracture density has greater control over drainage density for groundwater development and is associated with the presence of good aquifers. The weathered sandstone rocks may also be a source of water but of low transmissivity (Roy et al., 2005).

2. Methodology and data analyses

2.1. Groundwater sampling

Groundwater sampling points have been chosen based on surface manifestation from satellite images as well as the accessibility of the groundwater site. A total of 25 samples were collected from different parts of middle Andaman of which 24 samples were from groundwater and one sample from seawater as a reference. Most of the samples were collected from an open well except one sample from spring water (Sample no. 11).

The samples were collected in polypropylene plastic bottles for cation and anion analysis separately. The bottles were rinsed from the sampling water at least three times before the collection of samples. Also, precautions were taken to minimize the impact of the material of the pipe and biases on the representative sample. The groundwater samples were geolocated using Garmin GPS (global positioning system). The parameters like pH, electrical conductivity (EC), and total dissolved solids (TDS) were recorded using handheld probes. The water samples collected for cations were preserved by adding a few drops of Concentrated HNO₃ and stored at a cool temperature (4 °C). Further, samples were filtered through 0.45 m-pore filter paper before analysis.

2.2. Groundwater parameter analysis

Major anions and major cations analysis were done in the laboratory using standard methods given by the American public health association (APHA, 2005) and (Diatloff and Rengel, 2001). Sodium, Potassium, and Calcium were measured using the Elico flame photometer (Elico CL-378) and Magnesium was measured using ICP-OES (Agilent 5110). Major anions such as Carbonate, Bicarbonate, and Chloride were analysed by using the titrimetric method whereas Nitrate, Phosphate, and Sulphate were analysed using UV/Vis spectrophotometer (Perkin Elmer-Lambda 35) with TRI method, Malachite Green method, and Barium Sulphate method respectively (APHA, 2005). pH, EC, and TDS were measured on the sampling site using a probe "multiparameter test 35 series".

The accuracy of groundwater parameters was calculated using charge balance error (CBE). It assumes the neutrality of charge in natural water (Domenico and Schwartz, 1997).

$$CBE = \frac{\sum C - \sum A}{\sum C + \sum A}$$

where $\sum C$ and $\sum A$ are the sums of cations and anions (meq/L) respectively.

The value of Charge Balance Error (CBE) was found in the range of $\pm 5\%$ in all the water samples. The Average, minimum, Maximum and standard deviation of CBE of all the samples was found to be 0.02, -0.42, 0.24, and 0.19 respectively. As all the samples were within the acceptable limit, water parameters were assumed to be good for further analysis.

Firstly, major cations and major anions were converted from mg/L to meq/L to remove the effect of charge in the calculation. A total of ten ionic ratios were taken to estimate the seawater intrusion in the study area (Klassen and Allen, 2017; Lee and Song, 2007; Bear et al., 1999; Nadler et al., 1980; Rosenthal, 1988). These groundwater chemical ionic ratios were found to be Na/Cl, Na/Ca, Mg/Cl, Ca/Mg, Cl/(SO₄ + HCO₃), K/Cl, SO₄/Cl, Cl/HCO₃, (Ca + Mg)/Cl, and Ca/(HCO₃ + SO₄).

Further, the Base exchange index (BEX) was calculated to distinguish the undergoing process of salination or recharging/freshening (Stuyfzand, 2008). A positive value of BEX indicates refreshing water, a negative value represents salination and a zero value means the absence of base exchange.

$$BEX = \text{Na} + \text{K} + \text{Mg} - 1.0716 \times \text{Cl} \text{ (meq/L)}$$

The equiline graph is generated using MS-Excel 2019 whereas Durov and Schoeller's diagram was plotted using AqQA version 1.1.1. The earthquake data was taken from the USGS earth explorer from 1990 to 2022 with a Richter scale of >5.

ArcGIS 10.8 was used for generating the spatial map of ionic ratios using the inverse distance weightage method (IDW). Further maps were integrated using the spatial overlay technique.

3. Result and discussion

3.1. Evaluation of water quality parameters

Table 1 is a summary of the water quality parameters (meq/L) comprised of the minimum, maximum, mean, median, and standard deviation of the major ions. It was observed that the electrical conductivity value of water samples varied from 100 µS/cm to 1500 µS/cm with an average value of 548 µS/cm. 60% of samples were found above 500 µS/cm. Chloride concentration varied between 0.98 meq/L to 270.55 meq/L with an average value of 12.47 meq/L. Cl and EC are two parameters that are universally accepted indicators of seawater intrusion. The high value of Cl and EC is indicative of seawater intrusion. In our study area, a high value of chloride and EC were found in the samples taken near the coast. Chloride is the single parameter found in seawater

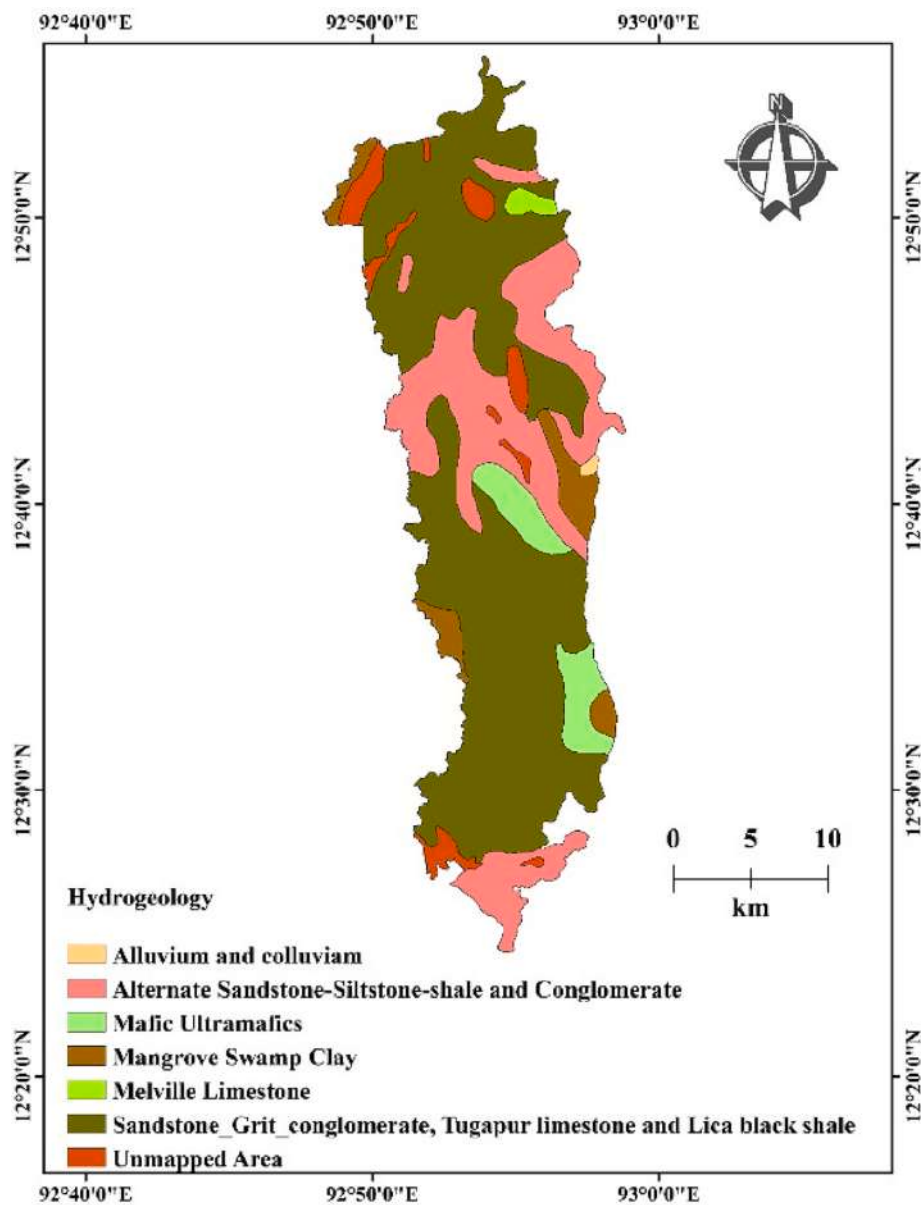


Fig. 3. Hydrology map of the study area.

Table 1
Statistical distribution concentration of major ions (meq/L) of middle Andaman.

	pH	EC	TDS	Na	K	Ca	Mg	CO ₃	HCO ₃	SO ₄	PO ₄	NO ₃	Cl	F
Mean	7.45	548	284.8	4.62	0.28	12	1.13	0.9	3.53	0.02	0.18	0.02	12.47	0.33
Min	6.2	100	30	0.13	0.01	0.5	0.29	0	1.28	0	0.01	0	0.98	0.07
Max	8.5	1500	740	87.45	5.09	175.12	2.09	1.7	5.53	0.14	0.38	0.05	270.55	1.43
S.D.	0.63	335.56	167.36	17.28	1	34.12	0.54	0.51	1.34	0.04	0.1	0.01	53.77	0.27

due to its conservative nature. It shares >55% of TDS in seawater and that makes it a very sensitive indicator of contamination of seawater in groundwater (Nadler et al., 1980; Moujabber et al., 2006; Jones et al., 1999; Panno et al., 2006).

It was found that the water sample taken from the sea, near Mayabunder Jatti (sample no. 25) also shown in Fig. 4 had a high concentration of Calcium (175.12 meq/L), Sodium (87.45 meq/L), Potassium (5.01 meq/L), Chloride (270 meq/L) and Sulphate (0.09 meq/L).

3.2. Schoeller diagram

In addition to the summarised data (Table 1), the Schoeller diagram illustrated the relative concentrations (meq/L) of major ions in each sample. It allowed to accommodate a large number of chemical constituents for comparison and investigation. As per Fig. 4, the pattern of ions obtained from different sources of groundwater indicated that the seawater sample (SEA1) showed the dominance of chloride and calcium ions. While the lower concentration of sodium with respect to chloride and calcium ions showed the presence of reverse ion exchange

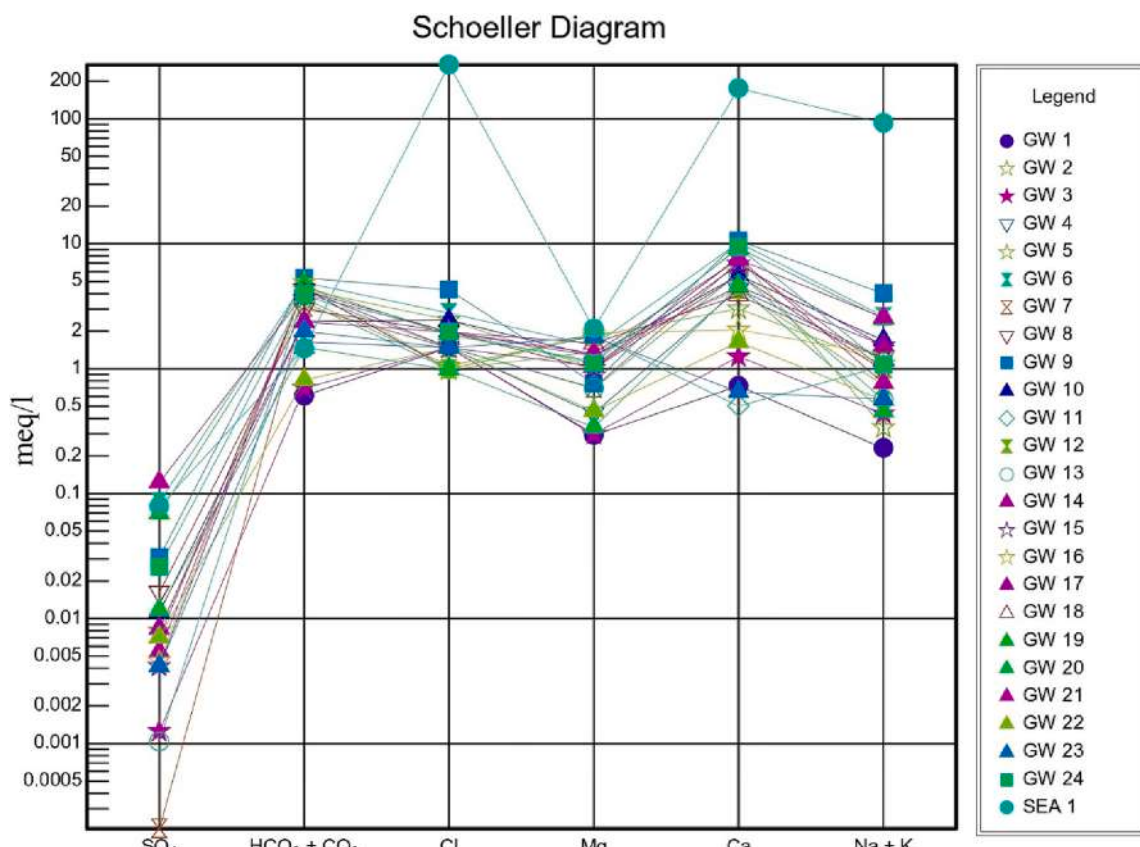


Fig. 4. Schoeller diagram of middle Andaman.

governing between sodium (from seawater) and calcium from limestone minerals. It was also found that bicarbonate has a higher value in all the samples except seawater whereas calcium was found dominant in all the samples including seawater. The chloride value (meq/L) was found higher value than sodium in 76% of the samples. The loss of sodium ions is probably due to the replacement of the sodium ion exchange process in groundwater. We may infer the possibility of seawater intrusion in the area.

3.3. Equiline graphs of Chloride with major ions

The concentrations of Chloride were plotted against the major ions (Na, Ca, Mg, K, SO_4 , NO_3 , HCO_3) and EC (Fig. 5), and the least r^2 value of linear regression was determined. Stoessell (1997) explained the good linear coefficient of determination between the Cl and major ions like Na, Ca, and K showed a possible mixing of freshwater with single-brine chemistry. The intrusion of seawater provided the replacement of Sodium with the same milliequivalent concentration of calcium and carbonate with chloride (Fig. 5a, f). Similarly, the analysis of seawater depicted a higher concentration of Potassium and chloride indicating the seawater influence in the aquifers. The equiline graphs (Fig. 5a, d, c) of potassium, calcium, and sodium showed a strong relation with chloride possibly due to the interaction of seawater with limestone and aquifers of the island. On the other hand, the equiline graph between EC and chloride did not show any linear correlation with each other. The dominance of EC over chloride and equal concentration (meq/L) of sodium and chloride suggested enrichment evaporation, NaCl aerosol, or direct mixing of seawater. The dominance of bicarbonate over chloride shows the weathering of carbonate minerals from limestone deposition in the study area. The dominance of chloride over nitrate and sulphate wipes out the possibility of anthropogenic influence in the aquifer. The highest value shown in the graph is the seawater

sample from the coast of Mayabunder in the middle Andaman (Umara et al., 2019; Lakshmanan et al., 2003).

3.4. Spatial map of ionic ratio

The summarised table of the mean, minimum, maximum, and standard deviation of the ionic ratios is shown in Table 2.

Equiline graphs and Schoeller showed that seawater intrusion is the major cause of low groundwater quality in most of the island's aquifers. The salinity caused by seawater intrusion has been associated with a lower value of sodium than chloride in groundwater compared to seawater (Vengosh, 2003). In the case of saltwater intrusion, the ratio of Na/Cl declines in saline groundwater, and that is lower than that of marine water (<0.86) (Schoeller, 1967). This is because when seawater intrudes into groundwater, a chemical exchange process takes place between rocks and seawater (Mercado, 1985; Nadler et al., 1980) and Calcium ions replace sodium ions resulting in depletion in sodium ion concentration but no change in chloride concentration. The ratio of Na/Cl ranges between 0.08 and 1.51 with an average value of 0.67. It was found that 68% of samples had Na/Cl ratio <0.86 . It was also observed that the contamination zone of the groundwater was higher in the 5 km spatial range from the shoreline. Further, 24% of samples showed contamination which indicated the possibility of anthropogenic influences where the ratio of Na/Cl was >1 (Vengosh, 2003).

When seawater intrudes; the ion exchange process takes place between alkali and alkaline earth metals. Na ion replaces Ca and Mg ions in the aquifer from carbonate minerals leading to the enrichment of Calcium, Magnesium, and bicarbonate ions into aquifers. The ratio of the sum of alkaline earth metal to chloride was found higher in groundwater compared to seawater. The ratio $(\text{Ca} + \text{Mg})/\text{Cl}$ was found in the range of 0.65 to 7.99 and an average value of 3.68 and a standard deviation of 1.83 (Table 2). There was an enrichment of Sulphate in seawater, an

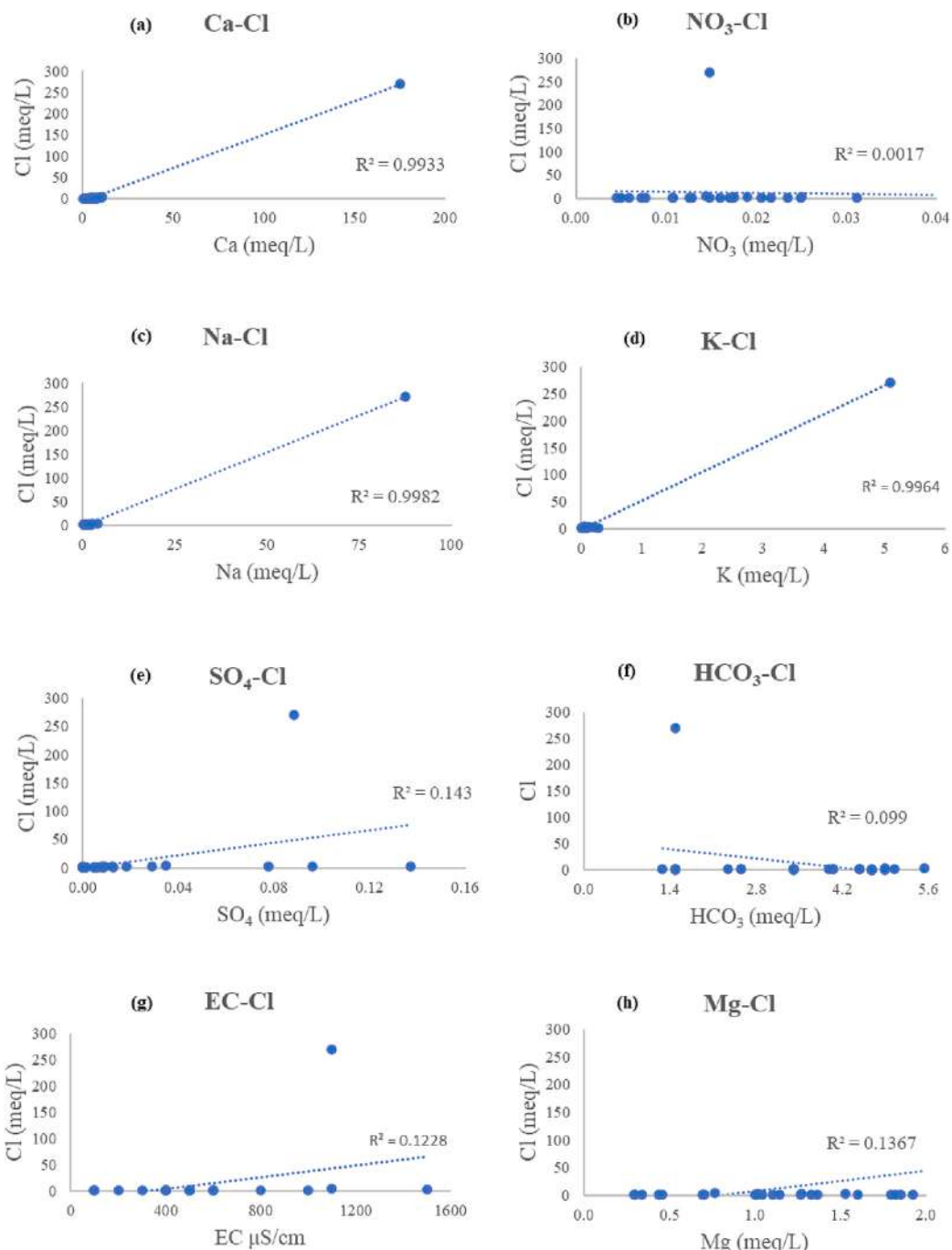


Fig. 5. Equiline graphs of chloride with major ions (a) Ca-Cl (b) NO₃-Cl (c) Na-Cl (d) K-Cl (e) SO₄-Cl (f) HCO₃-Cl (g) EC-Cl (h) Mg-Cl.

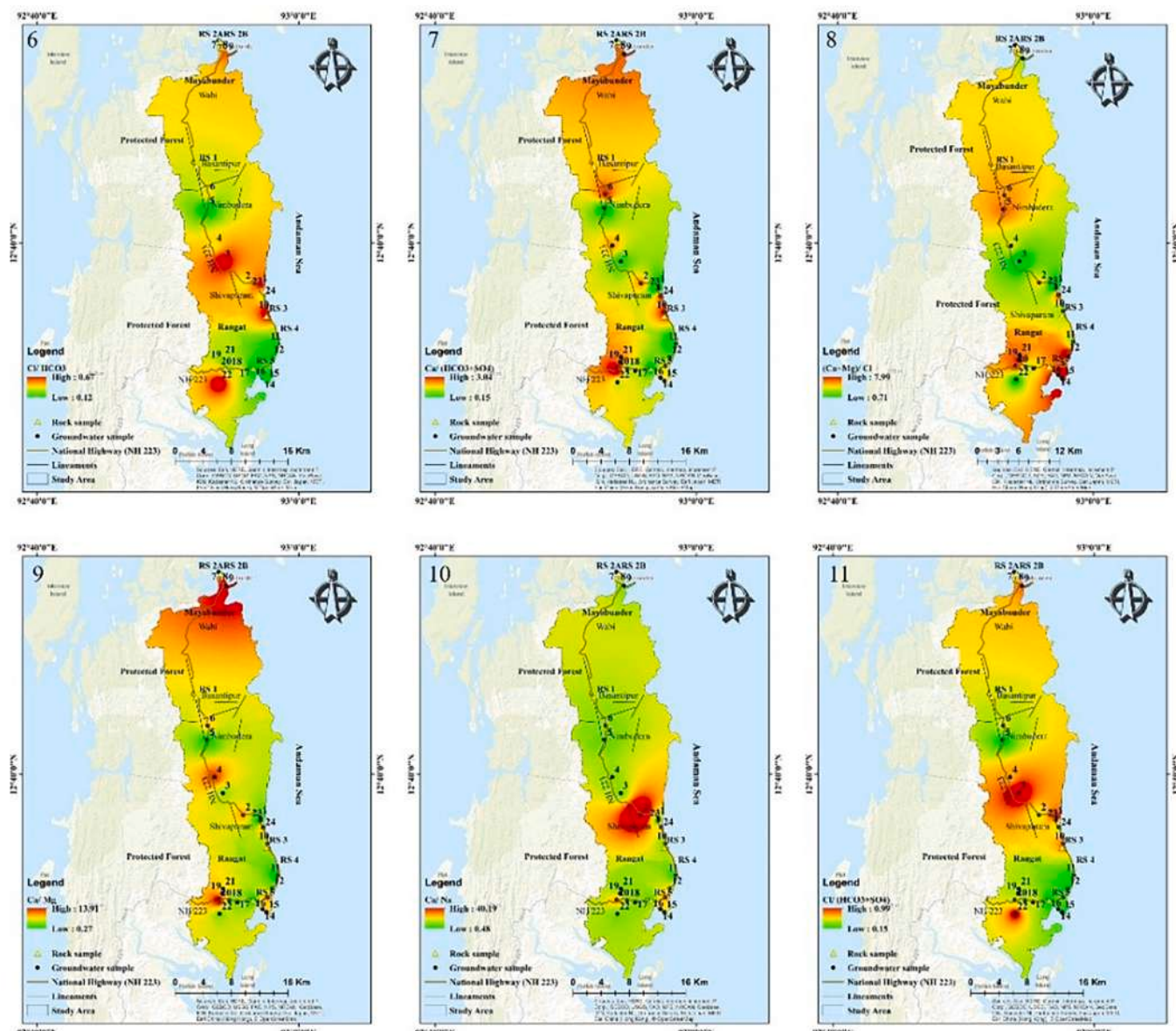
Table 2

Statistical distribution of ionic ratios of major ions of middle Andaman.

	EC	Ca/Mg	BEX	Cl/(HCO ₃ + CO ₃)	Ca/(HCO ₃ + SO ₄)	Mg/Cl	Ca/Na	Na/Cl	Cl/ HCO ₃	K/Cl	(Ca + Mg)/Cl	SO ₄ /Cl	Ca/SO ₄
Mean	548	8.92	-7.34	5.05	5.80	0.71	6.36	0.67	4.53	0.67	3.68	0.01	767.35
min	100	0.27	-195.3	0.15	0.15	0.01	0.48	0.08	0.12	0.08	0.65	0	54.31
max	1500	83.93	2.17	115.63	111.04	1.96	40.19	1.51	105.75	1.51	7.99	0.07	1490
SD	335.56	16.06	39.17	23.04	21.94	0.54	7.76	0.39	21.09	0.39	1.83	0.02	1123

interaction of seawater and groundwater may have led to the dissolution of calcium sulphate into the saline water. The higher concentration of ratio of calcium and sulphate indicates the seawater intrusion in the coastal aquifer (Fig. 12). For the ratio of Ca/SO₄, ratio values varied

between 54.31 and 1490 with a standard deviation of 1123. A ratio >1 indicates the intrusion of seawater into groundwater. EC is also a good indicator of saltwater intrusion and 16% percent of samples have found EC value >1000 (Lee and Song, 2007). This also confirmed the



Figs. 6–15. Represent the spatial map of ionic ratios: Cl/HCO_3 , $\text{Ca}/(\text{HCO}_3 + \text{SO}_4)$, $(\text{Ca} + \text{Mg})/\text{Cl}$, Ca/Na , $\text{Cl}/(\text{SO}_4 + \text{HCO}_3)$, Ca/SO_4 , K/Cl , Mg/Cl , and SO_4/Cl respectively.

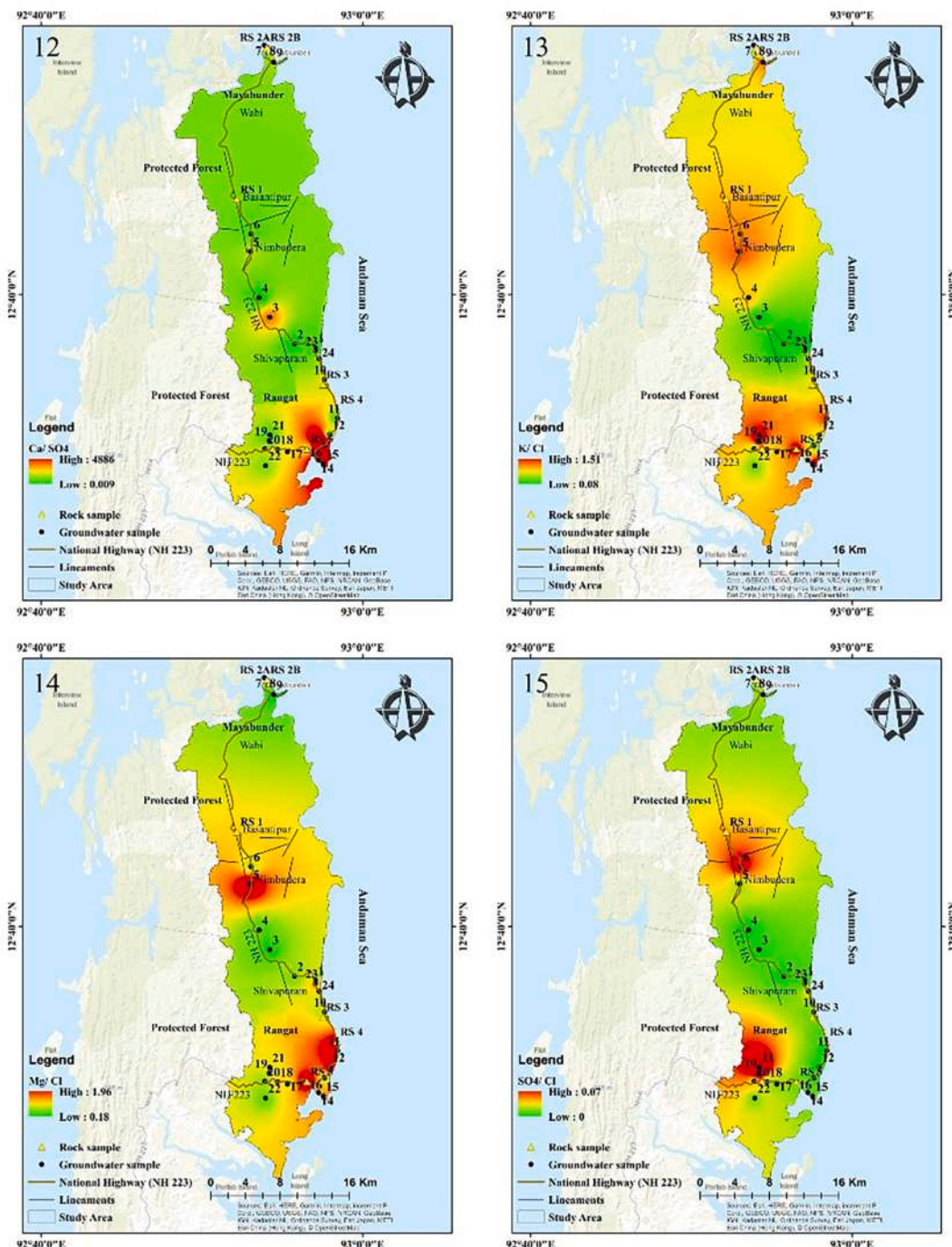
possibility of calcium dissolution from limestone caves and governs calcium enrichment in the coastal aquifer through to ion exchange process.

Fresh groundwater is usually abundant with both carbonate and bicarbonate ions and a small number of chloride ions as compared to seawater (Bear et al., 1999; Todd and Mays, 2004). Simpson ratio ($\text{Cl}/(\text{HCO}_3 + \text{CO}_3)$) can also be used to delineate the seawater contamination zone, as more chloride ions in groundwater contributed to the higher value of Simpson's ratio value. Freshwater is abundant with carbonate and bicarbonate ions giving a lower value of Simpson's ratio. In this way, the groundwater is classified into five classes; a ratio value <0.5 indicates good quality fresh water (0%), a value from 0.5 to 1.3 indicates slightly contaminated (36%), from 1.3 to 2.8 is moderately contaminated (60%), from 2.8 to 6.6 is injuriously contaminated (0%), and >6.6 is highly contaminated (0%). In the study area, no samples have values <0.5 and >2.8 which indicated slightly to moderately contaminated groundwater.

In coastal aquifers, the interaction of seawater-freshwater causes the

loss of sodium ions as it was replaced by calcium ions. The enrichment of calcium is a clear indicator of seawater intrusion. The source of calcium can be either leaching from surface soil or the dissolution of limestone occurring in the study area (Naily, 2018; Carol and Kruse, 2012; Mousjabber et al., 2006; Klassen et al., 2014). The value of $\text{Ca}/(\text{HCO}_3 + \text{SO}_4)$ lied between 0.15 and 111.04 with an average value of 5.80 (Fig. 7). The variation for K/Cl , Mg/Cl , and SO_4/Cl was found between 0.08 and 1.51, 0.01–1.96, and 0–0.07 respectively (Figs. 13, 14 & 15).

The value of $\text{Ca}/(\text{HCO}_3 + \text{SO}_4) > 1$ with low K/Cl , Mg/Cl , and SO_4/Cl also demarcated seawater intrusion in the coastal aquifer (Jones et al., 1999). 72% of the samples have found the ratio of $\text{Ca}/(\text{HCO}_3 + \text{SO}_4) > 1$ whereas 68% of the samples had a lower Na/Cl ratio (<0.86). Not a single sample was found to have a low ratio of K/Cl (<0.02). As seawater intrudes into groundwater, the absorption of K^+ on clay particles occurs due to silicate weathering, which decreases the concentration of K^+ in groundwater (Vengosh, 2003). The ratio of Mg/Cl varies from 0.01 to 1.96. Both sulphate and bicarbonates have a higher concentration in groundwater than in seawater. It was observed that 76% of the samples



Figs. 6–15. (continued).

had $\text{Ca}/(\text{HCO}_3 + \text{SO}_4) > 1$ and also had an Mg/Cl ratio < 1 . This indicated the increase in Cl concentrations in coastal aquifers. Similarly, the ratio of $\text{SO}_4/\text{Cl} < 1$ also indicates the intrusion of seawater in groundwater aquifer, it was observed that the samples having a ratio of $\text{Ca}/(\text{HCO}_3 + \text{SO}_4) > 1$ also had a ratio of $\text{SO}_4/\text{Cl} < 1$ (Abdalla, 2016).

The ratio of $\text{Ca}/\text{Na} > 1$ indicates the saltwater intrusion in groundwater (Gimenez and Morell, 1997) (Fig. 10). For the study area, the value of Ca/Na is distributed between 0.48 and 40.19 with an average value of 6.36; 96% of the samples may be contaminated with saltwater intrusion ($\text{Ca}/\text{Na} < 1$). The cation exchange process between seawater and calcium-rich rocks is the main cause of the enrichment of calcium ions in coastal aquifers. The Ca/Mg ratio varies from 0.27 to 80.93 with an average value of 8.92 and a standard deviation of 16.06 (Fig. 9). The

higher ratio of Ca/Mg again indicates the enrichment of calcium ions during the interaction of aquifers with seawater.

3.5. Correlation matrix of major ions

As per Table 3, a correlation matrix of major cations and anions was generated to understand the correlation of ions with each other. The green and red colors denote positive correlation and negative correlation. The dark and light shades represented strong correlation or weak correlation respectively.

The correlation matrix has shown that Total Dissolved Solid (TDS) was strongly correlated with EC. Carbonate, bicarbonate, and sulphate are positively correlated to EC and TDS. Carbonate was strongly

Table 3

Correlation matrix of major ions.

	pH	EC	TDS	Na	K	Ca	Mg	CO ₃	HCO ₃	SO ₄	PO ₄	NO ₃	Cl	F
pH	1.000													
EC	0.581	1.000												
TDS	0.577	0.995	1.000											
Na	0.100	0.381	0.405	1.000										
K	0.084	0.346	0.370	0.997	1.000									
Ca	0.119	0.402	0.427	0.997	0.996	1.000								
Mg	0.466	0.515	0.529	0.381	0.356	0.364	1.000							
CO ₃	0.626	0.502	0.513	-0.011	-0.037	-0.006	0.744	1.000						
HCO ₃	0.455	0.533	0.532	-0.291	-0.317	-0.264	0.359	0.469	1.000					
SO ₄	0.375	0.782	0.764	0.404	0.380	0.416	0.293	0.165	0.153	1.000				
PO ₄	0.352	0.056	0.062	-0.274	-0.258	-0.259	0.167	0.171	0.283	-0.034	1.000			
NO ₃	0.047	0.072	0.072	-0.043	-0.019	-0.025	0.038	-0.029	0.281	-0.073	0.269	1.000		
Cl	0.085	0.350	0.375	0.999	0.998	0.997	0.370	-0.019	-0.315	0.378	-0.278	-0.042	1.000	
F	0.167	0.534	0.548	0.858	0.860	0.877	0.266	0.036	-0.111	0.455	-0.089	0.016	0.853	1.000

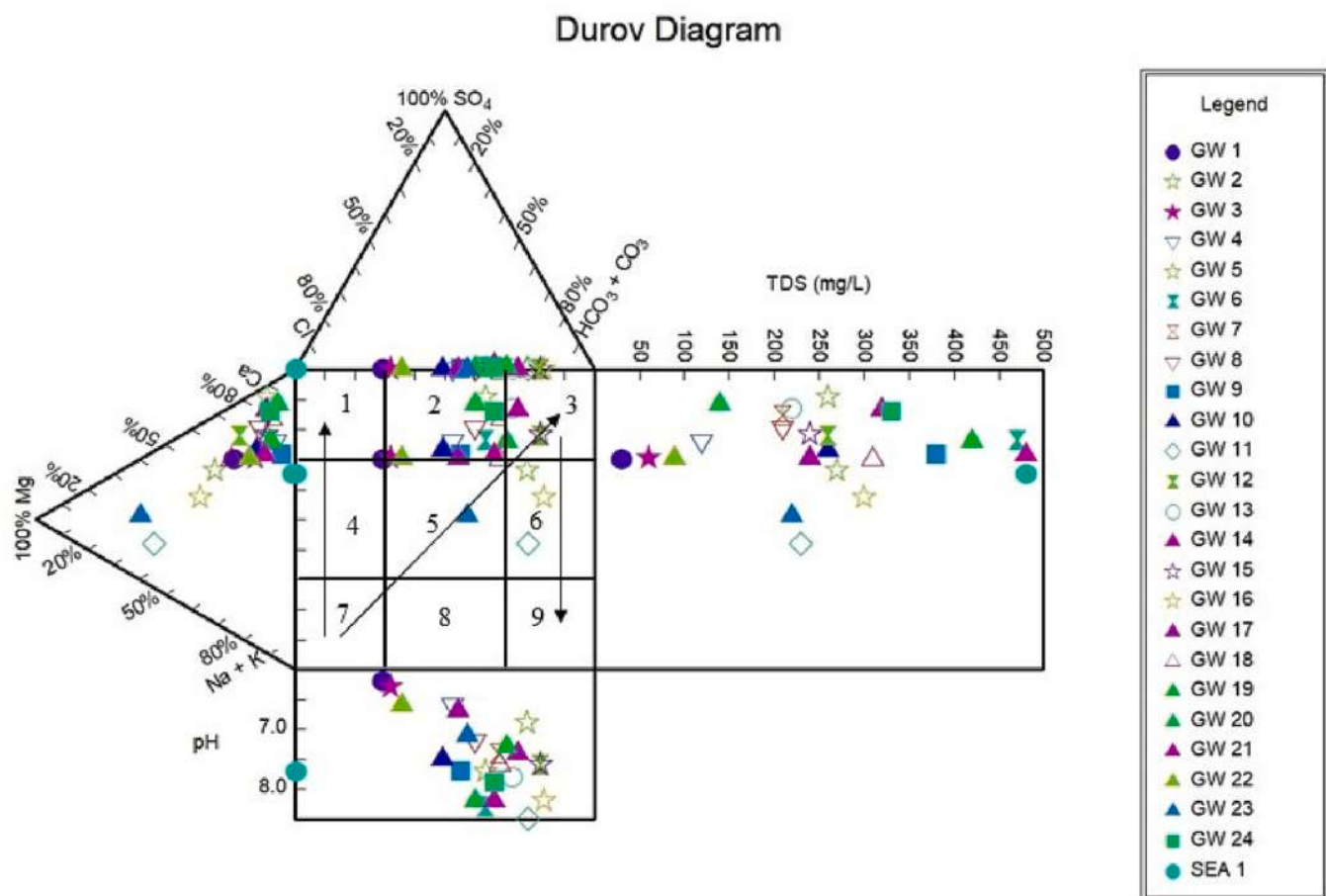


Fig. 16. Durov plot of the area.

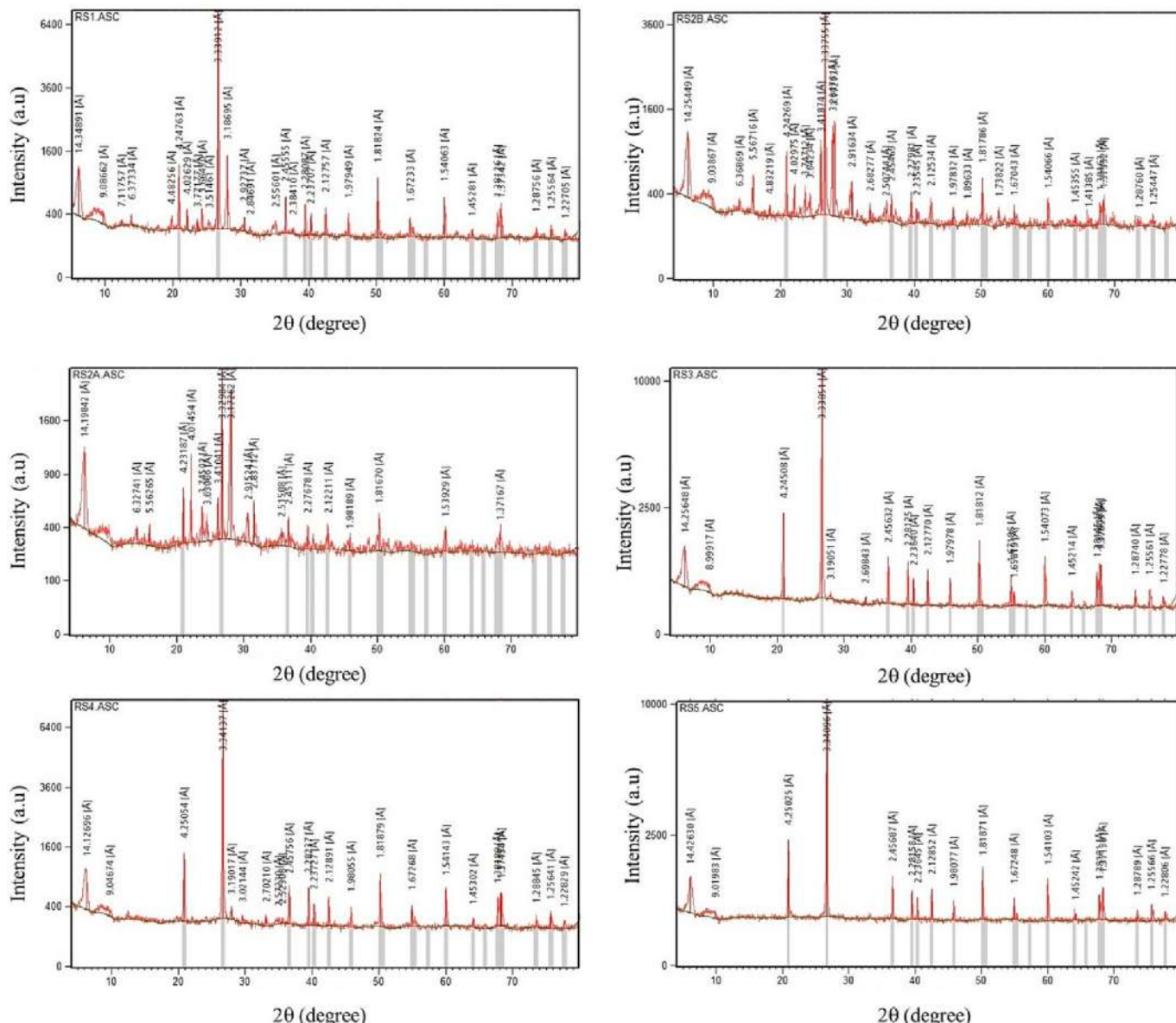
positively correlated to magnesium; and sodium, potassium, and calcium are strongly correlated to each other. This may confirm the dissolution of limestone with the interaction of Na from seawater intrusion and the release of K ions from weathering of rocks containing potassium.

Both chloride and fluoride are strongly correlated to sodium, potassium, calcium, and with each other. This strongly advocates the interaction of seawater with limestone minerals releasing calcium, potassium, and fluoride in the groundwater. The strongly correlated ions also revealed the same source or process (seawater and limestone) for their enrichment in groundwater.

3.6. Durov plot

The Durov diagram is another graph used to depict the water chemistry of water samples (Fig. 16). In advance of the Piper diagram, it uses other parameters pH and TDS for the water chemistry interpretation. Similar to the piper plot, it also uses the percentage of major cations and anions (meq/L) in the water samples. It calculates the percentage of

each cation group to the whole sum of the concentration of major cations- calcium, magnesium, and the sum of sodium and potassium. The percentage of each anion group is calculated with the summation of the concentration of sulphate, chloride, and the sum of both carbonate and bicarbonate. Lloyd and Heathcoat (1985) classified water into three major processes, ion exchange, simple dissolution or mixing, and reverse ion exchange. These processes are represented with the arrows (7 to 1) for ion exchange, (7 to 3) for simple dissolution or mixing, and (3 to 9) for reverse ion exchange. Most of the samples depicted an ion exchange process and simple dissolution or mixing at pH above 7 and TDS > 200. A few samples showed weak ion exchange processes in the aquifer. The dominant water type Ca-HCO₃ with significant Magnesium influence was observed in 48% of the samples. Na-HCO₃ indicating an ion exchange process was found in 24%, and non-dominating cations and anions were found in 12% of samples showing simple mixing and dissolution. Calcium and bicarbonate ions dominated in 56% and 76% of the samples respectively.



Figs. 17–23. XRD plot of rock samples (RS1, RS2A, RS2B, RS3, RS4, RS5) in the region, where the X-axis represents 2θ value and Y- the axis represents intensity value.

3.7. X-ray diffraction (XRD) data of the area

The mineralogical study for the rock samples found in the area was carried out using X-ray diffraction. The data obtained after XRD analysis provided a d-spacing value that was matched with the inventory of known minerals to confirm the presence of the minerals in the sample. The parent peak and a subordinate peak of d-spacing were compared with standard reference values given by (Lindholm, 1987) for the identification of minerals present in the samples. The graph in Figs. 17–23 was plotted using the software Xpert high score version 1.0a. The locations of rock samples are shown in Fig. 1.

The carbonate minerals found in middle Andaman after the analysis of rock samples were Aragonite found in rock samples (RS2A, RS2B)

having common Intensity peak values 3.396, 2.870, 2.484, 2.481, 2.410, Calcite found only in RS4 with an intensity peak value 3.030, 2.495, Chlorite was identified in RS1 with an intensity peak value 7.150, 2.870, 2.550, 2.475, 2.390, Chromite was observed in (RS1& RS4) with a common intensity peak value 2.950, 2.520, 2.400, Dolomite was observed in (RS1, RS2A, RS2B) with a common intensity peak value 4.030, 3.690, 2.886, 2.405, Magnetite was found in (RS1 & RS4) with a common intensity peak value 2.530, 2.419, Pyrite was confirmed in (RS2B, RS3, RS4) with a common intensity peak value 2.709, 2.423, 2.212. These minerals confirmed the presence of limestone deposits in the area. The presence of Aragonite showed evidence of burial and metamorphism of the rocks of the Mithakari formation.

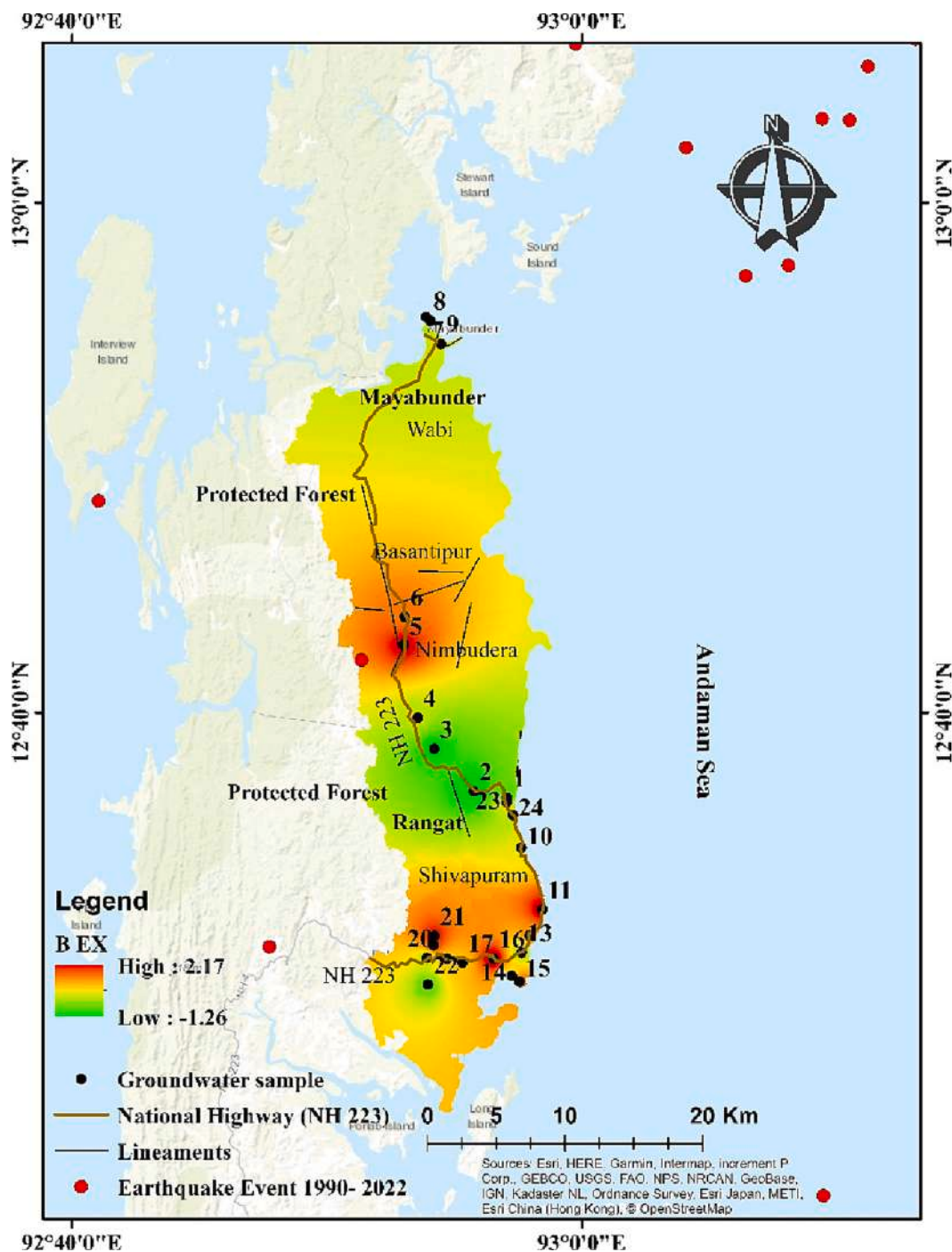


Fig. 24. BEX map of middle Andaman.

3.8. Base exchange index (BEX)

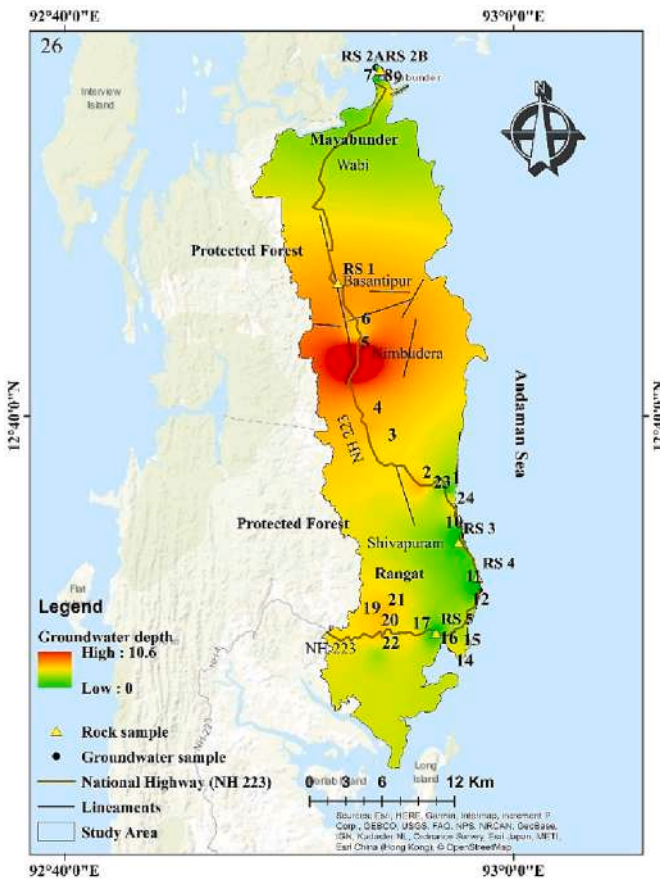
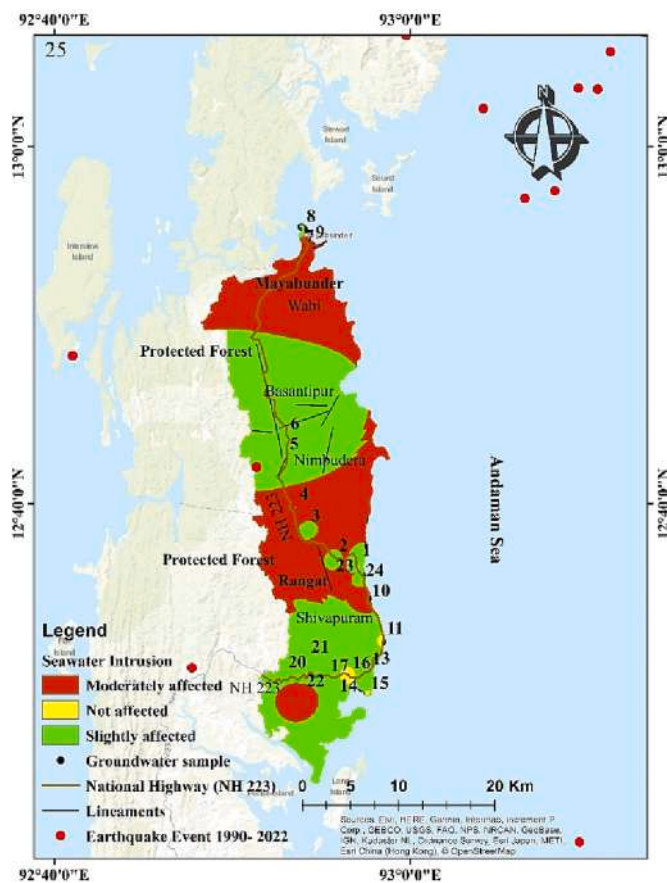
The base exchange index is an index of salinization that shows the negative value for seawater intrusion and positive values for the freshwater aquifer. It was observed that the BEX values were between -195.30 and 2.17 , with a mean value of -7.34 . The negative value of BEX indicated a higher concentration of $(\text{Na} + \text{Mg} + \text{K})$ relative to chloride ions. A zero value of BEX indicated the absence of base ion exchange in the area (Stuyfzand, 1989). The spatial map of BEX (Fig. 24) showed the effect of saltwater intrusion: a large portion in middle below Numbudera, a few spots in the southern region, and some parts of the northern region of the study area. BEX index showed that about 32% of groundwater samples are under the effect of seawater intrusion.

3.9. Integrated seawater intrusion

The integrated seawater intrusion diagram was made after the integration of all the ratio parameters on ArcGIS 10.8. It was classified based on the sum of the ionic ratios; strongly affected (≥ 8), Moderately affected (6, 7), Slightly affected (4, 5), and not affected (< 4). Fig. 25 showed the Moderately affected (44%), slightly affected (54%), and not affected (2%) saline groundwater in the area (Asare et al., 2021). Not a single sample was found strongly affected by seawater influences. The effect of seawater intrusion was found in the North and Middle with a small spot in the southern part as a moderately affected area. In comparison to groundwater depth (Fig. 26), the deep aquifers of Numbudera and Basantipur are less affected by seawater intrusion possibly due to groundwater recharge through interconnected fractures preventing seawater intrusion through the hydraulic gradient. The shallow aquifers of Mayabunder and Rangat were found moderately affected by seawater intrusion. The seashore extension of seawater intrusion was found above

Nimbudera and above Basantipur.

The integration map of Ionic ratio with earthquakes, active faults/fractured zone/ deep lineaments (Fig. 25). As the area already falls in earthquake zone V, seismic activities are very common in the study area. The earthquake shockwave also triggered the structural change in limestone deposits. Manchi and Sankaran (2009) studied the impact of the 2004 earthquakes on limestone caves and stated the impact caused the narrowing, widening, fractional, or complete shutting of present cave openings, (2) collapsed rocks inside caves, and (3) advanced existing cracks and fissures. The combination of active faults with earthquakes can be beneficial and disastrous for groundwater development. The connected fault found in the Nimbudera and Basantipur is found to be a good zone for groundwater recharge. The fault perpendicular to the sea provides an opening for seawater intrusion resulting in the dissolution of limestone as well. The seawater sample taken from Mayabunder was near the fault opening which lies perpendicular to the seashore that showed a higher amount of calcium ions than sodium. Generally, seawater usually contains NaCl dominance but the study area reported calcium chloride dominance in the sea. The higher value of bicarbonate in seawater again confirmed the limestone weathering in the study area. Similar to Mayabunder, Govindpur, and Monsdera are also having active faults perpendicular to seawater. The limestone minerals were present in all the rock samples in varied quantities. The middle of the study area has ophiolite group exposure overlying Mithakari and Bhartang formations. Geologically, the Mithakari formation has associated with a good aquifer zone with a good source of groundwater recharge zone. Sedimentary formation does not support the infiltration of surface water into the subsurface zone. Therefore, the sea level rise or extraction of groundwater may have developed a hydraulic gradient to infiltrate seawater in island aquifers. Similar way, seismic activities have created an explosion of the fracture within



Figs. 25–26. Integrated water intrusion and groundwater depth map of middle Andaman.

ophiolite that further provoked the Mithakari as well as Bhartang formations to develop a more interconnected fracture. Since some of the fractures have an opening in the sea, seawater can intrude through them. So, a precautionary measure must be taken so that the existing quality of the groundwater of the aquifer does not deteriorate over time.

4. Conclusion

The ionic ratio data showed the relative abundance of various constituents of water in the aquifer. The intrusion of seawater in freshwater changes the relative abundance of water parameters. We could successfully differentiate freshwater from seawater based on these ionic ratios. The Schoeller diagram aided in understanding the relative milli-equivalent proportion of each ion present in water and depicted limestone dissolution (higher concentration of calcium and bicarbonate) with a higher concentration of chloride than sodium (seawater effect). The GIS platform was found useful in the spatial visualization of BEX, ionic ratios, active faults, and geological formation. Bivariate plots have provided data on the enrichment of alkali metal salt and alkaline earth metal salts. The correlation matrix has depicted the strong relationships of chloride ions with major ions such as Na, K, Ca, and F (strongly correlated). Durov plots described the major water types (Ca-HCO₃ (48%) and Na-HCO₃ (24%)) and the processes (reverse ion exchange (56%) or mixing of seawater (12%) of the samples) taking place in the aquifer.

The shallow aquifer's proximity to the sea was found to be affected by seawater intrusion. The influence of seawater was found to be as follows: SO₄/Cl (100%) > Ca/SO₄ (100%) > Ca/Na (96%) > Mg/Cl (76%) > Ca/(HCO₃ + SO₄) (64%) > Cl/(HCO₃ + CO₃) (36%) > Cl/HCO₃ (16%) > (Ca + Mg)/Cl (2%) > Ca/Mg (0%) > K/Cl (0%). The integrated result has shown that the study area was found to be moderately affected (44%), slightly affected (54%), and not affected in 2% samples only.

Further X-ray diffraction plots of rock samples confirmed the presence of limestone minerals (Calcite, Aragonite Chlorite, Chromite, Dolomite, Magnetite, and Pyrite) in the area. The presence of limestone was indicative due to the dominance of calcium ions in coastal seawater. Further, the tectonic-metamorphic changes have been instrumental in the development of unconformity and lineament. These linear features needed to be monitored with utmost care to infer the possibility of seawater intrusion, especially in those areas where the openings of these fractures are associated with the coastal terrain. The current research has demarcated the salt-affected region of the coastal aquifer but it has not incorporated the effect of groundwater flow with an accurate hydraulic gradient. Even though the current research has described little about the role of earthquakes through active fault, data is still limited to understanding the role of tides, tsunamis, and disastrous events in the movement of seawater into aquifers of islands. There is a future possibility of studying groundwater modeling using geophysical data, time series analysis through machine learning techniques with accurate real-time weather data, tides movement, and groundwater flow detection using isotopes and age dating for understanding the lateral movement of seawater through the hydraulic gradient.

Declaration of Competing Interest

The authors declare that they have no known competing financial interests or personal relationships that could have appeared to influence the work reported in this paper.

Data availability

Data will be made available on request.

Acknowledgment

Authors show sincere gratitude to Lab 211, SES-JNU, AIRF-JNU, and

IUAC-New Delhi for instrumentation facilities and UGC for the scholarship.

References

- Abdalla, F., 2016. Ionic ratios as tracers to assess seawater intrusion and to identify salinity sources in Jazan coastal aquifer, Saudi Arabia. *Arab. J. Geosci.* 9 (1), 1–12.
- Abdalla, F., Al-Turki, A., Al Amri, A., 2015. Evaluation of groundwater resources in the southern Tihama plain, Saudi Arabia. *Arab. J. Geosci.* 8 (5), 3299–3310.
- Abdollahi-Nasab, A., Boufadel, M.C., Li, H., Weaver, J.W., 2010. Saltwater flushing by freshwater in a laboratory beach. *J. Hydrol.* 386 (1–4), 1–12.
- Adimalla, N., Dhakate, R., Kasarla, A., Taloor, A.K., 2020. Appraisal of groundwater quality for drinking and irrigation purposes in central Telangana, India. *Groundw. Sustain. Dev.* 10, 100334.
- Ahmed, M.A., Abdel Samie, S.G., Badawy, H.A., 2013. Factors controlling mechanisms of groundwater salinization and hydrogeochemical processes in the quaternary aquifer of the Eastern Nile Delta, Egypt. *Environ. Earth Sci.* 68 (2), 369–394.
- Akshitha, V., Balakrishna, K., Udayashankar, H.N., 2021. Assessment of hydrogeochemical characteristics and saltwater intrusion in selected coastal aquifers of southwestern India. *Mar. Pollut. Bull.* 173, 112989.
- Allow, K.A., 2012. The use of injection wells and a subsurface barrier in the prevention of seawater intrusion: a modeling approach. *Arab. J. Geosci.* 5 (5), 1151–1161.
- APHA, 2005. Standard Methods for the Examination of Water and Wastewater, 21st ed. American Public Health Association, Washington D.C.
- Appelo, C.A.J., Postma, D., 2005. Geochemistry, Groundwater, and Pollution, 2nd. ed. Balkema, Rotterdam.
- Asare, A., Appiah-Adjei, E.K., Ali, B., Owusu-Nimo, F., 2021. Assessment of seawater intrusion using ionic ratios: the case of coastal communities along the Central Region of Ghana. *Environ. Earth Sci.* 80, 1–14.
- Bandopadhyay, P.C., Carter, A., 2017. Introduction to the geography and geomorphology of the Andaman-Nicobar Islands. *Geol. Soc. Lond. Mem.* 47 (1), 9–18.
- Bandopadhyay, P.C., Ghosh, B., 2015. Provenance analysis of the Oligocene turbidites (Andaman Flysch), south Andaman Island: a geochemical approach. *J. Earth Syst. Sci.* 124, 1019–1037.
- Barlow, P.M., Reichard, E.G., 2010. Saltwater intrusion in coastal regions of North America. *Hydrogeol. J.* 18 (1), 247–260.
- Bear, J., Cheng, A.H.D., Sorek, S., Ouazar, D., Herrera, I. (Eds.), 1999. Seawater Intrusion in Coastal Aquifers: Concepts, Methods, and Practices, vol. 14. Springer Science & Business Media.
- Bhagat, C., Puri, M., Mohapatra, P.K., Kumar, M., 2021. Imprints of seawater intrusion on groundwater quality and evolution in the coastal districts of South Gujarat, India. *Case Stud. Chem. Environ. Eng.* 3, 100101.
- Carol, E.S., Kruse, E.E., 2012. Hydrochemical characterization of the water resources in the coastal environments of the outer Río de la Plata estuary, Argentina. *J. S. Am. Earth Sci.* 37, 113–121. <https://doi.org/10.1016/j.jsames.2012.02.009>.
- Challinor, J., 1967. Dictionary of Geology. University Press, Oxford/Great Britain, p. 39.
- Chidambaram, S., Anandhan, P., Prasanna, M.V., Thiyya, C., Thilagavathi, R., Sarathidasan, J., 2014. Hydrochemistry of groundwater in a coastal region and its repercussion on quality, a case study—Thoothukudi district, Tamil Nadu, India. *Arab. J. Geosci.* 7 (3), 939–950.
- Custodio, E., 2010. Coastal aquifers of Europe: an overview. *Hydrogeol. J.* 18 (1), 269–280.
- Darnault, C.J., Godinez, I.G., 2008. Coastal aquifers and saltwater intrusion. Overexploitation and contamination of shared groundwater resources: management. In: (Bio) Technological, and Political Approaches to Avoid Conflicts, pp. 185–201.
- Diatloff, E., Rengel, Z., 2001. Compilation of simple spectrophotometric techniques for the determination of elements in nutrient solutions. *J. Plant Nutr.* 24 (1), 75–86.
- Domenico, P.A., Schwartz, F.W., 1997. Physical and Chemical Hydrogeology. John Wiley & sons.
- Dragoni, W., Sukhija, B.S., 2008. Climate change and groundwater: a short review. *Geol. Soc. Lond., Spec. Publ.* 288 (1), 1–12.
- Elango, L., Kannan, R., 2007. Rock–water interaction and its control on chemical composition of groundwater. *Dev. Environ. Sci.* 5, 229–243.
- Ford, T.D., Cullingford, C.H.D., 1976. Science of Speleology. Academic Press.
- Ganeshiaha, K.N., Sanjappa, M., Rao, R., Murugan, C., Shivaprakash, K.N., 2019. Spatial distribution pattern of taxonomic and phylogenetic diversity of woody flora in Andaman and Nicobar Islands, India. *Forest Ecosyst.* 6, 1–14.
- Ganyaglo, S.Y., Osae, S., Akiti, T., Armah, T., Gourcy, L., Vitvar, T., Otoo, I.A., 2017. Application of geochemical and stable isotopic tracers to investigate groundwater salinity in the Ochi–Narkwa Basin, Ghana. *Hydrog. Sci. J.* 62 (8), 1301–1316.
- Gill, B., Webb, J., Stott, K., Cheng, X., Wilkinson, R., Cossens, B., 2017. Economic, social and resource management factors influencing groundwater trade: evidence from Victoria, Australia. *J. Hydrol.* 550, 253–267.
- Gimenez, E., Morell, I., 1997. Hydrogeochemical analysis of salinization processes in the coastal aquifer of Oropesa (Castellon, Spain). *Environ. Geol.* 29 (1), 118–131.
- Gulam Rasool, Bhat, Balaji, S., Ganai, M.Y., 2022. Tectonic Geomorphology and Seismic Hazard of the East Boundary Thrust in Northern Segment of the Sunda-Andaman Subduction Zone.
- Jafri, S.H., Balaram, V., Govil, P.K., 1993. Depositional environments of cretaceous radiolarian cherts from Andaman-Nicobar Islands, northeastern Indian Ocean. *Mar. Geol.* 112 (1–4), 291–301.
- Jones, B.F., Vengosh, A., Rosenthal, E., Yechiel, Y., 1999. Geochemical investigations. In: Seawater Intrusion in Coastal Aquifers—Concepts, Methods and Practices. Springer, Dordrecht, pp. 51–71.

- Kazakis, N., Pavlou, A., Vargemezis, G., Voudouris, K.S., Soulios, G., Pliakas, F., Tsokas, G., 2016. Seawater intrusion mapping using electrical resistivity tomography and hydrochemical data. An application in the coastal area of eastern Thermaikos Gulf, Greece. *Sci. Total Environ.* 543, 373–387.
- Klassen, J., Allen, D.M., 2017. Assessing the risk of saltwater intrusion in coastal aquifers. *J. Hydrol.* 551, 730–745.
- Klassen, J., Allen, D.M., Kirste, D., 2014. Chemical indicators of saltwater intrusion for the Gulf Islands. British Columbia. Final Report, Department of Earth Sciences, Simon Fraser University.
- Kumar, S., 1981. Geodynamics of Burma and Andaman-Nicobar region, based on tectonic stresses and regional seismicity. *Tectonophysics* 79 (1–2), 75–95.
- Lakshmanan, E., Kannan, R., Kumar, M.S., 2003. Major ion chemistry and identification of hydrogeochemical processes of ground water in a part of Kancheepuram district, Tamil Nadu, India. *Environ. Geosci.* 10 (4), 157–166.
- Lee, J.Y., Song, S.H., 2007. Groundwater chemistry and ionic ratios in a western coastal aquifer of Buan, Korea: implication for seawater intrusion. *Geosci. J.* 11 (3), 259–270.
- Li, P., Karunandhi, D., Subramani, T., Srinivasamoorthy, K., 2021. Sources and consequences of groundwater contamination. *Arch. Environ. Contam. Toxicol.* 80, 1–10.
- Lindholm, R.C., 1987. Mineral identification using X-ray diffraction. In: *A Practical Approach to Sedimentology*, pp. 124–153.
- Lloyd, J.W., Heathcoat, J.A., 1985. *Natural Inorganic Hydrochemistry in Relation to Groundwater: An Introduction*. Clarendon Press, Oxford.
- Louvat, D., Michelot, J.L., Aranyossy, J.F., 1999. Origin and residence time of salinity in the Åspö groundwater system. *Appl. Geochem.* 14 (7), 917–925.
- Manchi, S., Sankaran, R., 2009. Impact of the 2004 earthquake on the limestone caves in North and Middle Andaman Islands. *Curr. Sci.* 1230–1234.
- Marimuthu, S., Reynolds, D.A., La Salle, C.I.G., 2005. A field study of hydraulic, geochemical and stable isotope relationships in a coastal wetlands system. *J. Hydrol.* 315 (1–4), 93–116.
- Mercado, A., 1985. The use of hydrogeochemical patterns in carbonate sand and sandstone aquifers to identify intrusion and flushing of saline water. *Groundwater* 23 (5), 635–645.
- Milnes, E., 2011. Process-based groundwater salinisation risk assessment methodology: application to the Akrotiri aquifer (southern Cyprus). *J. Hydrol.* 399 (1–2), 29–47.
- Mohanty, A.K., Rao, V.G., 2019. Hydrogeochemical, seawater intrusion and oxygen isotope studies on a coastal region in the Puri District of Odisha, India. *Catena* 172, 558–571.
- Mondal, N.C., Singh, V.S., Saxena, V.K., Singh, V.P., 2011. Assessment of seawater impact using major hydrochemical ions: a case study from Sadras, Tamilnadu, India. *Environ. Monit. Assess.* 177 (1–4), 315–335.
- Moujabber, M.E., Samra, B.B., Darwish, T., Atallah, T., 2006. Comparison of different indicators for groundwater contamination by seawater intrusion on the Lebanese coast. *Water Resour. Manag.* 20 (2), 161–180.
- Mukherjee, S., 1986. Land subsidence in middle Andaman: A case study. *Hydrol. J.* 13 (3), 150–156.
- Nadler, A., Magaritz, M., Mazor, E., 1980. Chemical reactions of sea water with rocks and freshwater: experimental and field observations on brackish waters in Israel. *Geochim. Cosmochim. Acta* 44 (6), 879–886.
- Naidu, L.S., Rao, G., Rao, G., Mahesh, J., Padalu, G., Sarma, V.S., Prasad, P.R., Rao, S.M., Rao, B.M., 2013. An integrated approach to investigate saline water intrusion and to identify the salinity sources in the Central Godavari delta, Andhra Pradesh, India. *Arab. J. Geosci.* 6 (10), 3709–3724.
- Naily, W., 2018. Ratio of major ions in groundwater to determine saltwater intrusion in coastal areas. In: *IOP Conference Series: Earth and Environmental Science*, vol. 118. IOP Publishing, p. 012021. No. 1.
- Panno, S.V., Hackley, K.C., Hwang, H.H., Greenberg, S.E., Krapac, I.G., Landsberger, S., O'Kelly, D.J., 2006. Characterization and identification of na-cl sources in ground water. *Ground Water* 44 (2), 176–187.
- Post, V.E.A., 2005. Fresh and saline groundwater interaction in coastal aquifers: is our technology ready for the problems ahead? *Hydrogeol. J.* 13 (1), 120–123.
- Rajkumar, N., Subramani, T., Elango, L., 2010. Ground water contamination due to municipal solid waste disposal—A GIS based study in Erode City. *Int. J. Environ. Sci.* 1 (1), 39–55.
- Rajmohan, N., Elango, L.J.E.G., 2004. Identification and evolution of hydrogeochemical processes in the groundwater environment in an area of the Palar and Cheyyar River Basins, Southern India. *Environ. Geol.* 46, 47–61.
- Rani, N.S., Satyanarayana, A.N.V., Bhaskaran, P.K., Rice, L., Kantamaneni, K., 2021. Assessment of groundwater vulnerability using integrated remote sensing and GIS techniques for the West Bengal coast, India. *J. Contam. Hydrol.* 238, 103760.
- Rao, P.S.N., 1996. Phytogeography of the Andaman and Nicobar Islands, India. *Nat. J.* 50 (2), 56–79.
- Rena, V., Vishwakarma, C.A., Singh, P., Roy, N., Asthana, H., Kamal, V., Mukherjee, S., 2022. Hydrogeological investigation of fluoride ion in groundwater of Ruparail and Banganga basins, Bharatpur district, Rajasthan, India. *Environ. Earth Sci.* 81 (17), 430.
- Rosenthal, E., 1988. Hydrochemical changes induced by overexploitation of groundwater at common outlets of the bet Shean-Harod multiple-aquifer system, Israel. *J. Hydrol.* 97 (1–2), 107–128.
- Roy, P.S., Padalia, H., Chauhan, N., Porwal, M.C., Gupta, S., Biswas, S., Jagdale, R., 2005. Validation of geospatial model for biodiversity characterization at landscape level—A study in Andaman & Nicobar Islands, India. *Ecol. Model.* 185 (2–4), 349–369.
- Saidi, S., Bouri, S., Dhia, H.B., 2013. Groundwater management based on GIS techniques, chemical indicators and vulnerability to seawater intrusion modelling: application to the Mahdia-Ksour Essaf aquifer, Tunisia. *Environ. Earth Sci.* 70 (4), 1551–1568.
- Sajil Kumar, P.J., 2016. Deciphering the groundwater-saline water interaction in a complex coastal aquifer in South India using statistical and hydrochemical mixing models. *Model. Earth Syst. Environ.* 2 (4), 1–11.
- Sakram, G.S., Bhoopathi, R.V., Saxena, P.R., 2013. The impact of agricultural activity on the chemical quality of groundwater. Karanjavagu watershed, Medak district. *Andhra Pradesh Int. J. Adv. Scientific Tech. Res.* 3.
- Sankaran, R., 1998. An annotated list of the endemic avifauna of the Nicobar Islands. *Forktail* 17–22.
- Schoeller, H., 1967. *Geochemistry of groundwater—an international guide for research and practice*, 15. Chap, pp. 1–18.
- Selvakumar, S., Chandrasekar, N., Kumar, G., 2017. Hydrogeochemical characteristics and groundwater contamination in the rapid urban development areas of Coimbatore, India. *Water Resour. Industry* 17, 26–33.
- Singh, P., Asthana, H., Rena, V., Kumar, P., Kushawaha, J., Mukherjee, S., 2018. Hydrogeochemical processes controlling fluoride enrichment within alluvial and hard rock aquifers in a part of a semi-arid region of Northern India. *Environ. Earth Sci.* 77, 1–15.
- Singha, P., Dewangan, P., Kamesh Raju, K.A., Aswini, K.K., Ramakrushna Reddy, T., 2019. Geometry of the subducting Indian plate and local seismicity in the Andaman region from the passive OBS experiment. *Bull. Seismol. Soc. Am.* 109 (2), 797–811.
- Srinivasamoorthy, K., Vasanthaigar, M., Vijayaraghavan, K., Sarathidasan, R., Gopinath, S., 2013. Hydrochemistry of groundwater in a coastal region of Cuddalore district, Tamilnadu, India: implication for quality assessment. *Arab. J. Geosci.* 6, 441–454.
- Srinivasan, M.S., 1979. *Geology and mineral resources of the Andaman and Nicobar Islands*. Andaman Nicobar Informa. 1979, 44–52.
- Srivastava, P.K., Gupta, M., Mukherjee, S., 2012. Mapping spatial distribution of pollutants in groundwater of a tropical area of India using remote sensing and GIS. *Appl. Geomatics* 4, 21–32.
- Stoessell, R.K., 1997. Delineating the chemical composition of the salinity source for saline ground waters: an example from East-Central Concordia Parish, Louisiana. *Groundwater* 35 (3), 409–417.
- Stuyfzand, P.J., 1989. A new hydrochemical classification of water types. *Iahs Publ* 182, 89–98.
- Stuyfzand, P.J., 2008. Base exchange indices as indicators of salinization or freshening of (coastal) aquifers. In: *20th Salt Water Intrusion Meeting*, Naples, Florida, USA.
- Subramani, T., Elango, L., Damodarasamy, S.R., 2005. Groundwater quality and its suitability for drinking and agricultural use in Chithar River Basin, Tamil Nadu, India. *Environ. Geol.* 47, 1099–1110.
- Tamta, S.R., 2003. Groundwater contamination in India. *Ind. J. Public Admin.* 49 (3), 578–584.
- Todd, D.K., Mays, L.W., 2004. *Groundwater Hydrology*. John Wiley & Sons.
- Umarani, P., Ramu, A., Kumar, V., 2019. Hydrochemical and statistical evaluation of groundwater quality in coastal aquifers in Tamil Nadu, India. *Environ. Earth Sci.* 78, 1–14.
- Vengosh, A., 2003. Salinization and saline environments. *Treat. Geochem.* 9, 612.
- Werner, A.D., 2010. A review of seawater intrusion and its management in Australia. *Hydrogeol. J.* 18 (1), 281–285.
- Werner, A.D., Simmons, C.T., 2009. Impact of sea-level rise on seawater intrusion in coastal aquifers. *Groundwater* 47 (2), 197–204.